

PB 301114

REPORT NO.
UCB/EERC-79/05
MAY 1979

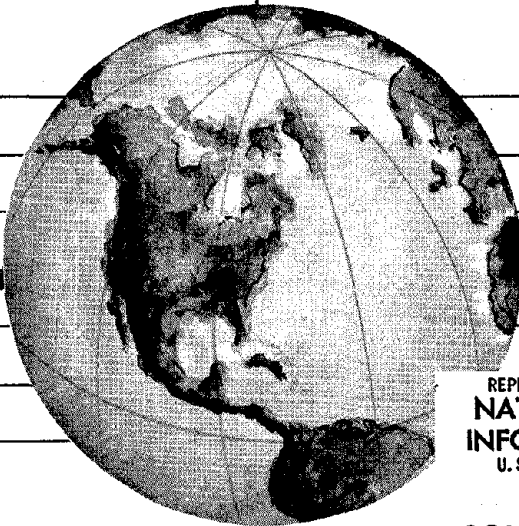
EARTHQUAKE ENGINEERING RESEARCH CENTER

MECHANICAL BEHAVIOR OF LIGHTWEIGHT CONCRETE CONFINED BY DIFFERENT TYPES OF LATERAL REINFORCEMENT

by

MIGUEL A. MANRIQUE
VITELMO V. BERTERO
EGOR P. POPOV

Report to Sponsor:
National Science Foundation



REPRODUCED BY
NATIONAL TECHNICAL
INFORMATION SERVICE
U. S. DEPARTMENT OF COMMERCE
SPRINGFIELD, VA. 22161

COLLEGE OF ENGINEERING

UNIVERSITY OF CALIFORNIA · Berkeley, California

BIBLIOGRAPHIC DATA SHEET	1. Report No. NSF/RA-790183	2.	3. Report Accession No. PB301114	
4. Title and Subtitle Mechanical Behavior of Lightweight Concrete confined by Different Types of Lateral Reinforcement			5. Report Date May 1979	
7. Author(s) M.A. Manrique, V.V. Bertero, E.P. Popov			8. Performing Organization Rept. No. UCB/EERC-79/05	
9. Performing Organization Name and Address Earthquake Engineering Research Center University of California - Richmond Field Station 47th. and Hoffman Blvd. Richmond, CA 94804			10. Project/Task/Work Unit No. 0-22002	
12. Sponsoring Organization Name and Address National Science Foundation 1800 G Street, N.W. Washington, D.C. 20550			11. Contract/Grant No. 9NV 76-04263 E	
15. Supplementary Notes			13. Type of Report & Period Covered	
			14.	
16. Abstract: Results of an experimental study carried out at Berkeley as part of an ongoing research program in order to evaluate the different aspects of the behavior of lightweight concrete are herein reported. The study focuses on the behavior of confined lightweight concrete when subjected to axial, monotonic loading. The effect on confined concrete of the following parameters was considered:				
<ul style="list-style-type: none"> (a) concrete cover (b) longitudinal reinforcement (c) lateral reinforcement arrangement <p>A total of 30 confined and unconfined specimens were tested. The effect of the mentioned parameters are evaluated; subsequently, the experimental results are compared with the results of a similar investigation carried out on normal weight concrete. Current codes-implied values of confinement effectiveness coefficient, and the values experimentally obtained are compared and the consequences (or effects) of the differences obtained are discussed.</p> <p>An analytical stress-strain relationship for longitudinally reinforced confined lightweight concrete is presented; this considers the effect of increase in strength and strain at maximum stress due to confinement as well as the effect of the different types of lateral reinforcement and the effect of the longitudinal reinforcement on the descending branch of the stress-strain relationship.</p> <p>Practical design implications of the present study are presented. The effects of avoiding buckling of the longitudinal reinforcement - by close spacing of the lateral reinforcement - on the ductility of the concrete and on the axial load-moment interaction diagrams obtained from current ACI assumptions of the material properties of both concrete and steel.</p>				
17a. COSATI Field/Group				
18. Availability Statement Release unlimited			19. Security Class (This Report) UNCLASSIFIED	21. No. of Pages 123
			20. Security Class (This Page) UNCLASSIFIED	22. Price PC A06 MF A01

MECHANICAL BEHAVIOR OF LIGHTWEIGHT CONCRETE CONFINED
BY DIFFERENT TYPES OF LATERAL REINFORCEMENT

by

Miguel A. Manrique
Research Assistant
Department of Civil Engineering
University of California, Berkeley

Vitelmo V. Bertero
Professor of Civil Engineering
Department of Civil Engineering
University of California, Berkeley

and

Egor P. Popov
Professor of Civil Engineering
Department of Civil Engineering
University of California, Berkeley

Report to Sponsor:
National Science Foundation

Report No. UCB/EERC-79/05
Earthquake Engineering Research Center
College of Engineering
University of California
Berkeley, California



ABSTRACT

Results of an experimental study carried out at Berkeley as part of an ongoing research program in order to evaluate the different aspects of the behavior of lightweight concrete are herein reported. The study focuses on the behavior of confined lightweight concrete when subjected to axial, monotonic loading. The effect on confined concrete of the following parameters was considered:

- (a) concrete cover
- (b) longitudinal reinforcement
- (c) lateral reinforcement arrangement

A total of 30 confined and unconfined specimens were tested. The effect of the mentioned parameters are evaluated; subsequently, the experimental results are compared with the results of a similar investigation carried out on normal weight concrete. Current codes-implied values of confinement effectiveness coefficient, and the values experimentally obtained are compared and the consequences (or effects) of the differences obtained are discussed.

An analytical stress-strain relationship for longitudinally reinforced confined lightweight concrete is presented; this considers the effect of increase in strength and strain at maximum stress due to confinement as well as the effect of the different types of lateral reinforcement and the effect of the longitudinal reinforcement on the descending branch of the stress-strain relationship.

Practical design implications of the present study are presented. The effects of avoiding buckling of the longitudinal reinforcement - by close spacing of the lateral reinforcement - on the ductility of the concrete and on the axial load-moment interaction diagrams of concrete sections is discussed and compared with similar diagrams obtained from current ACI assumptions of the material properties of both concrete and steel.

ACKNOWLEDGEMENTS

This report is based on the research carried out by M. A. Manrique to satisfy the requirements for the degree of Master of Engineering. This research was conducted under the direct supervision of Professors V. V. Bertero and E. P. Popov.

Financial support for this study was provided by the National Science Foundation under Grant No. 9NV 76-04263, Subproject No. 0-22002. The authors would like to acknowledge the assistance provided by B. Lotz, D. Clyde, and R. Parsons during the experimental testing of the specimens. The cooperation of R. Stephen and the machine shop personnel is appreciated.

In addition, the editorial assistance of M. C. Randall is appreciated. F. Jackson and R. Rhodes types the manuscript. D. Parodi and D. Ullman did the technical illustrations.

TABLE CONTENTS

ABSTRACT	i
ACKNOWLEDGEMENTS	ii
TABLE OF CONTENTS	iii
LIST OF TABLES	v
LIST OF FIGURES	vii
LIST OF NOTATIONS	xiii
1. INTRODUCTION	1
1.1 General	1
1.2 Objectives and Scope	2
2. TEST SPECIMENS	3
2.1 Description of Test Specimens	3
2.2 Materials	4
2.2.1 Concrete	4
2.2.2 Reinforcement	4
2.3 Fabrication and Casting of Specimens	5
2.4 Specimen Designation	6
3. EXPERIMENTAL SET-UP AND TESTING PROCEDURE	7
3.1 General	7
3.2 External Instrumentation	7
3.3 Internal Instrumentation	8
3.4 Data Acquisition System	8
3.5 Testing Procedure	8
4. EVALUATION OF EXPERIMENTAL RESULTS	11
4.1 Introductory Remarks	11
4.2 Unconfined Concrete Specimens	11
4.3 Confined Concrete Specimens	12
4.3.1 General	12
4.3.2 Effect of the Concrete Cover	13
4.3.3 Effect of Longitudinal Reinforcement	14
4.3.4 Effect of Type of Lateral Reinforcement	16
4.3.5 Effect of Buckling Delay and Strain Hardening of Longitudinal Steel on the Load-Strain Relationship of Confined Lightweight Concrete	21

5.	COMPARISON BETWEEN BEHAVIOR OF CONFINED LIGHTWEIGHT AND NORMAL WEIGHT CONCRETE	23
5.1	Introductory Remarks	23
5.2	Comparison of Strength of Normal and Lightweight Confined Concrete	23
5.3	Comparison of Deformation of Normal and Lightweight Confined Concrete	24
6.	CONFINEMENT EFFECTIVENESS OF LIGHTWEIGHT CONCRETE	25
6.1	Analysis and Assumptions of Code Values	25
6.2	Confinement Effectiveness Coefficients Obtained Experimentally	31
6.2.1	General	31
6.2.2	Experimental K_o for Concrete Confined by Square Spirals	33
6.2.3	Experimental K_o for Concrete Confined by Circular Spirals	34
6.2.4	Experimental K_o for Concrete Confined by Square Hoops	34
7.	ANALYTICAL RELATIONSHIPS	37
7.1	General	37
7.2	Analytical Expressions	37
8.	CONCLUSIONS	43
8.1	General	43
8.2	Experimental Study.	43
8.3	Analytical Curve	44
9.	IMPLICATIONS IN PRACTICAL DESIGN	47
9.1	Introductory Remarks	47
9.2	Buckling of the Longitudinal Reinforcement	48
9.3	Axial Load-Moment (P-M) Interaction Diagrams	50
	REFERENCES	55
	TABLES	57
	FIGURES	65

LIST OF TABLES

<u>Table</u>	<u>Page</u>
1.1 Main Characteristics of Specimens	59
2.1 Specified Mix Design	60
2.2 Mechanical Characteristics of Reinforcement	60
2.3 6" x 12" Standard Cylinder Compression Test Results	60
4.1 Mechanical Characteristics of Unconfined Concrete Specimens	61
4.2 Mechanical Characteristics of Confined Concrete Specimens (Square Spirals)	61
4.3 Mechanical Characteristics of Confined Concrete Specimens (Circular Spirals)	62
4.4 Mechanical Characteristics of Confined Concrete Specimens (Square Hoops)	62
5.1 Comparison Between Confined Normal and Lightweight Concrete	63
6.1 Experimental K_0 and K_f	63



LIST OF FIGURES

<u>Figure</u>		<u>Page</u>
1.1	Dimensions of Longitudinally Reinforced Specimens (Square Spirals)	67
1.2	Dimensions of Longitudinally Reinforced Specimens (Circular Spirals)	67
1.3	Dimensions of Longitudinally Reinforced Specimens (Square Hoops)	67
2.1	Stress-Strain Relationship of the Longitudinal Reinforcement and Dimensions of Coupon Tested	68
2.2	Stress-Strain Relationship of the Lateral Reinforcement	68
2.3	Steel Cage for Specimen with Square Hoops	69
2.4	Steel Cage for Specimen with Circular Spirals	69
2.5	Steel Cage for Specimen Without Longitudinal Reinforcement	69
2.6	Detail Showing How Specified Spacing of the Lateral Reinforce- ment Was Maintained in Circular Specimens Without Cover	69
2.7	Cross Section View of Steel Cage (Square Spirals)	70
2.8	Cross Section View of Steel Cage (Circular Spirals)	70
2.9	Cross Section View of Steel Cage (Square Hoops)	70
2.10	Stress-Strain Relationship of Standard 6 in. x 12 in. Cylinder	71
3.1	Qualitative Stress-Strain Relationships at and Outside Zone of Failure	71
3.2	Instrumentation and Data Acquisition System	72
3.3	External Instrumentation	72
3.4	Internal Instrumentation (Square Cross Section)	73
3.5	Internal Instrumentation (Circular Cross Section)	73
3.6a	Close-Up of Specimen (Square Cross Section)	73
3.6b	Close-Up of Specimen (Circular Cross Section)	73
4.1	Stress-Strain Relationship of Plain Concrete Control Specimen	74
4.2	Unconfined Specimen After Testing	74

Preceding page blank

<u>Figure</u>		<u>Page</u>
4.3	Typical Failure of Unconfined Specimen	75
4.4	Stress-Strain Relationship of Specimen Without Cover and Without Longitudinal Reinforcement, Square Spiral; (1AA-1) . .	75
4.5	Stress-Strain Relationship of Specimen Without Cover and Without Longitudinal Reinforcement, Square Spirals; (1AA-2) . .	76
4.6	Stress-Strain Relationship of Specimen With Cover and Without Longitudinal Reinforcement, Square Spirals; (1BA-1)	76
4.7	Stress-Strain Relationship of Specimen With Cover and Without Longitudinal Reinforcement, Square Spirals; (1BA-2)	77
4.8	Stress-Strain Relationship of Specimen With Cover and With Longitudinal Reinforcement, Square Spirals; (1BB-1)	77
4.9	Stress-Strain Relationship of Specimen With Cover and With Longitudinal Reinforcement, Square Spirals; (1BB-2)	78
4.10	Stress-Strain Relationship of Specimen Without Cover and Without Longitudinal Reinforcement, Circular Spirals; (2AA-1) .	78
4.11	Stress-Strain Relationship of Specimen Without Cover and Without Longitudinal Reinforcement, Circular Spirals; (2AA-2) .	79
4.12	Stress-Strain Relationship of Specimen With Cover and Without Longitudinal Reinforcement, Circular Spirals; (2BA-1)	79
4.13	Stress-Strain Relationship of Specimen With Cover and Without Longitudinal Reinforcement, Circular Spirals; (2BA-2)	80
4.14	Stress-Strain Relationship of Specimen Without Cover and With Longitudinal Reinforcement, Circular Spirals; (2AB-1)	80
4.15	Stress-Strain Relationship of Specimen Without Cover and With Longitudinal Reinforcement, Circular Spirals; (2AB-2)	81
4.16	Stress-Strain Relationship of Specimen With Cover and With Longitudinal Reinforcement, Circular Spirals; (2BB-1)	81
4.17	Stress-Strain Relationship of Specimen Without Cover and Without Longitudinal Reinforcement, Square Hoops; (3AA-1)	82
4.18	Stress-Strain Relationship of Specimen Without Cover and Without Longitudinal Reinforcement, Square Hoops; (3AA-2)	82
4.19	Stress-Strain Relationship of Specimen With Cover and Without Longitudinal Reinforcement, Square Hoops; (3BA-1)	83

<u>Figure</u>		<u>Page</u>
4.20	Stress-Strain Relationship of Specimen With Cover and Without Longitudinal Reinforcement, Square Hoops; (3BA-2)	83
4.21	Stress-Strain Relationship of Specimen Without Cover and With Longitudinal Reinforcement, Square Hoops; (3AB-1).	84
4.22	Stress-Strain Relationship of Specimen Without Cover and With Longitudinal Reinforcement, Square Hoops; (3AB-2)	84
4.23	Stress-Strain Relationship of Specimen With Cover and With Longitudinal Reinforcement, Square Hoops; (3BB-1)	85
4.24	Stress-Strain Relationship of Specimen With Cover and With Longitudinal Reinforcement, Square Hoops; (3BB-2)	85
4.25	Specimen Confined With Square Spirals After Testing (With Cover and Without Longitudinal Reinforcement)	86
4.26	Specimen Confined With Square Spirals After Testing (With Cover and Without Longitudinal Reinforcement)	86
4.27	Specimen Confined With Square Spirals After Testing (With Cover and With Longitudinal Reinforcement)	87
4.28	Specimen Confined With Circular Spirals After Testing (With Cover and Without Longitudinal Reinforcement)	87
4.29	Specimen Confined With Circular Spirals After Testing (With Cover and With Longitudinal Reinforcement)	88
4.30	Specimen Confined With Circular Spirals After Testing (Close-Up of Region of Failure).	88
4.31	Specimen Confined With Square Hoops After Testing (With Cover and Without Longitudinal Reinforcement)	89
4.32	Specimen Confined With Square Hoops After Testing (With Cover and Without Longitudinal Reinforcement)	89
4.33	Specimen Confined With Square Hoops After Testing (With Cover and With Longitudinal Reinforcement)	89
4.34	Effect of Concrete Cover on the Stress-Strain Relationship of Confined Concrete (Specimens Without Longitudinal Reinforcement)	90
4.35	Effect of Concrete Cover on the Stress-Strain Relationship of Confined Concrete (Specimens With Longitudinal Reinforcement).	90
4.36	Effect of the Longitudinal Reinforcement on the Stress-Strain Relationship of Confined Concrete (Specimens With Cover)	91

<u>Figure</u>		<u>Page</u>
4.37	Effect of the Longitudinal Reinforcement on the Stress-Strain Relationship of Confined Confined Concrete (Specimens with Cover)	91
4.38a	Effect of Configuration of the Longitudinal Reinforcement on the Basketing of the Concrete Core	92
4.38b	Longitudinal Variation of f_r on a Specimen	92
4.39a	Transversal Variation of f_r in Circular Cross Section	92
4.39b	Transversal Variation of f_r in Square Cross Section.	92
4.40	Effect of Type of Lateral Reinforcement on the Stress-Strain Relationship of Confined Lightweight Concrete	93
4.41	Free Body Diagrams Used in Determining f_r	93
4.42	Effect of Strain Hardening of the Longitudinal Reinforcement on Confined Concrete	94
5.1	Comparison of Normal and Lightweight Confined Concrete (Specimens Without Cover and Without Longitudinal Reinforcement)	94
5.2	Comparison of Normal and Lightweight Confined Concrete (Specimens With Cover and Without Longitudinal Reinforcement)	95
5.3	Comparison of Normal and Lightweight Confined Concrete (Specimens With Cover and With Longitudinal Reinforcement).	95
6.1	Variation of f_r (required) Vs. K_o for Different Values of A_g/A_c	96
7.1	Experimental and Analytical Stress-Strain Relationship of Confined Lightweight Concrete (Square Spirals)	96
7.2	Experimental and Analytical Stress-Strain Relationship of Confined Lightweight Concrete (Circular Spirals).	97
7.3	Experimental and Analytical Stress-Strain Relationship of Confined Lightweight Concrete (Square Hoops).	97
9.1a	Dimensions of Square Cross Section Used in Computing P-M Interaction Diagrams	98
9.1b	Dimensions of Circular Cross Section Used in Computing P-M Interaction Diagram	98
9.2a	Stress-Strain Relationship of Confined Concrete Used in the Analysis of Square Cross Section	98

<u>Figure</u>		<u>Page</u>
9.2b	Stress-Strain Relationship of Confined Concrete Used in the Analysis of Circular Cross Section	98
9.3a	Stress-Strain Relationship for Concrete Cover.	99
9.3b	Stress-Strain Relationship for Longitudinal Reinforcement . . .	99
9.4a	Equivalent Stress Block Assumptions and Implied Stress-Strain Relationship for Concrete	99
9.4b	Hognestad Stress-Strain Relationship for Concrete	99
9.4c	Elastic-Perfectly Plastic Relationship for Steel	99
9.5	Comparison of Axial Load-Moment (P-M) Interaction Diagrams for Square Cross Section Computed Using Hognestad's and the Equivalent Stress Block Relationship	100
9.6	Comparison of Axial Load-Moment (P-M) Interaction Diagrams for Circular Cross Section Computed Using Hognestad's and the Equivalent Stress Block Relationship	100
9.7	Comparison of Axial Load-Moment (P-M) Interaction Diagrams for Square Cross Section	101
9.8	Comparison of Axial Load-Moment (P-M) Interaction Diagrams for Circular Cross Section	101
9.9	Effect of Amount of Lateral Confining Pressure on the Axial Load-Moment (P-M) Interaction Diagrams for Normal and Lightweight Concrete	102
9.10	Nondimensional Stress-Strain Relationships for Confined Normal and Lightweight Concrete (Ref. 3)	102
9.11	Comparison of Axial Load-Moment (P-M) Interaction Curves Computed Using the Equivalent Stress Block Relationship and the Experimental Curves Reported in Reference 3	103

LIST OF NOTATIONS

- A = Constant which depends on the type of lateral reinforcement
- $A_c = A_{ch}$ = Area of core section out-to-out of the lateral reinforcement
- A_g = Area of gross section
- A_s = Total steel area of longitudinal reinforcement
- A_{sh} = Total cross sectional area of lateral reinforcement
- A_{st} = Area of one leg of lateral reinforcement
- D_b = Diameter of bar of longitudinal reinforcement
- D_c = Diameter of core section in circular specimens
- d_s = Diameter of gage wire used as transverse reinforcement
- E = Modulus of elasticity
- E_c = Modulus of elasticity of concrete
- $E_{c(0.45 f'_c)}$ = E_c within the range of $0 < f_c < 0.45 f'_c$
- $E_{c(0.45 f_c^U)}$ = E_c within the range of $0 < f_c < 0.45 f_c^U$
- E_c (ACI) = E_c based on ACI formulae
- E_s = Modulus of elasticity of steel
- E_{sh} = Tangent modulus at the onset of strain hardening of longitudinal steel
- $E_{t\ scr}$ = Tangent modulus of elasticity in the strain hardening range
- f'_c = Standard 6 in. x 12 in. cylinder compressive strength
- f_c = Stress in concrete
- f_c^U = Maximum strength of unconfined concrete specimen of similar size as the confined specimens

Preceding page blank

- $f_{C \max}^C$ = Maximum strength of confined concrete
 f_f = Stress in concrete at failure
 f_s = Stress in the longitudinal reinforcement
 f_{scr} = Critical buckling stress of the longitudinal reinforcement
 f_r = Lateral confinement pressure
 f_s'' = Stress in the lateral reinforcement
 f_y = Specified yield stress of transverse reinforcement
 $f_y'' = f_{yh}$ = Specified yield stress of transverse reinforcement
 f_{su} = Specified ultimate stress of longitudinal reinforcement
 h_c = Lateral core dimension of square cross section specimens measured out-to-out of the lateral reinforcement
 k = Effective length coefficient value which depends on the support conditions offered by the lateral reinforcement
 K = Maximum stress ratio
 K_o = Confinement effectiveness coefficient at maximum stress
 K_f = Confinement effectiveness coefficient at failure
 ℓ_h = Maximum unsupported length of rectangular hoop measured between perpendicular legs of the hoop or supplementary crossties
 P_b = Balanced failure axial load capacity
 P_e = Maximum design axial load
 $r = \epsilon_{su} - \epsilon_{sh}$
 $R = S/h_c$ or S/D_c
 S = Spacing of the lateral reinforcement
 $x = \epsilon_s - \epsilon_{sh}$

- Z = Parameter that defines the slope of the descending branch of the $f_c - \epsilon_c$ relationship
- ϵ = Strain
- ϵ_c = Concrete strain
- ϵ_0 = Concrete strain at maximum stress of 6 in. x 12 in. standard cylinder
- ϵ_0^U = Concrete strain at maximum stress of unconfined specimen of similar size as the confined specimen
- ϵ_0^C = Concrete strain at maximum stress of confined specimen
- ϵ_f = Concrete strain failure
- ϵ_{cu} = Concrete strain at ultimate stress
- ϵ_s = Steel strain
- ϵ_y = Yielding strain of the longitudinal reinforcement
- ϵ_{sh} = Steel strain at onset of strain hardening
- ϵ_{su} = Steel strain at ultimate stress
- $\epsilon_{0.2K}$ = Concrete strain when $f_c/f'_c = 0.2K$
- ρ_s = Volumetric ratio of longitudinal reinforcement
- ρ'_s = Volumetric ratio of lateral reinforcement
- ϕ = Capacity Reduction Factor



1. INTRODUCTION

1.1 General

In earthquake-resistant design, economic considerations usually require that structural members be able to absorb and dissipate large amounts of energy through significant inelastic deformations.

In earthquake-resistant concrete construction, the positive characteristics of concrete - good durability; architectural and structural versatility - are not sufficient to render efficient, economic, and safe structures. There are three main drawbacks to the use of concrete as a structural material in areas of high seismic risk:

- (a) It has a relatively low strength/unit weight ratio
- (b) It has a very low resistance to tension
- (c) It has a low deformation capacity

It is highly desirable to find ways to improve these properties of plain, normal weight concrete. The use of lightweight aggregate as a constituent material permits lessening of the unit weight of the concrete ideally without diminishing its strength, and deformability. This is attractive to the designer because of the possibilities of reducing the mass of the structure, leading to lower inertia forces in the event of a severe ground motion.

Results of investigations at the University of California, Berkeley, [1,2,3] and elsewhere [4] regarding the behavior of confined and unconfined concrete with different types of aggregate indicate that confinement of concrete is effective in increasing its strength and deformation capacity. Investigators agree that the deformation and strength characteristics of confined concrete are sensitive to the kind of aggregate and relative amount of confinement pressure used and that the increase in compressive strength due to lateral confinement is greater for normal weight than for lightweight concrete.

Significant differences in the behavior of lightweight and normal weight concrete do exist; the use of lightweight concrete in seismic-resistant construction is not warranted without properly accounting for these differences. Recommendations have recently been made that research should be done to improve the deformability of concrete and to improve its ratio of strength per unit weight and modulus of elasticity per unit weight [5].

However, the available literature reports no experimental program which considers the separate effects of design parameters such as: the concrete cover; different types of lateral reinforcement; and effects of the longitudinal reinforcement for lightweight concrete. All these

parameters have considerable practical significance. As part of an ongoing experimental program being carried out at Berkeley to evaluate all aspects of the behavior of structural members made with lightweight aggregate, an experimental study on the mechanical behavior of confined lightweight concrete when subjected to monotonic axial compressive loads has been planned.

The determination of the stress-strain relationship for confined lightweight aggregate concrete, and the design implications when it is used in reinforced concrete members, are the main concerns of this study. The effects of the three design parameters mentioned above on the strength and deformation of short lightweight concrete columns are also of primary consideration. Because of its practical significance emphasis is placed on the specimens containing all three parameters.

1.2 Objectives and Scope

The main objective of the experimental study reported herein was to gather reliable information regarding the mechanical behavior of lightweight aggregate concrete under monotonic axial compressive loading. This information would permit the formulation of a reliable stress-strain relationship for confined lightweight aggregate concrete.

In attempting to fulfill this objective, a parametric study was considered which would account for the effects of the following variables:

- (a) concrete cover
- (b) longitudinal reinforcement
- (c) lateral reinforcement arrangement

A second objective of this investigation was to compare the experimental results of tests carried out by Vallenias, Bertero, and Popov [6] on similar size normal weight concrete specimens considering the same parameters. The final objective was to discuss the implications of cover spalling, and strain hardening of steel on the practical design of confined reinforced concrete structural members.

Three groups of specimens were tested (10 specimens in each group), each with a different type of lateral reinforcement:

- (a) specimens with square spirals
- (b) specimens with circular spirals
- (c) specimens with square hoops

Two plain concrete specimens of a size similar to the confined specimens were cast with each group. The average results of the plain specimens were compared with the results of the confined specimens. Table 1.1 gives a summary of the main characteristics of the specimens tested in this study. The dimensions of the specimens are shown in Figs. 1.1 to 1.3.

2. TEST SPECIMENS

2.1 Description of Test Specimens

In this study, the different parameters affecting the behavior of the specimen were isolated in order to find their individual effect on confined concrete. A total of 30 specimens were tested. The specimens were cast vertically in sets of ten specimens each. Of these ten specimens, eight contained the parameters previously mentioned (concrete cover, lateral reinforcement, longitudinal reinforcement), and two were plain concrete control specimens. The specimens in all three groups had a length of 30 in. (762 mm) and when cover was used, its thickness was 0.5 in. (12.7 mm). Specimens with rectangular hoops, rectangular spirals, and cover had cross sectional dimensions of 10 in. x 10 in. (254 mm x 254 mm). Similar specimens without cover had cross sectional dimensions of 9 in. x 9 in. (229 mm x 229 mm). For the specimens with cover, this represented 19% of the total cross section.

The specimens with circular spirals had a diameter of 11 in. (279.4 mm) in the case of specimens with cover, and 10 in. (254 mm) for the specimens without cover. The cover was about 17% of the cross sectional area. The specimen's core area is measured from out to out of the lateral reinforcement.

Longitudinal reinforcement was included in four specimens in each group; it consisted of eight #6 (diameter 0.75 in. [19.05 mm]) deformed reinforcing steel bars distributed around the perimeter of the cross section, as can be seen in Figs. 1.1, 1.2, and 1.3. The total area of the longitudinal reinforcing bars was 3.53 in.² (2277.4 mm²). The longitudinal reinforcement ratio for the square cross section specimens varied from $\rho_s = 0.0436$ for the specimens without cover to $\rho_s = 0.0353$ for the specimens with cover. In the case of the circular cross section specimens, the longitudinal reinforcement ratio varied from $\rho_s = 0.0449$ for the specimens without cover to $\rho_s = 0.0371$ for the specimens with cover.

The lateral reinforcement of all specimens consisted of #7 gage wire (diameter: 0.179 in. [4.55 mm]). In the specimens with square cross sections, the spacing of the lateral reinforcement was 1.33 in. (33.78 mm) and the lateral reinforcement volumetric ratio,

$$\rho'_s = \frac{\text{volume of confining steel}}{\text{volume of confined concrete}}$$

was 0.0144 for the specimens with square spirals and square hoops. It may be noted that in the case of specimens with square hoops if the length of the extension hook of the hoops, (see Fig. 1.3) is included in the calculation of the volumetric ratio, then $\rho'_s = 0.0152$. In the case of specimens with circular spirals, the spacing of the lateral reinforcement was 0.7 in. (17.78 mm), and the volumetric ratio of the lateral reinforcement was $\rho'_s = 0.0144$.

In order to make meaningful comparisons, the area of the core (out-to-out of the lateral reinforcement), and the volumetric ratio of the lateral reinforcement, were kept as close as possible for the three groups of specimens. The standard compression test of 6 in. x 12 in. (152 mm x 305 mm) cylinders was used as an index of the strength of the concrete.

2.2 Materials

2.2.1 Concrete

Portland cement type I and II, natural sand, and a locally manufactured lightweight aggregate were used in this study. A mix design was used, suggested by the manufacturer of the lightweight aggregate [7], to give a strength of 4500 psi (31.03 MPa) at 28 days. However, the cylinder strength obtained from samples of this mix was approximately 5200 psi (35.85 MPa) at 28 days. The values of the strengths varied from 5100 psi (35.16 MPa) to 5350 psi (36.89 MPa) and those of the strain at maximum stress varied from 0.00285 in/in to 0.00305 in/in.

The lightweight aggregate used was expanded shale. The manufacturing process of this aggregate consists of taking raw shale containing elemental carbon and iron oxide which is then moisturized and extruded into cord-like lengths of regulated diameter. The cords are broken down into pellet-shaped pieces. These pellets expand when subjected to burning temperatures as high as 2050° F. By this burning process the pellet is transformed into a vitreous-coated nugget with a honeycombed inner structure.

The lightweight aggregate had a maximum size of 3/8 in. (9.52 mm) with an approximate unit weight when moist of 44 lbs/c.f. (704 kg/m³). Its moisture content at the time of mixing was approximately 11.5%.

The mix design used was the same for the three groups of specimens; minor modifications in the water-cement ratio were necessary in some mixes in order to obtain a uniform slump in all mixes. Table 2.1 shows the mix design used in this study.

The average unit weight of the concrete at the time of casting was 114.1 lbs/c.f. (1830 kg/m³). The air-dry unit weight at 28 days is about 5 lbs/c.f. less than the unit weight at the time of casting. The air content of the mix varied from 6% to 6-1/4% and the slump obtained varied from 2-1/4 in. (57.15 mm) to 2-3/4 in (69.85 mm).

2.2.2 Reinforcement

Deformed #6 steel bars with a nominal diameter of 0.75 in. (19.5 mm) were used as longitudinal reinforcement. Figure 2.1 shows the stress-strain relationship for this longitudinal reinforcement obtained by averaging the results of two coupons tested in tension.

The lateral reinforcement consisted of #7 plain gage wire, with a diameter of 0.179 in (4.546 mm). Some variation of the properties were observed for this reinforcement from coupon to coupon; presumably, this is due to the manufacturing process. Figure 2.2 shows the results of the stress-strain relationship obtained in tension test runs on this reinforcement.

Table 2.2 summarizes the mechanical characteristics of both longitudinal and lateral steel.

2.3 Fabrication and Casting of Specimens

A total of 30 specimens were fabricated, and three different configurations of the lateral reinforcement were considered. The specimens with a square cross sectional area had either two hoops at the same level or two square spirals, one interior and one exterior, having the same pitch (see Figs. 1.1 and 1.3). In the case of specimens with longitudinal reinforcement, the hoops or spirals were fastened to the reinforcement by means of flexible wire (see Figs. 2.3 and 2.4). For specimens without longitudinal reinforcement, longitudinal flexible wire was used to keep the specified spacing between the hoops, or spirals, throughout the length of the cage. This operation, repeated at the middle and each corner of the hoop, was sufficient to allow the cage to be placed in the forms without disturbing the spacing (see Fig. 2.5). A similar procedure was used for the circular specimens with cover. For circular cross-section specimens without cover, the spirals were kept in place by means of U-shaped pieces of flexible wire; these were passed horizontally through holes punched in the forms at the specified spacing along the specimen (see Fig. 2.6).

Figures 2.7 to 2.9 show cross section views of the cages ready to be placed into the forms before casting.

Transverse steel rods 1/4 in. (6.35 mm) in diameter were used to attach the designed instrumentation. Four of these rods were running in the North-South direction and two were running in the East-West; they were spaced at six in. (152.4 mm), which corresponds to the gage length of the instrumentation used.

All specimens were cast in the vertical position. In the case of specimens with a square cross sectional area, wood forms were used; whereas for specimens with a circular cross section, commercially available forms were used. Ten specimens were cast at one time; after casting, the specimens were covered with wet burlap and left in the laboratory for five-six days. The forms were then stripped and the specimens were stored in the laboratory at 70° F until the date of testing. The age of the specimens at the time of testing varied from 26 days to 32 days, with most of the specimens at 28-30 days.

In order to avoid premature failure due to stress concentration at the ends of the specimen where the axial load is applied, the lateral confinement in these regions, six in. (152.5 mm) at the top and six in. (152 mm) at the bottom, was increased by reducing the spacing to 0.67 in. (17.08 mm). However, at the time of testing, additional 3/4 in. (19.05 mm) thick steel plates had to be used in order to avoid premature failure at the ends of the specimen. In this manner failure was forced to occur along the instrumented region, i.e., within the central 18 in. (457.2 mm).

Concrete samples taken from each batch were cast in 6 in. x 12 in. (152 mm x 305 mm) cylinders in order to monitor the strength of the specimens and to have an indication of the strength of the concrete at the time of testing.

Table 2.3 contains the results of the compression test of these cylinders at 28 days after casting. The secant modulus of elasticity taken at 45% of the maximum strength is also shown. Figure 2.3 shows an average $f_c - \epsilon_c$ relationship obtained from the standard cylinder tests.

2.4 Specimen Designation

Alphanumeric characters (e.g. 3AB-1) were used to more readily identify the specimens. Their significance is as follows:

- The first number indicates the casting sequence of the three groups of specimens and denotes a particular type of lateral reinforcement:

- (1) Specimens with rectangular spirals
- (2) Specimens with circular spirals
- (3) Specimens with square ties

- The letter after the first number indicates either:

- (A) Specimen has no cover
- (B) Specimen has cover

- The next letter indicates:

- (A) Specimen has no longitudinal reinforcement
- (B) Specimen has longitudinal reinforcement

- The last number is used to distinguish between identical specimens; since there are two specimens of each kind, this number can be either one or two.

3. EXPERIMENTAL SET-UP AND TESTING PROCEDURE

3.1 General

A primary objective of the experimental phase of this study was to accurately measure the concrete's inelastic deformations at the zone of failure, rather than relying on an average of inelastic deformations. Figure 3.1 depicts the difference in stress-strain curves obtained from deformations measured in three different regions along the length of the specimen. From this figure, it can be observed that, when the stress resistance begins to decrease along the descending branch of the stress-strain curve, most inelastic deformations occur in one region (the middle region in Fig. 3.1). As the test progresses, this region may be the only one contributing significantly to the total deformation of the specimen. The strain in the other regions of the specimen (upper and lower regions in Fig. 3.1) may remain constant or even decrease.

For these reasons, and because the actual zone of failure is uncertain, it was deemed necessary to instrument individually different consecutive regions of the specimen along the full length where failure could occur.

In the present study, two kinds of instrumentation were used, external and internal. Figure 3.2 shows a diagram of the complete instrumentation and data acquisition system. A detailed discussion of the instrumentation follows.

3.2 External Instrumentation

Part of the external instrumentation can be seen in Fig. 3.3. Axial deformations were measured along the possible region of failure of the specimen, that is, 18 in. (457.2 mm). For this purpose, 3 pairs of clip gages of six in. (152.4 mm) gage length were used, these gages were placed on opposite faces of the specimen and are denoted as follows. CGT N means a clip gage placed at the top north side of the specimen, M or B instead of T would indicate middle or bottom region, and S instead of N indicates that the gage is being placed on the south side. These clip gages were attached to circular rods of 1/4 in. (6.35 mm) in diameter which were embedded across the specimen. At the other two faces of the specimen two LVDTs* were used to measure axial deformations at the middle section, these were denoted as LVDT E (placed on the east side) and LVDT W (placed on the west side of the specimen). These LVDTs were placed over a gage length of six in. (152.4 mm). The overall deformation of the specimen was measured with a pair of linear potentiometers (LP E and LP W) placed opposite each other; the gage length was 30 in. (762 mm). The clip gages have the advantage that they remain operational even after spalling of the cover of the specimen; the LVDTs are more susceptible to being disturbed by spalling of the cover. The use of the described instrumentation ensured measurement of deformations well into the inelastic range.

Transverse deformations were monitored at the middle section of the specimen by horizontal LVDTs fixed to steel posts. These posts were attached

*LVDTs stands for Linear Variable Differential Transformers

to the testing floor with hydrostone. Wire connected to the LVDTs were attached to the specimens by means of a hook attached either to the main reinforcement or to one of the spirals, depending upon the type of specimen. For the case of plain concrete specimens, it was necessary to epoxy a small aluminum angle to the concrete surface. In some specimens, the longitudinal strains of a reinforcing bar were measured by means of a clip gage attached to pins soldered to the bar. The gage length used for this clip gage was six in. (152.4 mm).

3.3 Internal Instrumentation

This instrumentation consisted of weldable and foil type strain gages. Weldable strain gages were placed on the interior face of a reinforcing bar, and a foil type strain gage was placed on the exterior face (see Figs. 3.4 and 3.5). The spacing between ties or spirals did not allow for the placement of a weldable strain gage at the exterior face of the reinforcing bar. These strain gages monitored the longitudinal strains in the steel bar as well as indicated when buckling of the instrumented bar began. Both strain gages were placed on the reinforcing bars at the middle section of the specimen. Strains in the lateral reinforcement were monitored with weldable strain gages for the specimens with cover and foil type strain gages for the specimens without cover. The specimens with a square cross section had one strain gage on the exterior hoop and one strain gage on the interior hoop. These gages were placed on the upper part of the wire so that effects of bending of the lateral reinforcement could be eliminated. The specimens with circular spirals had one weldable strain gage on the lateral reinforcement to measure the confining stresses developed by this reinforcement (See Figs. 3.6a and 3.6b).

3.4 Data Acquisition System

The data acquisition system consisted of four XYY' recorders which provided a continuous record of the specimen's deformations and a low speed scanner whose center is a NOVA minicomputer. A total of 17 transducers were monitored, the output of nine of them sent simultaneously to XYY' recorders. Each X channel of the XYY' recorder was connected in series to the axial load transducer. The amplifiers for the YY' channels were calibrated to give plots of load versus strains. The specimens were tested at the University of California Richmond Field Station using the 4,000,000 lbs. capacity Universal testing machine.

3.5 Testing Procedure

Before testing, the specimens were capped with approximately 1" - to 1 - 1/2" of hydrostone at the top and bottom in order to ensure good contact surface. The specimens were tested under monotonically increasing axial compressive load up to collapse.

The loading rate was in the order of 100 kips/min. up to attainment of maximum load and from then on at approximately 30 μ e/sec. Testing time for one specimen varied between 30-35 minutes. The testing of a specimen was considered complete after the specimen showed a sudden decrease in resistance or when the damage was so severe that consecutive strain readings

would not be reliable. Readings of all 17 channels were taken at intervals of 40 kips in the initial stages of loading. Near maximum load readings were taken at intervals of 20 kips. Once peak load was attained, readings were taken at constant intervals of strain (at every 0.0015 in/in) up to the end of the test. The testing machine used does not operate on displacement control, therefore, at each reading level, it was necessary to keep the load constant for six to eight seconds in order for the scanner to read and print all 17 channels.



4. EVALUATION OF EXPERIMENTAL RESULTS

4.1 Introductory Remarks

In this chapter experimental results in the form of stress-strain relationships are discussed, first for unconfined and then for confined specimens. The relationships presented correspond to the region of the specimen where most inelastic deformations occurred, and were measured over a length of 6 in. (152.4 mm). In the case of confined specimens, comparisons of experimental results of specimens within each group are made in order to determine the effect of two parameters: the concrete cover and the longitudinal reinforcement. Then the results from each of the three groups containing these two parameters are compared in order to evaluate the effect of the type of lateral reinforcement on the stress-strain relationship of confined concrete. This latter comparison was made only for the specimens containing both cover and longitudinal reinforcement because of their practical significance. Finally, the effects of confinement on longitudinally reinforced specimens and its influence on the load versus strain relationship of concrete is discussed.

4.2 Unconfined Concrete Specimens

Six plain unconfined concrete specimens of similar size, shape, and concrete mix to those of the confined specimens were cast so that the behavior of the confined and unconfined specimens could be compared.

The unconfined specimens were cast and tested in three groups: each group of two specimens was cast and tested simultaneously with confined specimens which contained the same kind of lateral reinforcement. The specimens were tested at either 26 or 27 days after they were cast.

A typical curve obtained from the testing of these specimens is shown in Fig. 4.1. Since the testing machine does not operate on displacement control, attempts to further develop the descending branch of the stress-strain curve were not successful. Other investigators [2,4] have reported special methods to develop the post-peak descending portion of the plain lightweight concrete curve. The main purpose of the various different testing arrangements was to avoid a sudden release of energy from the testing machine to the specimen when the specimen starts to unload. In this manner it is possible to develop the full stress-strain curve. In the future, attempts should be made to obtain the full curve.

The stress-strain relationship was computed by averaging the readings obtained from two LVDTs placed on opposite faces of the specimen. The LVDTs were attached to a special extensometer whose gage length was 12 in. (304.8 mm).

The experimental results obtained for the three groups of specimens are summarized in Table 4.1 in both SI and English units. As can be observed from this table, the strength of the unconfined control specimens was consistently lower than the 6 x 12 cylinder strength. The average ratio

of unconfined control specimen strength to 6 x 12 cylinder strength was 86.3%. This difference in the strength of different sized specimens may arise from the fact that smaller specimens are better compacted and exhibit a smaller amount of bleeding; therefore their concrete is of somewhat better quality [8].

Failure of the unconfined control specimens occurred suddenly, without previous indication of external crushing. Splitting tension cracks running along the length of the specimen were observed after the test. This type of failure is a consequence of a sudden energy release by the testing machine which occurs when the specimen starts unloading, and which the specimen is unable to absorb. Figures 4.2 and 4.3 show these specimens after testing. Comparison of experimental values for the modulus of elasticity (secant modulus at 45% of maximum stress) with the values computed using the ACI Code formula indicate that this formula consistently gives larger values than those obtained experimentally. However, this overestimation never exceeded 13%.

4.3 Confined Concrete Specimens

4.3.1 General

This study included the testing of specimens both with and without concrete cover; and with and without longitudinal reinforcement. The experimental determination of the relationship between the total load and the longitudinal strain is straightforward. However, the true stress on the specimen when the cover starts to spall is more complicated to determine, since it is very difficult to accurately ascertain the effects of arch formation in between hoops, or spirals, once the cover starts spalling. Experimental observation indicates that in most specimens fine longitudinal cracking appeared on the concrete cover at a strain of 0.002 in./in. (mm/mm). This cracking was followed by some flaking (crushing) on the different faces of the specimens; then the cover began to spall off the specimen. Based mostly on this experimental observation, the concrete cover was assumed to start spalling at a strain of 0.002 in./in. which is smaller than that observed in tests of unconfined concrete. The main reason for this smaller strain is due to the discontinuity between core and cover introduced by the lateral reinforcement (see discussion in section 4.3.2).

The ultimate strain of the concrete cover is difficult to determine experimentally. In this study, the contribution of the concrete cover to the load carrying capacity of the specimen was assumed to end at a strain of 0.0045 in./in. (mm/mm). This assumption agrees well with experimental observations, since at this strain the cover had - in most cases - spalled off the specimen. A linear reduction in the area of the specimen from $A_g = 100 \text{ in.}^2$ (63516 mm²) starting at a concrete strain of 0.002 in./in. to $A_c = 81 \text{ in.}^2$ (52258 mm²) (out-to-out of hoop or spiral) at a strain of 0.0045 in./in. was adopted.

In the case of specimens with longitudinal reinforcement, the contribution of this reinforcement to the specimen's resistance had to be subtracted from the total load in order to obtain the $f_c - \epsilon_c$ of the concrete alone.

The resistance of the longitudinal reinforcement was evaluated from

the average strain obtained from two weldable strain gages placed opposite each other in one longitudinal bar. The steel stress corresponding to the average strain was taken from the stress-strain curve obtained from testing steel coupons under tension. The force contributed by the steel was then subtracted from the specimen's total load and the stress in the concrete was computed.

The longitudinal strains in the steel and in the concrete are identical up to or slightly beyond the point where the specimen reaches maximum load. From then on, there may be some discrepancy in the strain values, especially when inelastic deformations are concentrated outside the middle region of the specimen because the steel strains are being measured only in the middle region. It was observed that, in cases when the specimen failed in its middle region, the measured strains between steel and concrete were quite compatible over a larger strain range.

At very large deformations, and at the region where the largest inelastic deformations occur, concrete strains tend to be larger than steel strains, indicating some slippage between steel and concrete. Also, concrete and steel strains cease to be compatible as soon as buckling of the longitudinal steel occurs where the gage is located.

In considering the effect of steel on the concrete stress-strain relationship, compatibility of strains between the two materials at large deformations was assumed. The actual experimentally obtained stress-strain relationship, including the strain hardening portion of the stress-strain relationship for the steel, was considered. In other words, no idealization of this part of the curve was done.

Finally, the experimental results are depicted in the form of stress-strain relationships in Figs. 4.4 to 4.24. In all these figures the corresponding curve for plain concrete is included to compare the behavior of both types of concrete: unconfined and confined. Figures 4.25 to 4.33 show the tested specimens after failure. A summary of the experimental results is presented in Tables 4.2 to 4.4.

4.3.2 Effect of the Concrete Cover

To predict mechanical behavior of concrete members it is necessary to distinguish between two types of concrete: the unconfined concrete of the cover and a concrete core which is confined by regularly spaced hoops or spirals. These two elements have different mechanical properties and, upon being loaded, follow different stress-strain paths. They may be able to undergo the same deformations up to the point when the confining steel begins to be effective. At this point, due to Poisson's effect and because of the confinement of the core section, the volumetric strains of both cover and core begin to differ substantially: lateral strains in the core are constrained by the confining steel and therefore are smaller than those in the cover. This causes separation between core and cover, converting the concrete cover into a slender and discontinuous part of the specimen, which is therefore less effective in resisting loads. (The discontinuity is introduced by the lateral reinforcement.) Figures 4.34 and 4.35 depict the comparison of specimens with and without cover for both unreinforced and longitudinally reinforced specimens.

The main effect of the concrete cover was to permit an early and more

effective confinement due to the reduction of the detrimental effect of shrinkage strains in the specimen's core. All this resulted in an increase in the strength of the concrete. In the ascending branch of the $f_c - \epsilon_c$ curve, the strains in the lateral reinforcement for the specimen without cover are smaller than for the specimens with cover. At about 85% to 90% of the computed maximum stress the strains in the lateral reinforcement correspond to stresses typically in the order of 20 ksi (137.9 MPa) in specimens without cover, and 40 ksi (275.8 MPa) for the specimens with cover. This indicates that the effects of shrinkage are more detrimental in the specimens without cover, since in this case the development of larger lateral strains are necessary before the lateral reinforcement can confine the concrete.

It appears that these shrinkage strains cause a delay in the confining action allowing the specimen to respond mostly as if it was unconfined; and therefore impairing a substantial increase in strength. However, as the longitudinal and lateral strains are increased, the concrete core, which may have already suffered extensive internal cracking, begins to develop confining stresses making it feasible to develop the descending branch of the $f_c - \epsilon_c$ curve. Similar findings are reported in reference 9.

Experimental observations indicate that the spalling of the cover occurred faster in the specimens with circular spirals than in specimens with square hoops, this is due mainly to the smaller spacing of the lateral reinforcement used in specimens with circular spirals. Therefore, the transition between cover and core is more discontinuous in this kind of specimen making the cover less effective as a load carrying element.

4.3.3 Effect of Longitudinal Reinforcement

In a reinforced concrete structural element, the presence of the longitudinal reinforcement can significantly affect the mechanical characteristics of the concrete by:

- (a) Working as a spreader; redistributing stresses from weak to stronger regions; and
- (b) Offering better confinement by improving the basketing of the concrete.

The longitudinal reinforcement improved the descending branch of the $f_c - \epsilon_c$ relationship with respect to the concrete in the specimens that did not contain this parameter. This is possible as long as buckling of the reinforcement is delayed long enough by close spacing of the lateral reinforcement.

However, once buckling of the reinforcement begins to take place, the concrete inside the core starts to lose its state of triaxial pressure, because of the lesser amount of lateral restraint existing as buckling of the longitudinal reinforcement develops, leading to an eventual loss of most of the confinement. Figures 4.36 and 4.37 show the effect of the longitudinal reinforcement on the $f_c - \epsilon_c$ relationship of lightweight concrete. In the case of specimens with square cross section, buckling of the reinforcement began to develop in between the hoops or square spirals. As

buckling developed, the longitudinal reinforcement pushed out against the lateral reinforcement. In most cases, the interior hoop failed by rupturing at a corner region rather than by slipping.

In the case of specimens with circular spirals, rupture of the lateral reinforcement permitted buckling of the longitudinal reinforcement which was followed by rapid deterioration of the concrete.

As expected, the yielding of the longitudinal reinforcement ($\epsilon_y = 0.002$) occurred before the specimen offered its maximum resistance. Experimental results indicated that this yielding occurred at 85% to 95% of the maximum attained load. Visible fine cracking of the concrete cover in some of the faces of the specimen was also noticed at this stage of loading. Some eccentricity of loading was present due to nonuniform spalling of the cover. However, the close spacing of the lateral reinforcement, and the total contact between longitudinal and lateral reinforcement at every hoop or spiral level, minimized the lateral displacement of the longitudinal reinforcement and delayed the buckling of it. Upon complete spalling of the cover at the region of failure, the load again became concentric.

Buckling of the longitudinal reinforcement occurred at longitudinal strains ranging from 0.036 to 0.045 in./in. (mm/mm) for the specimens with square spirals; 0.028 to 0.054 in./in. (mm/mm) for the specimens with circular spirals; and 0.033 to 0.05 in./in. (mm/mm) for the specimens with square hoops. The average critical buckling strain for these specimens was 0.045 in./in. (mm/mm). At this strain level, from Fig. 2.1 it can be determined that $E_{t\text{ scr}} = 450$ ksi (3102.75 MPa) and $f_{\text{scr}} = 88$ ksi (606.8 MPa). The spacing of the lateral reinforcement necessary to prevent buckling can now be computed from Euler's formula:

$$S = \frac{\pi D_b}{4k} \sqrt{\frac{E_{t\text{ scr}}}{f_{\text{scr}}}} \quad 4.1$$

where

S = spacing of lateral reinforcement

D_b = diameter of longitudinal reinforcement

$E_{t\text{ scr}}$ = tangent modulus of elasticity in the strain-hardening range

f_{scr} = critical stress in the longitudinal reinforcement corresponding to ϵ_{cr}

and

k = effective length coefficient, the value of which depends on the support conditions offered by the lateral reinforcement.

In the case of square -cross-sections, the longitudinal bars are laterally supported by the corner of a hoop (or spiral). If the actual spacing, 1.33 inches (33.78 mm), is used in formula 4.1, the value of the effective length coefficient (k), applicable to the experimental results, is then:

$$k = \frac{\pi \cdot 0.75}{4 \cdot 1.33} \sqrt{\frac{450}{88}} = 1.0.$$

In the case of specimens with circular cross-sections, the actual pitch of the lateral spiral was 0.7 inches (17.78 mm). However, buckling of the longitudinal reinforcement in this kind of specimen occurred after the rupture of the circular spiral and, therefore, the above result is not applicable to these specimens.

The experimental results show that the strength increase due to confinement was in the order of 10% for specimens with cover whether there was longitudinal reinforcement or not. These results indicate that the longitudinal reinforcement did not contribute to an increase of the lightweight concrete strength. An explanation for this behavior follows:

Figures 4.38a and 4.38b show how the configuration of the longitudinal reinforcement leads to larger effective confined areas as well as more efficient redistribution of confining stress which could, in general, improve the strength of the confined concrete. However, the level of concrete strength of the specimens tested was high: 5.2 ksi (35.852 MPa) to 5.325 ksi (36.71 MPa). A 10% increase in strength due to lateral confinement means the aggregate particles have to sustain stresses in the range of 5.72 ksi (39.44 MPa) to 5.858 ksi (40.39 MPa). At this level of stress, it is likely that the lightweight aggregate particles experienced localized crushing and the longitudinal reinforcement could not create any further increase in strength.

4.3.4. Effect of Type of Lateral Reinforcement

In a laterally confined structural member, confining forces are developed discretely at every level of the lateral reinforcement. Although these forces vary in between levels, the overall effect is to impose a triaxial stress condition on the concrete.

The consequence of this effective triaxial state of stress is to significantly increase both the concrete's compressive strength and its capacity to develop large inelastic deformations by: (a) arresting the formation and the opening of microcracks; and (b) increasing friction in between microcracked surfaces.

As the longitudinal stress increases on a specimen, the lateral pressure offered by the lateral steel increases. Then, depending upon the strength and amount of the concrete cover, the specimen may or may not attain maximum capacity with the cover still intact. Once the specimen reaches its maximum resistance, the cover spalls off and a drop in capacity is observed, the magnitude of which is also dependent upon the cover properties. Beyond this stage, the behavior of the confined concrete depends on the state of the lateral confining pressure and the state of stress of the lightweight aggregate particles.

In the case when lateral confinement is provided by circular spirals, the lateral confining pressure (f_r) is directly determined by the amount (ρ'_s) and the mechanical properties of the lateral reinforcement (f_s''), i.e., $f_r = f(\rho'_s, f_s'')$. This is because in this case only tension stresses can be developed and, therefore, confinement can be considered uniform along the spiral (Fig. 4.39a).

If confinement is provided by square hoops or square spirals, the lateral confining pressure is less effective and varies along the length of the hoop (Fig. 4.39b). In this case, the concrete in the vicinity of the corner regions is effectively restrained by the lateral reinforcement. However, in regions away from the hoop corners, the deformation of the concrete in the lateral directions is subjected to a much lower flexural-type confinement because the lateral restraint is provided by the bending resistance of the hoop or square spiral (Fig. 4.39b).

Figure 4.40 exhibits the experimental results obtained for concrete confined with the three types of lateral reinforcement tested in this study. For the level of concrete strength used, the average results indicate that the three types of specimens responded similarly up to attaining maximum stress. However, the descending branch of the $f_c - \epsilon_c$ curve presented marked differences due to the different effectiveness of the confinement in the three cases.

Figures 4.41a, 4.41b, and 4.41c show the free-body diagrams used for determination of the confinement pressure. From Fig. 4.41a, it will be seen that, in the case of a square-cross section, the chosen free-body diagram will give the maximum f_r .

$$4A_{st} f_s'' = f_r h_c S$$

$$f_r = \frac{4A_{st} f_s''}{h_c S} \quad 4.2$$

Also, the volumetric ratio of the lateral reinforcement is:

$$\rho'_s = \frac{(4h_c + 2\sqrt{2}h_c) A_{st}}{h_c^2 S}$$

or

$$\rho'_s = \frac{2(2 + \sqrt{2}) A_{st}}{h_c S} \quad 4.3$$

Therefore, f_r can be expressed as

$$f_r = \frac{2\rho'_s f''_s}{2 + \sqrt{2}} \quad 4.4$$

where

A_{st} = area of one leg of lateral reinforcement

h_c = lateral dimension of the core

f_r = lateral confinement pressure

S = spacing of the lateral reinforcement

f''_s = stress in the lateral reinforcement

and

ρ'_s = volumetric ratio of the lateral reinforcement.

From the free body diagram in Fig. 4.41b, it can be seen that a different f_r is obtained for the same type of section, that is,

$$2A_{st} f''_s + \frac{2\sqrt{2}}{2} A_{st} f''_s = f_r h_c S \quad 4.5$$

$$f_r = \frac{A_{st} f''_s (2 + \sqrt{2})}{h_c S} \quad 4.6$$

Expressing equation 4.6 in terms of the volumetric ratio of the lateral reinforcement (Equation 4.3):

$$f_r = \frac{\rho'_s f_s'' (2 + \sqrt{2})}{2 (2 + \sqrt{2})}$$

$$f_r = \frac{\rho'_s f_s''}{2} \quad 4.7$$

For the amount of lateral reinforcement provided for the specimens with square spirals ($\rho'_s = 0.0144$) and using $f_s'' = f_y'' = 67.5$ ksi. (465.41 MPa), the values of f_r obtained are:

From Equation 4.4:

$$f_r = \frac{2 \cdot 0.0144 \cdot 67.5}{2 + \sqrt{2}} = 0.569 \text{ ksi (3.923 MPa):}$$

From Equation 4.7:

$$f_r = \frac{0.0144 \cdot 67.5}{2} = 0.486 \text{ ksi (3.351 MPa).}$$

Comparison of these two values indicates that f_r depends on the assumed free-body diagram. This proves that, for the case of square cross-section specimens, a uniform lateral confinement pressure across the whole section does not exist, as it varies depending on the section where the free-body diagram is chosen.

In the case of a circular cross-section, uniform confinement pressure exists across the whole section. From the free-body diagram in Fig. 4.41d, it is seen that:

$$2A_{st} f_s'' = f_r D_c S$$

$$f_r = \frac{2A_{st} f_s''}{D_c S} \quad 4.8$$

Where D_c = diameter of concrete core (out-to-out of spiral), the volumetric ratio is

$$\rho'_s = \frac{4A_{st}}{D_c S}, \quad 4.9$$

therefore,

$$f_r = \frac{\rho'_s f''_s}{2}. \quad 4.10$$

If

$$\rho'_s = 0.0144,$$

and

$$f''_s = f''_y = 67.5 \text{ ksi (465.41 MPa)},$$

then

$$f_r = \frac{0.0144 \cdot 67.5}{2} = 0.486 \text{ ksi (3.351 MPa)}.$$

Comparison of results from Equations 4.10 and 4.7 indicates that the lateral confining pressure is the same for square and circular cross-sections when the free-body diagram shown in Fig. 4.41b is chosen for the square cross section specimens.

The minimum value of f_r that can be obtained for a square cross section corresponds to the free body diagram shown in Fig. 4.41c. For this free body, by summing forces in either a vertical or a horizontal direction, Equation 4.11 is obtained

$$A_{st} f''_s + \frac{2\sqrt{2}}{2} A_{st} f''_s = \frac{\sqrt{2}}{2} f_r \sqrt{2} h_c S \quad 4.11$$

$$f_r = \frac{(1 + \sqrt{2}) A_{st} f''_s}{h_c S}.$$

Expressing 4.11 in terms of ρ'_s

$$f_r = \frac{(1 + \sqrt{2}) \rho'_s f_s''}{2(2 + \sqrt{2})}$$

If

$$\rho'_s = 0.0144$$

and

$$f_s'' = f_y'' = 67.5 \text{ ksi (465.41 MPa),}$$

then

$$f_r = \frac{(1 + \sqrt{2}) 0.0144 \cdot 67.5}{2(2 + \sqrt{2})} = 0.343 \text{ ksi (2.365 MPa)}$$

Comparison of results obtained from Equation 4.11 (square cross section) and 4.12 (circular cross section) indicates that, for the same amount of lateral reinforcement (ρ'_s), the square spirals are about 70% as effective as the circular spirals.

4.3.5. Effect of Buckling Delay and Strain Hardening of Longitudinal Steel on the Load-Strain Relationship of Confined Lightweight Concrete

Of special practical significance is the consideration of load vs. strain capacity of structural members closely confined by lateral reinforcement. Figure 4.42 depicts the total experimental load for the circular test specimen. For the value of f_r used (0.486 ksi, 3.351 MPa), the concrete curve experienced a smooth descending branch. However, if the lateral reinforcement is closely spaced, and total contact between lateral and longitudinal reinforcement is ensured at every hoop or spiral level, lateral displacement and buckling of the longitudinal bars can be delayed considerably. Then, because of strain hardening of the steel, the specimen is able to clearly define two peak load values at very different strains. The first peak load attained was 614 kips (2731.01 KN) and the strain in the concrete was 0.0041 while the second peak load was 610 kips (2713.22 MPa), but the longitudinal strain in the concrete was 0.042--more than a tenfold increase in deformation. It is evident that, if higher values of f_r are used, this behavior will be considerably improved. The practical significance of this is discussed in greater detail in Chapter IX.

5. COMPARISON BETWEEN BEHAVIOR OF CONFINED LIGHTWEIGHT AND NORMAL WEIGHT CONCRETE

5.1 Introductory Remarks

In this chapter, the experimental results of the present investigation are compared with those of a similar experimental program carried out at the University of California, Berkeley, by Vallenias, Bertero, and Popov [6] in order to determine the mechanical characteristics of confined normal weight concrete.

The experimental program for normal weight concrete consisted of testing specimens with and without concrete cover as well as with and without longitudinal reinforcement. The normal weight specimens contained the same amount of both lateral and longitudinal reinforcement as the specimens in the present investigation. However, specimens with only one type of lateral reinforcement (square hoops) were tested. Therefore, in this section the results reported in reference [6] will be compared with the results from similar lightweight concrete specimens confined with square hoops. Figures 5.1 to 5.3 depict the behavior of the two types of concrete.

5.2. Comparison of Strength of Normal and Lightweight Confined Concrete

The principal experimental results from this investigation and from reference [6] are summarized in Table 5.1. Normal weight concrete specimens without longitudinal reinforcement experienced an increase in strength with respect to the 6 in. x 12 in. cylinder tests of 13% and 15% for specimens without and with cover, respectively.

In the case of longitudinally reinforced specimens, the normal weight concrete experienced a further increase in strength with respect to the 6 in. x 12 in. cylinder tests of about 6% and 8% (which can be attributed to the longitudinal reinforcement). Thus, the total strength increase was 19% and 23% for specimens without and with cover, respectively. The lightweight concrete in similar specimens experienced increases in strength of 2% and 10.8%.

The discussion above indicates that, when the same type of longitudinal steel configuration is used for both normal and lightweight concrete, an increase in strength due to longitudinal reinforcement can be expected in normal weight concrete. Because of the higher resistance of strength of normal weight aggregate, as compared with lightweight aggregate, the strength of normal weight concrete can increase with the additional confinement pressure offered by the basketing due to longitudinal reinforcement.

Preceding page blank

5.3 Comparison of Deformation of Normal and Lightweight Confined Concrete

Table 5.1 displays the differences in strain values at maximum stress obtained for normal and lightweight concretes. The absolute values of strain at maximum stress vary from 0.0085 in./in. (mm/mm) to 0.01 in./in. (mm/mm) for normal weight concrete and from 0.0040 in./in. (mm/mm) to 0.0045 in./in. (mm/mm) for lightweight concrete.

The increase in strain at maximum stress for a confined specimen (ϵ_0^C) with respect to the same strain in the 6 in. x 12 in. cylinder (ϵ_0) varies between 193% to 280% for normal weight concrete and only 23% to 58% for the lightweight concrete, indicating a tremendous difference in the strain under which maximum strength is attained. Another way to see this difference in deformation at maximum strength is by forming ratios of ϵ_0^C for normal weight to ϵ_0^C for lightweight. Table 5.1 shows that these ratios vary from 2.00 to 2.63, indicating that the normal weight concrete can experience at least twice as much deformation at maximum stress than the lightweight concrete.

6. CONFINEMENT EFFECTIVENESS OF LIGHTWEIGHT CONCRETE

6.1. Analysis and Assumptions of Code Values

In the design of compression members, that is, when

$$P_e > 0.4P_b \quad 6.1$$

where P_e = maximum design axial load and P_b = balanced failure axial load capacity. The ACI Code [10] provisions for seismic design (Appendix A, ACI 10-3) stipulate that, where a spiral is used, the volumetric ratio, ρ'_s , shall not be less than

$$\rho'_s = 0.45 \frac{f'_c}{f''_y} \left(\frac{A_g}{A_c} - 1 \right) \quad 6.2$$

nor less than

$$\rho'_s = 0.12 \frac{f'_c}{f''_y} \quad 6.3$$

where

ρ'_s = ratio of volume of spiral to total volume of the core
(out-to-out of spiral)

A_g = gross area of the section

A_c = area of core measured to outside diameter of spiral

f'_c = specified compressive strength of concrete

and

f''_y = specified yield strength of transverse steel.

Equation 6.2 is based on the following assumptions:

- (a) The lateral reinforcement becomes effective only after the cover spalls off.
- (b) The contribution of the lateral reinforcement to the strength of a concentrically loaded member is equal to or slightly greater than the capacity that is lost when the cover spalls off.
- (c) The additional amount of strength provided by the spirals is about 4.1 times the lateral confining pressure times the core area.

Using assumptions (a), (b), and (c), Equation 6.2 is derived as follows:

$$A_g - A_c = \text{area loss}$$

$$(A_g - A_c) \phi f'_c = \text{strength loss}$$

and

$$K_o f_r A_c = \text{strength gain.}$$

Assuming strength loss equals strength gain, then:

$$(A_g - A_c) \phi f'_c = K_o f_r A_c$$

or

$$K_o f_r = \phi f'_c \left(\frac{A_g}{A_c} - 1 \right). \quad 6.4$$

But, from Figure 4.41d, Equation 4.8 is obtained:

$$f_r = \frac{2A_{st} f'_s}{D_c S};$$

also,

$$\rho'_s = \frac{\text{Volume of confining steel}}{\text{Volume of confined concrete}}$$

$$\rho'_s = \frac{A_{st} 2\pi \frac{D_c}{2}}{\frac{\pi D_c^2 S}{4}} = \frac{4A_{st}}{D_c S}$$

(these terms have already been defined in Chapter 4). Therefore, expressing f_r in terms of ρ'_s , Equation 4.10 is obtained:

$$f_r = \rho'_s \frac{f''_s}{2}$$

Substituting 4.10 into 6.4 and given $K_o = 4.1$ and $\phi = 0.85$,

$$4.1 \rho'_s \frac{f''_s}{2} = 0.85 f'_c \left(\frac{A_g}{A_c} - 1 \right)$$

$$\rho'_s = \frac{1.7}{4.1} \left(\frac{A_g}{A_c} - 1 \right) \frac{f'_c}{f''_s}$$

$$\rho'_s = 0.415 \left(\frac{A_g}{A_c} - 1 \right) \frac{f'_c}{f''_s} \quad 6.5$$

which is equal to the ACI equation if 0.415 is rounded off to 0.45 and $f''_s = f''_y$. (Therefore, $K_{o_{\text{actual}}} = 3.77$ if $\phi = 0.85$). The second criteria of the ACI Code (Equation 6.3) is:

$$\rho'_s = 0.12 \frac{f'_c}{f_y}$$

It gives a minimum lateral confining pressure required in the design of large sections. Equating 6.2 and 6.3

$$0.45 \left(\frac{A_g}{A_c} - 1 \right) \frac{f'_c}{f''_y} = 0.12 \frac{f'_c}{f_y}$$

It is seen that, for values $A_g/A_c \leq 1.267$, Equation 6.3 will control the design.

In the design of square (or rectangular) sections, the ACI Code considers that the effective confining pressure of a section confined by square hoops is 50% that of a circular section which contains the same amount of lateral reinforcement. Therefore, in order to provide for equal effectiveness of confinement between the two sections:

$$f_{r_{\text{circular}}} = 0.5 \left(f_{r_{\text{rectangular}}} \right) \quad 6.6$$

For a square cross section and from the free-body diagram in Figure 4.41a

$$f_{r_{\text{square}}} = \frac{4A_{st} f_s''}{h_c S}$$

also, from Fig. 4.41d

$$f_{r_{\text{circular}}} = \frac{2A_{st} f_s''}{D_c S}$$

From Equation 6.6:

$$\frac{2A_{st} f_s''}{D_c S} = 0.5 \left(\frac{4A_{st} f_s''}{h_c S} \right) \quad 6.7$$

and from Equation 4.9:

$$\rho_s' = \frac{4A_{st}}{D_c S}$$

$$D_c = \frac{4A_{st}}{\rho_s' S} \quad 6.8$$

Putting Equation 6.8 into 6.7, one obtains:

$$A_{st} = \frac{h_c \rho_s' S}{4} \quad 6.9$$

which is equal to ACI Equation A-4 if $\ell_h = h_c/2$.

The implied confinement effectiveness coefficient can be calculated as follows: From general Equation 6.4:

$$K_o f_r = 0.85 f'_c \left(\frac{A_g}{A_c} - 1 \right);$$

and, since

$$f_{r_square} = \frac{4A_{st} f_s''}{h_c S},$$

by putting Equation 4.2 into 6.4

$$K_o \frac{4A_{st} f_s''}{h_c S} = 0.85 f'_c \left(\frac{A_g}{A_c} - 1 \right)$$

one obtains

$$A_{st} = \frac{0.85}{4K_o} h_c S \frac{f'_c}{f_s''} \left(\frac{A_g}{A_c} - 1 \right). \quad 6.10$$

Equating 6.10 and 6.9 (ACI A-4):

$$\frac{0.85}{4K_o} h_c S \frac{f'_c}{f_s''} \left(\frac{A_g}{A_c} - 1 \right) = \frac{h_c 0.45 \left(\frac{A_g}{A_c} - 1 \right) \frac{f'_c}{f_s''} S}{4}$$

and yields

$$K_{o_square} = 1.88$$

which is the confinement effectiveness coefficient implied by the ACI Code.

The UBC requirements (11) for lateral reinforcement are given by UBC Formula 26.5:

$$A_{sh} \geq .3 S_h h_c \frac{f'_c}{f_{yh}} \left(\frac{A_g}{A_{ch}} - 1 \right) \quad 6.11$$

or

$$A_{sh} \geq 0.12 S_h h_c \frac{f'_c}{f_{yh}} \quad 6.12$$

where

A_{ch} = area of rectangular core of column measured out to out of hoop, square inches

A_{sh} = total cross sectional area of rectangular hoop

S_h = center-to-center spacing of hoops, inches

and

f_{yh} = specified yield strength of hoop reinforcement, psi.

Equating 6.10 and 6.11 and considering that, in this case, $4A_{st} = A_{sh}''$

$$\frac{4(0.85)}{4K_o} h_c S \frac{f'_c}{f_s''} \left(\frac{A_g}{A_c} - 1 \right) = .3 S_h h_c \frac{f'_c}{f_{yh}} \left(\frac{A_g}{A_{ch}} - 1 \right).$$

In these formulas, if $S = S_h$, $f_s'' = f_{yh}$, and $A_{ch} = A_c$, then $K_o = 2.83$. Comparing this value ($K_o = 2.83$) with the one given by the ACI, ($K_o = 1.88$) indicates that, for the rectangular cross section under consideration in this study, the UBC requires two-thirds the amount of reinforcement of the ACI Code. Equation 6.12 will control the minimum lateral reinforcement requirements for values of $A_g/A_c \leq 1.4$.

The variations in lateral confining pressure demand, as a function of confinement effectiveness K_o (Equation 6.4), have been plotted in Fig. 6.1 for different values of A_g/A_c . The required lateral confining pressure for circular and rectangular cross sections according to both ACI and UBC codes are also shown.

From Fig. 6.1, it should also be noted that, for low values of A_g/A_c , the variation in K_o is not very important since the absolute variation in f_r with K_o is small. However, as the A_g/A_c ratio is increased, and the values of K_o decrease, the demand for lateral pressure increases rapidly. For example, for $A_g/A_c = 1.25$, the required $f_r/0.85 f'_c$ is 0.0625 when $K_o = 4$ and is 0.125 when $K_o = 2$ (a difference of 0.0625). However, if $A_g/A_c = 2.5$ (a 100% increase), the difference between f_r at $K_o = 4$ and $K_o = 2$ becomes 0.375 (a 500% increase in demand).

6.2 Confinement Effectiveness Coefficients Obtained Experimentally

6.2.1 General

For the purpose of consistency with the previous section, the values of the confinement effectiveness coefficient, K_o , were calculated using the free-body diagram (as shown in Fig. 4.41a) for the square cross section specimens. Figure 4.41d shows how K_o was calculated for the circular cross-section specimens. Therefore,

$$f_r = \frac{4A_{st} f_s''}{h_c S} \quad (\text{square cross section})$$

$$f_r = \frac{2A_{st} f_s''}{D_c S} \quad (\text{circular cross section})$$

In this study, values of f_r were calculated, assuming yielding of lateral reinforcement ($f_s'' = f_s''^y$). This assumption may lead to conservative values of K_o in cases when f_s'' was actually less than $f_s''^y$. Experimentally, it was observed that in some cases the lateral reinforcement did not yield at maximum stress, whereas, in other cases yielding strains of this reinforcement were recorded. The basic equation to determine K_o from experimental data is:

$$f_{c_{\max}}^c = f_c^U + K_o f_r \quad 6.13$$

$$K_o = \frac{f_{c_{\max}}^c - f_c^U}{f_r} \quad 6.14$$

where

K_o = confinement effectiveness coefficient

$f_{c_{\max}}^c$ = maximum compression strength of confined concrete

f_c^U = compressive strength of unconfined control specimen

and

f_r = lateral confining pressure

by substituting in Equations 4.2 and 4.6 for

$$A_{st} = 0.025 \text{ in.}^2$$

$$f_s'' = f_y'' = 67.5 \text{ ksi}$$

$$f_r = \frac{4 \cdot 0.025 \cdot 67.5}{9 \cdot 1.33} = 0.564 \text{ ksi (for circular sections)}$$

and

$$f_r = \frac{2 \cdot 0.025 \cdot 67.5}{10 \cdot 0.7} = 0.482 \text{ ksi (for circular sections).}$$

Similarly, the confinement effectiveness coefficient at failure (K_f), can be determined from:

$$K_f = \frac{f_f - f_c^U}{f_r} \quad 6.15$$

where f_f is defined in the following manner:

- (a) In specimens without longitudinal reinforcement when the stress in the concrete has dropped by 50% or at the concrete stress level when the lateral reinforcement has ruptured leading to rapid deterioration of strength.
- (b) In specimens with longitudinal reinforcement at the concrete stress level when buckling of the longitudinal reinforcement occurs or, at rupture of the lateral reinforcement, whichever occurs first.

Values of K_o and K_f have been summarized in Table 6.1 along with concrete strain values corresponding to the stresses mentioned.

6.2.2 Experimental K_o for Concrete Confined by Square Spirals

Specimens Without Longitudinal Reinforcement. As can be observed from Table 6.1, the K_o values attained for specimens without cover (1AA-1 and 1AA-2) were 1.67 and 1.72. For the specimens with cover (1BA-1 and 1BA-2), the K_o values were 2.59 and 2.23. The discrepancy in the K_o values in each group is minimal. The K_o values for specimens with cover are on the average about 40% larger than the K_o values of specimens without cover.

Specimens with Longitudinal Reinforcement. Only the K_o values for the specimens with cover are presented. When the specimens without cover were tested without restraining steel plates at both ends of the specimen, the longitudinal reinforcement buckled at the upper 6 inches (152.4 mm) of the specimen before the specimen attained its maximum capacity. Therefore, the K_o values for these specimens are not realistic. For the specimens with cover (1BB-1 and 1BB-2), K_o values were 1.52 and 2.50. This relatively large discrepancy in K_o values is because failure took place in the middle and lower instrumented regions of specimen 1BB-2 while, in specimen 1BB-1, failure occurred in the upper instrumented region. Since the strength of the specimen is governed by its weakest section and, since the upper regions of the specimens are often the weakest, due to a larger amount of bleeding and segregation that can occur at the time of casting, it is correct to assume that the discrepancy found in K_o values is due to a reduced carrying capacity as a consequence of lower strength at the upper region of the specimen.

6.2.3 Experimental K_o for Concrete Confined by Circular Spirals

Specimens without Longitudinal Reinforcement. Circular specimens without cover (2AA-1 and 2AA-2) attained identical coefficients of $K_o = 2.36$ while, in specimens with cover (2BA-1 and 2BA-2), the K_o values were 1.9 and 1.56, respectively. This situation is different from the one observed for specimens with square spirals or square hoops where it was observed that the specimens with cover had higher K_o values. This can be explained by considering that the concrete cover in specimens with circular spirals can spall more easily than in the square cross-section specimens because of the closer spacing of the lateral reinforcement (0.7 in. [17.78 mm] versus 1.33 in. [33.78 mm]) and, therefore, more discontinuity exists between the concrete cover and the inside core.

Therefore, the cover in the specimens described above was less effective in resisting loads. This was confirmed experimentally when the cover spalled abruptly along the whole length of the specimen just as it reached peak load. The resulting deterioration of the concrete core caused significant reduction in the effective cross-sectional area of the specimen.

Since this reduction in effective cross sectional area was ignored, computations indicate a lower increase in compressive strength. One way to consider this effect in an approximate fashion would be to assume that the effective cross-sectional area of the specimen would be the area enclosed by the inside-to-inside spiral rather than outside-to-outside as was assumed in the original computations. In this case, the cross-sectional area would be 73.0 inches² (47097 mm²) versus the original area of 78.53 inches² (50.664 mm²). K_o values would be 2.78 and 2.4 (versus original values of 1.96 and 1.56). These new K_o values are higher than those obtained for specimens without cover.

Specimens with Longitudinal Reinforcement. These specimens attained similar values of K_o (2.47 and 2.36). The maximum difference between them was 4.6%.

6.2.4 Experimental K_o for Concrete Confined by Square Hoops

Specimens without Longitudinal Reinforcement. Values of K_o for these specimens are, in general, pretty uniform. However, a distinction can be made between specimens without cover (3AA-1 and 3AA-2) and those with cover (3BA-1 and 3BA-2). Values of K_o found for specimens without cover average 2.07, whereas the specimens with cover averaged 2.26. The difference encountered in these values can be attributed to shrinkage effects.

Specimens with Longitudinal Reinforcement. These specimens have the same trend as those without longitudinal reinforcement. K_o values are higher for specimens with cover. Specimens without cover (3AB-1 and 3AB-2) attained an average K_o of 1.65; the specimens with cover (3BB-1 and 3BB-2) averaged $K_o = 2.62$. This difference may be due to the fact that the specimens without cover are more severely affected by early shrinkage of concrete. Because of

Poisson's effect, when the specimen is loaded in the longitudinal direction, large lateral strains need to be developed in the concrete before the lateral and longitudinal reinforcement acting as confinement elements become effective. This delaying in confinement permits the specimen to respond, as in an unconfined condition, with development of extensive microcracking. Therefore, the specimen without cover will not experience as much an increase in strength as the one with cover.

7. ANALYTICAL RELATIONSHIP

7.1 General

In order for an analytical expression to closely approximate the experimental results, it should account for the following factors:

- (a) Increase in the concrete's compressive strength due to lateral confinement, in the order of 10% with respect to standard 6 x 12 in. cylinder strength for longitudinally reinforced specimens with cover.
- (b) Increase in the values of strain at maximum stress, in the order of 50% with respect to similar strain in 6 x 12 in. cylinders.
- (c) The varying behavior of the descending branch of the stress-strain curve due to different confinement arrangements (square spirals, circular spirals, square hoops).

Emphasis will be placed on trying to determine an analytical expression for confined, longitudinally reinforced concrete, as this is the type of reinforced concrete that is used in practice.

7.2 Analytical Expressions

A maximum stress ratio defined as $K = f_c^C \text{ max} / f_c'$, can be introduced to account for the increase in maximum stress due to confinement.

The parameter, K , is assumed to be dependent on the spacing, S , amount, ρ_s' , and grade, f_y'' , of the lateral reinforcement, as well as the specimen's cross section core dimension (h_c or D_c) and the strength of the concrete.

From the general relationship:

$$\frac{f_c^C \text{ max}}{f_c'} = 1 + K_0 \frac{f_r}{f_c'} \quad 7.1$$

Sargin [12] postulated that:

$$K = \frac{f_c \text{ max}}{f_c'} = 1 + C_1 (1 + C_2 R^\alpha)^\beta \rho_s' \frac{f_y''}{(f_c')^\gamma} \quad 7.2$$

where:

$C_1, C_2, \alpha, \beta, \gamma$ = constants evaluated for best fit of experimental data

Preceding page blank

and

$$R = \frac{S}{h_c} \text{ or } \frac{S}{D_c} \text{ depending on type of cross section.}$$

In this study a modified version of Sargin's formulation is proposed; this accounts for the difference in the strength increase for normal and lightweight concrete. Then for square cross sections:

$$K = 1 + 0.0073 \left(1 - 0.245 \frac{S}{h_c}\right) \rho'_s \frac{f''_y}{f'_c} \quad 7.3$$

where

- K = maximum stress ratio
- S = spacing (in.)
- h_c = square cross section core dimension (in.)
- ρ'_s = volumetric ratio of the lateral reinforcement
- f''_y = yield stress of lateral reinforcement, psi
- f'_c = 6 x 12 in. cylinder strength, psi

The effect of the lateral reinforcement in increasing the strain values at maximum stress (ϵ_0^C) is accounted for as follows:

$$\frac{\epsilon_0^C}{\epsilon_0} = 1 + 0.039 \left(1 - 0.734 \frac{S}{h_c}\right) \frac{\rho'_s f''_y}{f''_c} \quad 7.4$$

where

- ϵ_0^C = strain at maximum stress for confined specimen
- ϵ_0 = strain at maximum stress for 6 x 12 in. cylinder

The corresponding equations for the case of circular confinement are:

$$K = 1 + 0.0073 \left(1 + 0.245 \frac{S}{D_c}\right) \frac{\rho'_s f''_y}{f'_c} \quad 7.5$$

$$\frac{\epsilon_0^c}{\epsilon_0} = 1 + 0.039 \left(1 + 0.734 \frac{S}{D_c}\right) \frac{\rho_s' f_y''}{f_c'} \quad 7.6$$

Once parameters K and $\epsilon_0^c / \epsilon_0$ have been defined, an analytical stress-strain relationship for lightweight concrete can be considered. The analytical expression will contain 3 regions:

(a) Region AB $\epsilon_c \leq \epsilon_0^c$

In this region, the mathematical model should satisfy the following conditions:

$$\frac{f_c}{f_c'} = 0 @ \epsilon_c = 0 \quad (\text{curve passes through origin})$$

$$\frac{f_c}{f_c'} = K @ \epsilon_c = \epsilon_0^c \quad (K \text{ and } \epsilon_0^c \text{ are peak coordinates in non-dimensional curve})$$

$$\frac{\partial \left(\frac{f_c}{f_c'} \right)}{\partial \epsilon_c} = \frac{E_c}{f_c'} @ \epsilon_c = 0 \quad (\text{the slope of the curve equals the modulus of elasticity})$$

$$\frac{\partial \left(\frac{f_c}{f_c'} \right)}{\partial \epsilon_c} = 0 @ \epsilon_c = \epsilon_0^c \quad (\text{curve has maximum } \epsilon_c = \epsilon_0^c)$$

The analytical model should be non-dimensional, with the power of the independent variable as low as possible to obtain a smooth variation along the ascending branch of the curve [12]. The mathematical model should be of the form:

$$\frac{f_c}{f_c'} = \frac{A + BX + CX^2}{1 + DX}$$

Application of the above conditions yields:

$$\frac{f_c}{f'_c} = \frac{\frac{E_c \epsilon_0^c}{f'_c} \left(\frac{\epsilon_c}{\epsilon_0^c} \right) - K \left(\frac{\epsilon_c}{\epsilon_0^c} \right)^2}{1 + \left[\frac{E_c \epsilon_0^c}{K f'_c} - 2 \right] \left(\frac{\epsilon_c}{\epsilon_0^c} \right)} \quad 7.7$$

where

f_c = stress in confined concrete

f'_c = strength of 6 x 12 in. cylinder

E_c = modulus of elasticity; taken as $34,000 \sqrt{f'_c}$

K = maximum stress ratio (Equations 7.3 or 7.5)

ϵ_0^c = strain at maximum stress in confined specimen (Equations 7.4 or 7.6)

(b) Region BC $\epsilon_0^c \leq \epsilon_c \leq \epsilon_0 \cdot 2K$ or $\epsilon_0^c \leq \epsilon_c \leq \epsilon_{cr}$

The descending branch of the stress-strain analytical curve is linear and its slope is a function of the: (1) volumetric ratio of the lateral reinforcement; (2) concrete strength; (3) dimensions of the cross section; and (4) spacing and arrangement of lateral reinforcement. In this region, an expression similar to Kent and Park's [13] is used:

$$\frac{f_c}{f'_c} = K \left[1 - Z (\epsilon_c - \epsilon_0^c) \right] \quad 7.8$$

$$Z = \frac{0.5}{A_{p_s}' \sqrt{R} + \left(\frac{3 + 0.003 f'_c}{f'_c - 1000} \right) - 0.003} \quad 7.9$$

where:

K = maximum stress ratio (equation 7.3 or 7.5)

ϵ_0^c = strain at maximum stress for confined specimen

ρ'_s = lateral steel volumetric ratio

R = ratio of core dimension to spacing of the lateral reinforcement

$$R = \frac{h_c}{S} \quad \text{or} \quad \frac{D_c}{S}$$

S = pitch of lateral reinforcement

A = constant which depends on the type of lateral reinforcement; it reflects the effect of lateral reinforcement in improving the descending branch of the stress-strain curve, i.e.,

$$A = 3/4 \text{ for square hoops}$$

$$A = 8/9 \text{ for square or circular spirals}$$

Because the proposed relationship is for confined concrete containing longitudinal reinforcement, Region BC should be limited by either:

(1) the concrete strain at which the stress has dropped to 0.2K ($\epsilon_{0.2K}$)
or

(2) the critical strain at which buckling of the longitudinal reinforcement can occur (ϵ_{cr}). A way to develop the desired critical strain in design is explained in Section 9.1

If $\epsilon_{cr} < \epsilon_{0.2K}$, a rapid rate of increase in the slope of the curve in this region will begin at ϵ_{cr} . The curve may then be conservatively assumed to have infinite slope at this point. Caution needs to be exercised to assure that premature buckling would not occur due to inadequate ductility of the hoops or spirals.

$$(c) \text{ Region CD } \quad \epsilon_c \geq \epsilon_{0.2K} \quad \text{or} \quad \epsilon_c \geq \epsilon_{cr}$$

$$\frac{f_c}{f'_c} = 0.2K \quad 7.10$$

This equation takes into account the ability of the concrete to sustain some stress at very large strains.

The experimental and analytical curves are depicted in Figs. 7.1 to 7.3. These figures show a good agreement between the experimental results and the proposed analytical relationships.



8. CONCLUSIONS

8.1 General

In the present study, only one type of lightweight aggregate was used; the strength of the concrete varied from $f'_c = 5100$ psi (35.16 MPa) to $f'_c = 5350$ psi (36.89 MPa). Therefore, these conclusions apply only to this type of aggregate and level of concrete strength. It is widely accepted that the properties of lightweight aggregate vary depending on the type of raw material, as well as on the manufacturing process. Therefore, it is necessary to do similar studies using different types of aggregate and different levels of concrete strengths in order to be able to draw more general conclusions.

This section summarizes the conclusions drawn from the tests performed on unconfined and confined specimens fabricated with lightweight aggregate concrete. The parameters varied were:

- (a) the concrete cover
- (b) the longitudinal reinforcement
- (c) the different arrangements of the lateral reinforcement

Special emphasis is placed on the results obtained from specimens containing concrete cover and longitudinal reinforcement because this is the way that concrete is most frequently used in structural applications.

8.2 Experimental Study

(a) In general, the specimens with cover attained higher values of K_0 than those without cover. The improvement with respect to the specimens without cover was in some instances as great as 50%.

(b) For specimens confined by circular spirals, the average $K_0 = 2.45$, which is 59.7% of the value assumed for this type of confinement in current codes ($K_0 = 4.1$).

(c) For concrete confined by square hoops or square spirals, the average K_0 was 2.09, which is about 85% of the K_0 found for circular spiral confinement. The difference between the experimentally obtained values of K_0 for the circular and square cross sections is not very significant. This is because, for the values of A_g/A_c corresponding to the specimens tested in this study (1.23 for circular cross-section and 1.21 for square cross-section specimens), the demand for f_r does not vary much as a function of K_0 , especially in the range of $K_0 = 2$ to $K_0 = 4$. Therefore, the confinement effectiveness coefficients are not expected to vary significantly. This is confirmed experimentally.

(d) Based on the arrangement and amount of longitudinal reinforcement used for the specimens tested in this study, it is found that the longitudinal

Preceding page blank

steel does not contribute to an increase in the strength of the confined lightweight aggregate concrete. The ratios $f_{c \max}^c / f_c'$ are, in general, similar for specimens with and without longitudinal reinforcement. (Tables 4.2 to 4.4).

(e) The longitudinal reinforcement considerably improves the descending branch of the stress-strain curve up to the critical buckling strain of the longitudinal reinforcement.

(f) The lateral reinforcement, through its confinement pressure, increases the compressive strength of the specimens with respect to the 6 x 12 in. standard cylinder strength by an average of 10% in specimens with cover (average of three groups of specimens, i.e., square and circular spirals, and square hoops) and an average of 6% for specimens without cover.

(g) The arrangement (type) of lateral reinforcement considerably influences the descending branch of the stress-strain curve. The worst behavior corresponded to specimens with rectangular ties; the best behavior corresponded to circular specimens with circular spirals (Fig. 4.40).

(h) Due to the effect of the size of the specimen, the compressive strength of the unconfined control specimens was consistently lower than the strength obtained from 6 x 12 in. standard cylinder results. The average f_c^u / f_c' ratio for all the groups of specimens was 0.86.

(i) The ACI code formulae for the modulus of elasticity overestimates the values of the secant modulus of elasticity of the concrete (at 45% of maximum stress) by as much as 13% in some cases.

8.3 Analytical Curve

Based on the experimental results, an analytical relationship is proposed for the specimens with cover and with longitudinal reinforcement. The complete $f_c - \epsilon_c$ relationship comprises three regions, as follows:

(a) Region AB $\epsilon_c \leq \epsilon_c^0$

$$\frac{f_c}{f_c'} = \frac{\frac{E_c \epsilon_c^0}{f_c'} \left(\frac{\epsilon_c}{\epsilon_c^0} \right) - K \left(\frac{\epsilon_c}{\epsilon_c^0} \right)^2}{1 + \left[\frac{E_c \epsilon_c^0}{k f_c'} - 2 \right] \left(\frac{\epsilon_c}{\epsilon_c^0} \right)}$$

(b) Region BC

$$\epsilon_0^C \leq \epsilon_c \leq \epsilon_{0.2K} \quad \text{or}$$

$$\epsilon_0^C \leq \epsilon_c \leq \epsilon_{cr}$$

$$\frac{f_c}{f'_c} = K [1 - Z (\epsilon_c - \epsilon_0^C)] \quad 7.8$$

$$Z = \frac{0.5}{A\rho'_s \sqrt{R} + \left(\frac{3 + 0.003 f'_c}{f'_c - 1000} \right) - 0.003} \quad 7.9$$

(c) Region CD $\epsilon_c \geq \epsilon_{0.2K}$ or $\epsilon_c \geq \epsilon_{cr}$

$$\frac{f_c}{f'_c} = 0.2K$$

The analytical relationship presented here is a good approximation of the experimental results as can be observed from Figs. 7.1 to 7.3.

9. IMPLICATIONS IN PRACTICAL DESIGN

9.1 Introductory Remarks

In earthquake-resistant design, it is highly desirable that the structure and, therefore, each of its structural members possess large energy-absorption and energy-dissipation capacities. To achieve such large energy capacities, it is not only necessary that the structural materials be capable of developing high strength but that this strength remain stable under large inelastic deformations. The need for a large deformation capacity, usually referred to loosely as "ductility," cannot be overemphasized.

To achieve such large energy capacities in concrete structures, it is necessary to use confined, reinforced concrete. For this type of concrete, the energy-absorption and energy-dissipation capacities are greatly affected by the following two parameters:

(a) The lateral confining pressure (f_r), that is, the state of triaxial stress created on the confined concrete by the lateral confining steel forces. This triaxial stress condition improves the compressive strength of the concrete as well as its resistance against shear and bond failure. It also significantly increases the concrete's deformation capacity.

(b) The critical buckling strain (ϵ_{cr}) that the longitudinal reinforcement is able to develop before buckling. It is possible that by close spacing of the lateral reinforcement, buckling of the longitudinal reinforcement can be delayed until the steel is in strain-hardening range and, therefore, can offer a larger resistance. This increase in steel resistance compensates somewhat for the decrease in concrete strength that occurs at these large strains. Therefore, the axial load strength of a structural member can be maintained or increased (depending on ρ'_s and the rate and maximum value of the strain hardening) at very large deformations.

The objective of this chapter is to discuss the implications of the experimental results and the effects of the two parameters described above on the practical design of structural members. Requirements are presented for delaying the buckling of the longitudinal reinforcement until it reaches the strain-hardening range. As previously discussed, this permits the structural member to develop large inelastic deformation (ductility).

Next, Axial Load-Moment (P-M) interaction diagrams for a circular and square cross-section are computed using:

(a) A fictitious $f_c - \epsilon_c$ relationship for the concrete, implied when assuming the equivalent stress-block distribution.

(b) A more realistic idealization of the $f_c - \epsilon_c$ relationship for unconfined concrete as proposed by Hognestad.

(c) An elasto-perfectly plastic relationship for the longitudinal steel.

P-M interaction diagrams for the same sections are computed considering strain hardening of the longitudinal steel, and using the $f_c - \epsilon_c$ relationships found experimentally for concrete. These diagrams are compared with diagrams computed based on: the material properties for concrete described in (a) above and the material properties for steel described in (c).

Preceding page blank

The volumetric ratio of the lateral reinforcement of specimens tested in this investigation was approximately the same as that required by current codes [10,11]. Results were also available for a previous experimental program [3] carried out at Berkeley on specimens of a similar size but containing about twice the volumetric ratio of lateral reinforcement required by current codes. This spectrum of available stress-strain relationships for confined concrete provoked an interest in comparing the Axial Load - Moment (P-M) interaction diagrams. This comparison was made by comparing the interaction diagrams computed by using the confined concrete relationship as obtained in the two experimental programs described above with those obtained by assuming a concrete relationship derived by assuming the equivalent stress block distribution.

9.2 Buckling of the Longitudinal Reinforcement

The critical buckling strain (ϵ_{cr}) that the longitudinal reinforcement is able to develop before buckling depends upon the spacing of the lateral reinforcement. The corresponding buckling stress can be found by the usual formulae:

$$f_{scr} = \left(\frac{\pi D_b}{4kS} \right)^2 E_{t scr} \quad 9.1$$

where

f_{scr} = critical buckling stress of longitudinal reinforcement

D_b = diameter of longitudinal bar

S = spacing of the lateral reinforcement

k = factor depending on end conditions

$E_{t scr}$ = tangent modulus of elasticity in the strain hardening region of the longitudinal reinforced steel and corresponding to ϵ_{cr} .

This equation cannot be applied in design without knowledge of the $E_{t scr}$ and the critical f_{scr} which corresponds to ϵ_{cr} .

This knowledge can be achieved by an idealization of the strain hardening region of the reinforcing steel $f_s - \epsilon_s$ relationship. A good idealization can be obtained using a cubic polynomial:

$$f_s = ax^3 + bx^2 + E_{sh}x + f_y \quad 9.2$$

where

$$x = \epsilon_s - \epsilon_{sh}$$

$$a = \frac{E_{sh}}{r^2} - \frac{2(f_{su} - f_y)}{r^3}; \quad r = \epsilon_{su} - \epsilon_{sh}$$

$$b = \frac{3[(f_{su} - f_y) - 2/3 E_{sh} r]}{r^2}$$

For grade 60 steel, the following values are taken:

$\epsilon_{sh} = 0.01$ (steel strain at onset of strain hardening)

$\epsilon_{su} = 0.2$ (steel strain at ultimate stress)

$E_{sh} = E_s/30 = 1000$ ksi (tangent modulus of steel at the onset of strain hardening)

$f_y = 60$ ksi

$f_{su} = 100$ ksi (ultimate stress of steel).

The tangent modulus, $E_{t \text{ scr}}$, can now be found by differentiation of Equation 9.2:

$$E_{t \text{ scr}} = \frac{df_s}{dx} = 3ax^2 + 2bx + E_{sh} \quad 9.3$$

Values of f_s and $E_{t \text{ scr}}$, given by Equations 9.2 and 9.3, have been calculated for the range of strains corresponding to the concrete $f_c - \epsilon_c$ relationships presented. These values are shown in Table 9.1.

TABLE 9.1 CRITICAL f_s and $E_{t \text{ scr}}$

ϵ_s	f_s (ksi)	$E_{t \text{ scr}}$ (ksi)
0.01	60	1000
0.02	69.29	860.77
0.03	77.24	731.16
0.04	83.95	611.17
0.045	86.86	554.78
0.05	89.50	500.80
0.06	94.00	400.00

Equation 9.1 can now be written in form useful for design (assuming $k = 1$):

$$\frac{S}{D_b} = \frac{\pi}{4} \sqrt{\frac{E_t \text{ scr}}{f_s}} \quad 9.4$$

In this way, with the values of Table 9.1 a value of spacing, S , can be selected in order to develop the desired critical steel strain. As a check of the accuracy of this equation, in section 4.3.3 it was found that the average critical buckling strain was 0.045 in./in. (mm/mm). By applying the corresponding values of f_s and $E_t \text{ scr}$, as given in Table 9.1, it is seen from equation 9-4 that:

$$S = 0.75 \frac{\pi}{4} \sqrt{\frac{554.78}{86.86}} = 1.48 \text{ in.}$$

which is 11% higher than the actually provided spacing (1.33 in.).

9.3 Axial Load-Moment (P-M) Interaction Diagrams

Two types of reinforced concrete columns were chosen to analyze the effects of confinement on the flexural behavior of structural members:

- (a) a square 30 in. x 30 in. (762 mm x 762 mm) cross section column; and,
- (b) a circular 33 in. (838.2 mm) in diameter column. (see Figs 9.1a and 9.1b respectively.)

Both sections contained eight #18 reinforcing bars. The hoops in the square section had a 4 in. (101.6 mm) spacing whereas the spiral's pitch in the circular section was 2.1 in. (53.34 mm). The volumetric ratio of the lateral reinforcement, as well as the ratio A_g/A_c , were similar on both columns.

The analysis of the P-M diagrams for the section of these columns was performed by using a computer program [14]. The computer program allows modeling of progressive spalling of the concrete cover as this reaches its maximum resistance at a given strain. Also, different $f_c - \epsilon_c$ relationships for concrete core and cover may be used.

Figures 9.2a and 9.2b show the $f_c - \epsilon_c$ relationships for the confined concrete in the core of the column section, which were used in the analysis of the square and circular cross sections respectively. Figure 9.3a shows the $f_c - \epsilon_c$ relationship that was used for the unconfined concrete in the cover of both types of sections. The reinforcing steel $f_s - \epsilon_s$ relationship used is shown in Fig. 9.3b. The strain hardening portion of this relationship was idealized as a cubic polynomial.

The same sections of the columns were analyzed using a fictitious $f_c - \epsilon_c$ relationship for the concrete which is implied when assuming the equivalent stress-block distribution and a more realistic $f_c - \epsilon_c$ relationship which was proposed by Hognestad and widely used in practical application. The longitudinal steel was idealized as an elastic-perfectly plastic relationship. The relationships are depicted in Figs. 9.4a, 9.4b, and 9.4c

Figures 9.5 and 9.6 show the axial load-moment interaction diagrams computed, according to the above $f_c - \epsilon_c$ relationships, for a square cross-section and a circular cross-section, respectively. From these figures, it was observed that higher values of axial load and moment capacities are obtained by using the equivalent rectangular stress-block distribution than they are by using Hognestad's relationship.

In Fig. 9.7, a comparison is made of the P-M interaction curves for the square cross-section using the previously mentioned relationships. It can be observed that, at a concrete strain of $\epsilon_c = 0.0045$ (although, under pure axial load, the cover has completely spalled), the axial-load strength of the column's concrete core differs very little from that calculated using the ACI equivalent stress-block distribution over the whole cross-section. It is also clear that the P-M interactions curve--as determined by the fictitious $f_c - \epsilon_c$ --is unconservative for loads above the balanced point. When the confined concrete $f_c - \epsilon_c$ relationship which is obtained experimentally is used, it can be seen that, at very large deformations, the flexural capacity is increased. This is mainly because of the steel's strain hardening. For loads below the balanced point, if buckling is delayed, the lateral confinement will allow for increases in moment capacity from 23267 k-in. (fictitious $f_c - \epsilon_c$ curve) to 34059 k-in. (confined concrete curve) or an increase of 46% when $P = 0$. Also, due to the strain hardening of the longitudinal steel, the axial-tension capacity of the column is actually about 50% above the one predicted according to the elasto-perfectly plastic assumption of Fig. 9.4c. These considerations are important in seismic-resistant design because a column may undergo tension under a strong seismic ground motion due to overturning moment effects.

Figure 9.8 shows the same type of comparison but for a circular cross-section. In this case, the $f_c - \epsilon_c$ relationship used for the confined concrete is shown in Fig. 9.2b.

For this type of cross-section, the required amount of lateral reinforcement is given by ACI Equation 10.3:

$$\rho'_{s \text{ required}} = 0.45 \left(\frac{A_g}{A_c} - 1 \right) \frac{f'_c}{f_y} = 0.45 \left(\frac{855.3}{706.8} - 1 \right) \frac{5.2}{60} = 0.009$$

or, as specified in ACI A.6.4.2:

$$\rho'_{s \text{ provided}} = 0.12 \frac{f'_c}{f_y} = 0.12 \cdot \frac{5.2}{60} = 0.0104$$

which is larger than 0.009 and, therefore, controls the required volumetric ratio in this case. The provided volumetric ratio is

$$\rho'_{s\text{ provided}} = \frac{4A_{st}}{D_c S} = \frac{4 \cdot 0.2}{30 \cdot 2.1} = 0.013 > 0.0104$$

which is larger than $\rho'_{s\text{ required}}$ by about 25%.

For a section with the above characteristics, the following interaction curves have been plotted in Fig. 9.8:

(a) An interaction P-M curve based on the $f_c - \epsilon_c$ implied when assuming the equivalent rectangular stress-block distribution, an elastic-perfectly plastic relationship for the steel and, assuming the maximum concrete strain, $\epsilon_c = 0.003$.

(b) An interaction P-M curve for the case when the concrete cover and confined core reach a strain $\epsilon_c = 0.003$ at the maximum compressive fiber of the cross-section (i.e., $f_{c(\text{cover})} = f'_c$). From Fig. 9.8, it can be observed that, at this concrete strain, the axial load strength of the column is a maximum.

(c) An interaction P-M curve for the case when the extreme fiber of the concrete cover and confined core reached $\epsilon_c = 0.0045$ on the cross-section are assumed to have spalled of the column.

(d) An interaction P-M curve for the case when the confined concrete reached a strain of $\epsilon_c = 0.05$ which is close to the experimentally obtained buckling strain of the longitudinal reinforcement for a reinforced column where concrete is laterally confined with circular spirals.

As can be observed from a comparison of results presented in Figs. 9.7 and 9.8, the performance of the circular column section at very large strains is better than the behavior of the square cross-section column at similar strains. This is due to the more beneficial effect of circular spiral confinement on strength of the concrete at these large strains. For the ratio, A_g/A_c , used in this section, the axial load strength is maintained up to the strain when the cover begins to spall off. However, the envelope curve based on the stress block and $\epsilon_c = 0.003$ overestimates the flexural capacity of the section when strains in the confined core and concrete cover reach $\epsilon_c = 0.003$ or $\epsilon_c = 0.045$. It is only when large concrete strains have developed ($\epsilon_c = 0.05$) that the capacities based on the two different $f_c - \epsilon_c$ (equivalent stress block vs. confined concrete) are similar for loads above the balanced point and as observed for the square cross-section, the moment, as well as the tension capacity of the column as predicted by the relationship for the

confined concrete, are considerably larger than those predicted by the fictitious $f_c - \epsilon_c$ derived from the equivalent rectangular stress block and the elastic-perfectly plastic $f_s - \epsilon_s$ of Fig. 9.4c.

Figure 9.9 compares the effect of increasing the lateral confining pressure, i.e., the amount of lateral reinforcement, for normal weight and lightweight concrete on columns with circular cross-section. In this case, $f_c - \epsilon_c$ relationships for the concrete are shown in Fig. 9.10 for normal and lightweight concrete, respectively. These relationships were found experimentally from tests carried out at the University of California in trying to determine the effects of lateral reinforcement on the behavior of normal and lightweight concrete columns [3]. The confinement characteristics of these sections are shown in Fig. 9.10. As can be observed from Fig. 9.9, for an increase of about three times in the lateral reinforcement (from 0.0134 to 0.043), the increase in axial and flexural capacity is considerable. The effect on normal weight concrete is even more remarkable. In Fig. 9.11 the interaction curves based on ACI's relationship are compared with the curves obtained by considering $\rho'_s = 0.043$. It is observed that it is only at this very high level of confinement that the ACI based curves are on the conservative side.*

From the above discussion it needs to be noted:

(a) There is a tremendous difference in axial and flexural capacity exhibited by similar reinforced concrete sections, one fabricated with normal weight concrete and the other with lightweight concrete. This indicates that present ACI code minimum requirements for lateral reinforcement may not be satisfactory when lightweight concrete is used.

(b) A design philosophy based on the criteria of strength only (a fictitious $f_c - \epsilon_c$ implied by the equivalent stress block or a Hognestad's type relationship) may lead to an unconservative design. This is because spalling of the cover (especially in cases where the ratio A_g/A_c is large) signifies loss in capacity. It is only when a high volumetric ratio of lateral reinforcement is provided and large concrete strains are developed (which requires special precautions in designing and detailing the lateral reinforcement) that the original axial and flexural strength will be recovered once the cover has spalled.

*ACI relationships for concrete imply either a Hognestad's relationship or a fictitious one based on the equivalent rectangular stress-block distribution.

REFERENCES

1. Bresler, B., and Bertero, V. V., "Influence of High Strain Rate and Cyclic Loading on Behavior of Unconfined and Confined Concrete in Compression," Paper presented at the "Journadas Sudamericanas de Ingenieria Estructural," V Symposium Panamericano de Estructuras, Caracas, Venezuela, 1975.
2. Bresler, B., "Lightweight Aggregate Reinforced Concrete Columns," Special Publication No. 29, ACI Paper SP 29-7, pp. 81-130.
3. Bertero, V. V., and Bresler, B., "Effect of Amount of Lateral Confining Pressure on the Strength and Deformation Characteristics of Normal and Lightweight Concrete," In-House Report, Department of Civil Engineering, University of California, Berkeley.
4. Shah, S. P., Naaman, A. E., and Moreno, J., "Effect of Compressive Strength and Confinement on the Ductility of Lightweight Concrete," Paper presented at the ACI Convention held in Houston, Texas, November, 1978. To be published in a special ACI publication.
5. Bertero, V. V., and Vallenias, J., "Confined Concrete: Research and Development Needs," Workshop on Earthquake Resistant Concrete Building Construction, University of California, Berkeley, July 11-15, 1977.
6. Vallenias, J., Bertero, V. V., and Popov, E. P., "Concrete Confined by Rectangular Hoops and Subjected to Axial Loads," Report No. UCB/EERC-77/13, Earthquake Engineering Research Center, College of Engineering, University of California Berkeley, 1977.
7. PC-7, Lightweight Aggregate, Port Costa Products Company Brochure.
8. Bresler, B., ed., Reinforced Concrete Engineering, Vol. 1, John Wiley & Sons, Inc., 1974
9. Burdett, E. G., and Hilsdorf, H. K., "Behavior of Laterally Reinforced Concrete Columns," Journal of the Structural Division ASCE, Vol. 97,
10. Building Code Requirements for Reinforced Concrete (ACI, 318-71), American Concrete Institute, Detroit, Michigan, 1971.
11. Uniform Building Code, International Conference of Building Officials, Whittier, California, 1973.
12. Sargin M., "Stress-Strain Relationships for Concrete and the Analysis of Structural Concrete Sections," Study No. 4, University of Waterloo, Ontario, Canada, 1971.
13. Kent, D. C., and Park, R., "Flexural Members with Confined Concrete," Journal of the Structural Division, ASCE, Vol. 97 ST7 (July, 1971), pp. 1969-1990.

Preceding page blank

14. Mahin, S. A., and Bertero, V. V., "RCCOLA: A Computer Program for Reinforced Concrete Column Analysis," User's Manual, Department of Civil Engineering, University of California, Berkeley, August, 1977.

T A B L E S



TABLE 1.1 MAIN CHARACTERISTIC OF SPECIMENS

No. & Notation Parameter	WITH LONGITUDINAL REINFORCEMENT						WITHOUT LONGITUDINAL REINFORCEMENT						
	WITH COVER			WITHOUT COVER			WITH COVER			WITHOUT COVER			
	SQUARE SPIRALS	CIRCULAR SPIRALS	SQUARE HOOPS	SQUARE SPIRALS	CIRCULAR SPIRALS	SQUARE HOOPS	SQUARE SPIRALS	CIRCULAR SPIRALS	SQUARE HOOPS	SQUARE SPIRALS	CIRCULAR SPIRALS	SQUARE HOOPS	
	1BB-1 1BB-2	2BB-1 2BB-2	3BB-1 3BB-2	1AB-1 1AB-2	2AB-1 2AB-2	3AB-1 3AB-2	1BA-1 1BA-2	2BA-1 2BA-2	3BA-1 3BA-2	1AA-1 1AA-2	2AA-1 2AA-2	3AA-1 3AA-2	
SPECIMEN DIMENSIONS	Length, in.	30	30	30	30	30	30	30	30	30	30	30	
	Lateral dimension, in.	10	11	10	9	10	9	10	11	10	9	10	
	Cover, in.	0.5	0.5	0.5				0.5	0.5	0.5			
	Gross area (A_g), in. ²	96.47	91.50	96.47	77.47	75.00	77.47	100.0	95.03	100.0	81.0	78.54	81.0
Core area (A_c), in. ²	77.47	75.00	77.47	77.47	75.00	77.47	81.00	78.54	81.00	81.0	78.54	81.0	
LATERAL STEEL	Type: gage wire	#7	#7	#7	#7	#7	#7	#7	#7	#7	#7	#7	
	Diameter (d_s), in.	0.179	0.179	0.179	0.179	0.179	0.179	0.179	0.179	0.179	0.179	0.179	
	Area (A_{st}), in. ²	0.025	0.025	0.025	0.025	0.025	0.025	0.025	0.025	0.025	0.025	0.025	
	f'_y , ksi	67.5	67.5	67.5	67.5	67.5	67.5	67.5	67.5	67.5	67.5	67.5	
	Volumetric ratio ρ_s^*	0.0144	0.0144	0.0144	0.0144	0.0144	0.0144	0.0144	0.0144	0.0144	0.0144	0.0144	
	spacing (S), in.	1.33	0.7	1.33	1.33	0.7	1.33	1.33	0.7	1.33	1.33	0.7	1.33
LONGITUDINAL STEEL	N^0 and size	8#6	8#6	8#6	8#6	8#6	8#6	8#6	8#6	8#6	8#6	8#6	
	Diameter (D_b), in.	0.75	0.75	0.75	0.75	0.75	0.75	0.75	0.75	0.75	0.75	0.75	
	Total area (A_s), in. ²	3.53	3.53	3.53	3.53	3.53	3.53	3.53	3.53	3.53	3.53	3.53	
	f'_y , ksi	60	60	60	60	60	60	60	60	60	60	60	
	ρ_s	0.0353	0.0371	0.0353	0.0436	0.0449	0.0436	0.0436	0.0436	0.0436	0.0436	0.0436	

NOTATION OF SPECIMENS:
 i.e.: 3 A B - 2
 1 (first specimen)
 2 (second specimen)
 A (with longitudinal steel)
 B (without longitudinal steel)
 A (with cover)
 B (without cover)
 1 (square spiral)
 2 (circular spiral)
 3 (square hoops)

* ρ_s = Volume of confining steel / Volume of confined concrete

TABLE 2.1 SPECIFIED MIX DESIGN

MATERIAL	Weight for 1 cu. yd. (lbs.)
Cement Type I & II	564#
Water	292#
Lightweight Aggregate	674#
Natural Sand	1464#
Air Entraining Agent	10 ml
Water Reducing Agent	85 ml

TABLE 2.2 MECHANICAL CHARACTERISTICS OF REINFORCEMENT

TYPE	STRENGTH (ksi)			STRAIN			MODULUS OF ELASTICITY (ksi)	
	UPPER YIELD	LOWER YIELD	ULTIMATE	AT YIELD	AT ONSET OF STRAIN HARDENING	AT ULTIMATE STRESS	ELASTIC	AT ONSET OF STRAIN HARDENING
Longitudinal Steel	65.0	60.0	99.5	0.002	0.012	0.150	30,000	1250
Lateral Steel	67.5		70.0	0.0042		0.022	27,601	

TABLE 2.3 6" x 12" STANDARD CYLINDER COMPRESSION TEST RESULTS

	Average f'_c (ksi) (MPa)	Average ϵ_o	$E_c (0.45f'_c)$ (ksi) (MPa)
1. Mix for specimens with square spirals	5.3 (36.7)	0.0029	2554.5 (17613.3)
2. Mix for specimens with circular spirals	5.3 (36.5)	0.0030	2495.0 (17203.0)
3. Mix for specimens with square hoops	5.2 (35.9)	0.0029	2515.0 (17341.0)

TABLE 4.1 MECHANICAL CHARACTERISTICS OF UNCONFINED CONCRETE SPECIMENS

GROUP	CROSS SECTION DIMENSIONS in. x in. (mm. x mm.)	MAXIMUM ATTAINED LOADS kips (kN)	f_c^U ksi (MPa)	ϵ_o^U	$E_c(0.45f_c^U)$ ksi (MPa)	E_c (ACI) ksi (MPa)	$\frac{f_c^U}{f_c'}$	$\frac{\epsilon_o^U}{\epsilon_o}$
SQUARE SPIRALS	9 x 9 (229 x 229)	380.0 (1690.2)	4.69 (32.34)	0.0024	2453.0 (16913.4)	2744.2 (18921.1)	0.88	0.83
	10 x 10 (254 x 254)	480.0 (2135.0)	4.80 (33.10)	0.0025	2742.0 (18906.1)		0.90	0.86
CIRCULAR SPIRALS	9 (254)	376.0 (1672.4)	4.78 (32.96)	0.0026	2534.5 (17475.4)	2737.7 (18876.6)	0.90	0.87
	10 (279)	432.0 (1921.45)	4.54 (31.30)	0.0024	2728.0 (18809.6)		0.86	0.80
SQUARE HOOPS	9 x 9 (229 x 229)	336.0 (1494.49)	4.15 (28.62)	0.002	2408.6 (16607.3)	2711.8 (18697.7)	0.80	0.7
	10 x 10 (254 x 254)	442.0 (1965.97)	4.42 (30.48)	0.0025	2486.2 (17142.4)		0.84	0.88

TABLE 4.2 MECHANICAL CHARACTERISTICS OF CONFINED CONCRETE SPECIMENS (SQUARE SPIRALS)

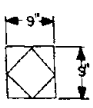
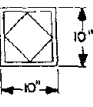
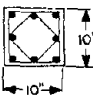
PARAMETER SPECIMEN	f_c^C max (ksi)	f_c^C max / f_c'	f_c^C max / f_c^U	ϵ_o^C	K_o	f_f (ksi)	E_f	K_f
	5.67	1.07	1.20	0.0048	1.67	2.84	0.049	-3.36
	5.70	1.07	1.20	0.0036	1.72	2.85	0.043	-3.55
	6.20	1.16	1.30	0.0045	2.59	3.10	0.042	-2.40
	6.00	1.12	1.26	0.0045	2.23	3.00	0.052	-3.00
	5.60	1.05	1.18	0.0044	1.52	4.00	0.036	-1.31
	6.15	1.15	1.30	0.0045	2.50	3.07	0.042	-2.96

TABLE 4.3 MECHANICAL CHARACTERISTICS OF CONFINED CONCRETE SPECIMENS (CIRCULAR SPIRALS)





PARAMETER SPECIMEN	$f_c^c \text{ max}$ (ksi)	$f_c^c \text{ max}/f_c'$	$f_c^c \text{ max}/f_c^U$	ϵ_0^c	K_0	f_f (ksi)	ϵ_f	K_f
	5.80	1.09	1.24	0.0041	2.36	4.10	0.024	-1.15
	5.80	1.09	1.24	0.0036	2.36	4.30	0.027	-0.75
	5.58	1.05	1.20	0.0045	1.90	3.80	0.031	-1.77
	5.41	1.02	1.16	0.0044	1.56	3.95	0.041	-1.47
	5.85	1.10	1.26	0.0050	2.47	4.50	0.028	-0.33
	5.80	1.09	1.24	0.0041	2.36	3.86	0.045	-1.66
	5.85	1.10	1.26	0.0045	2.47	2.47	0.054	-3.44

TABLE 4.4 MECHANICAL CHARACTERISTICS OF CONFINED CONCRETE SPECIMENS (SQUARE HOOPS)


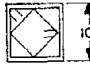


PARAMETER	$f_c^c \text{ max}$ (ksi)	$f_c^c \text{ max}/f_c'$	$f_c^c \text{ max}/f_c^U$	ϵ_0^c	K_0	f_f (ksi)	ϵ_f	K_f
	5.55	1.067	1.29	0.0042	2.23	2.78	0.048	-2.69
	5.38	1.035	1.25	0.0042	1.91	2.69	0.035	-2.85
	5.50	1.057	1.28	0.0045	2.12	2.75	0.05	-2.74
	5.70	1.10	1.36	0.0045	2.4	2.85	0.036	-2.39
	5.28	1.02	1.22	0.0038	1.7	2.44	0.045	-3.29
	5.23	1.01	1.21	0.0042	1.6	1.55	0.047	-4.87
	5.65	1.08	1.31	0.0045	2.39	2.3	0.046	-3.5
	5.91	1.136	1.37	0.0045	2.85	2.96	0.0336	-2.37

TABLE 5.1 COMPARISON BETWEEN CONFINED NORMAL AND LIGHTWEIGHT CONCRETE





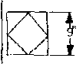

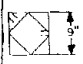
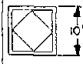

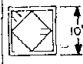

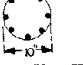




GROUP	PARAMETER SPECIMEN	Normalweight Concrete* (reference 8)			Lightweight Concrete*			$\frac{\epsilon_c^c(\text{normalweight})}{\epsilon_c^c(\text{lightweight})}$
		$\frac{f_c^c \text{ max}}{f_c^t}$	ϵ_c^c	$\frac{\epsilon_c^c}{\epsilon_c}$	$\frac{f_c^c \text{ max}}{f_c^t}$	ϵ_c^c	$\frac{\epsilon_c^c}{\epsilon_c}$	
1		1.135	0.011	3.8	1.051	0.0042	1.474	2.62
2		1.15	0.009	3.1	1.094	0.0045	1.579	2.00
3		1.19	0.0085	2.93	1.02	0.004	1.404	2.08
4		1.23	0.009	3.1	1.102	0.0045	1.579	2.00

TABLE 6.1 EXPERIMENTAL K_O AND K_F

SQUARE SPIRALS: $f_c^U = 4.74$ (ksi) $\epsilon_c^U = 0.0024$					CIRCULAR SPIRALS: $f_c^U = 4.66$ (ksi) $\epsilon_c^U = 0.0023$					SQUARE HOOPS: $f_c^U = 4.30$ (ksi) $\epsilon_c^U = 0.0023$				
PARAMETER SPECIMEN	ϵ_c^c	K_O	ϵ_f	K_F	PARAMETER SPECIMEN	ϵ_c^c	K_O	ϵ_f	K_F	PARAMETER SPECIMEN	ϵ_c^c	K_O	ϵ_f	K_F
	0.0048	1.67	0.050	-3.36		0.0041	2.36	0.024	-1.15		0.0042	2.23	0.048	-2.69
	0.0036	1.72	0.042	-3.35		0.0036	2.36	0.027	-0.75		0.042	1.91	0.035	-2.85
	0.0045	2.59	0.042	-2.90		0.0045	1.90 (2.78)*	0.031	-1.77		0.0045	2.12	0.050	-2.74
	0.0045	2.23	0.052	-3.00		0.0044	1.56 (2.40)*	0.041	-1.47		0.0045	2.40	0.036	-2.39
	**					0.0050	2.47	0.028	-0.33		0.0038	1.70	0.045	-3.20
	0.0041	2.36	0.045	-1.66		0.0042	1.60	0.047	-4.87					
	0.0044	1.52	0.036	-1.31		0.0045	2.47	0.054	-3.00		0.0045	2.39	0.046	-3.50
	0.0045	2.50	0.045	-2.96		0.0045	2.85	0.034	-2.37					

*See discussion in Section 6.2.3.

**Values not reported. See Section 6.2.2.

FIGURES

Preceding page blank

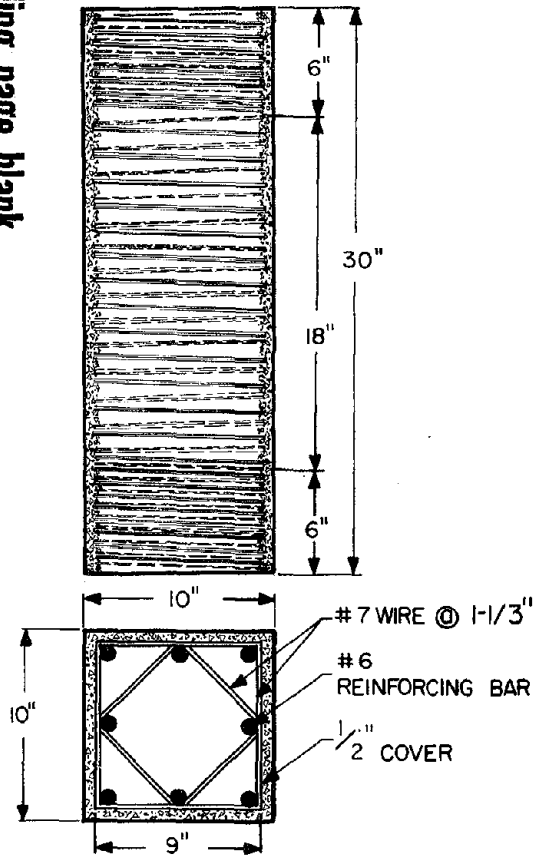


FIG. 1.1 DIMENSIONS OF LONGITUDINALLY REINFORCED SPECIMENS (SQUARE SPIRALS)

SIDE VIEW

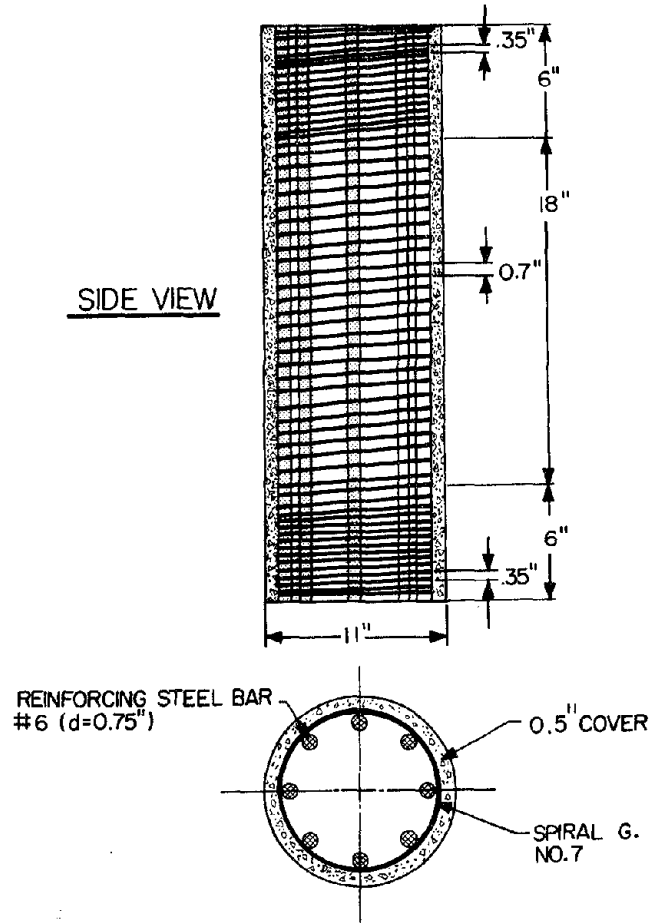


FIG. 1.2 DIMENSIONS OF LONGITUDINALLY REINFORCED SPECIMENS (CIRCULAR SPIRALS)

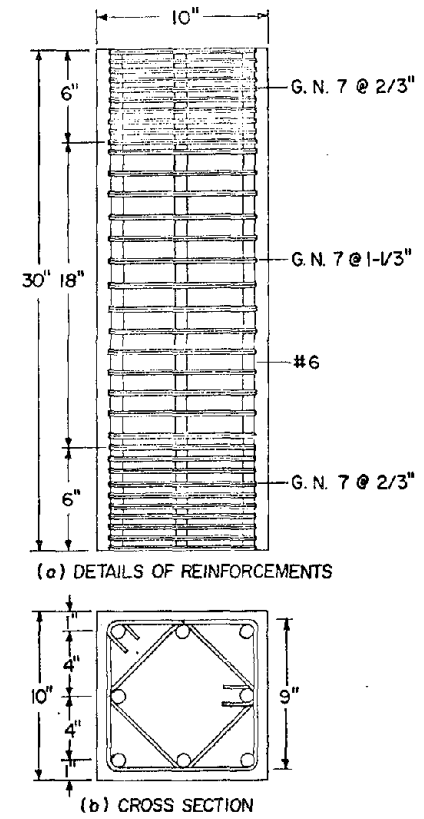


FIG. 1.3 DIMENSIONS OF LONGITUDINALLY REINFORCED SPECIMENS (SQUARE HOOPS)

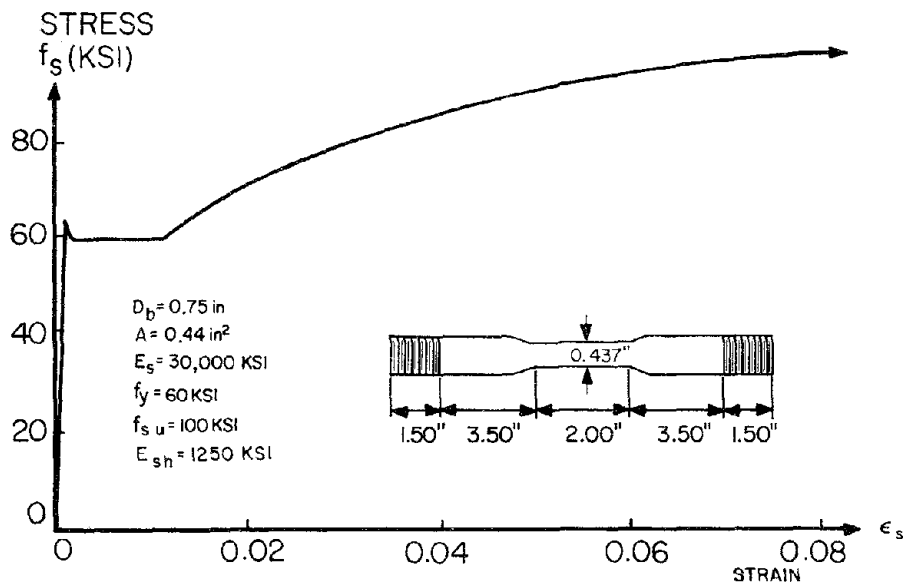


FIG. 2.1 STRESS-STRAIN RELATIONSHIP OF THE LONGITUDINAL REINFORCEMENT AND DIMENSIONS OF COUPON TESTED

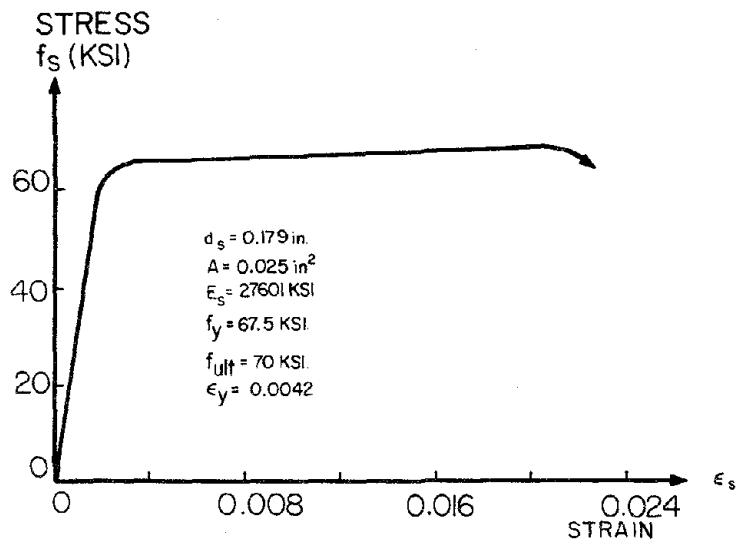


FIG. 2.2 STRESS-STRAIN RELATIONSHIP OF LATERAL REINFORCEMENT

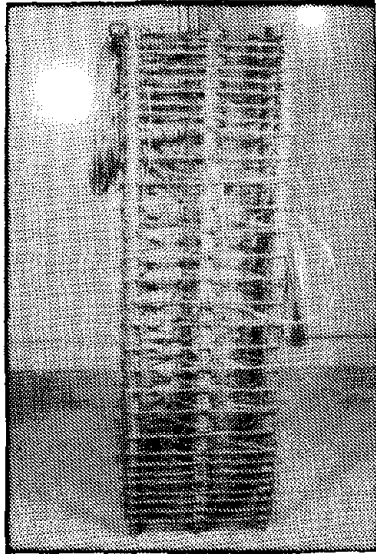


FIG. 2.3 STEEL CAGE FOR SPECIMEN WITH SQUARE HOOPS

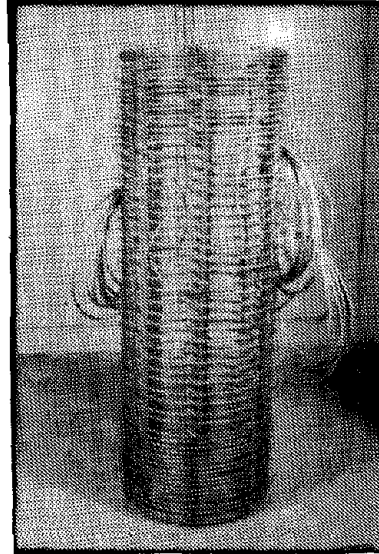


FIG. 2.4 STEEL CAGE FOR SPECIMEN WITH CIRCULAR SPIRALS



FIG. 2.5 STEEL CAGE FOR SPECIMEN WITHOUT LONGITUDINAL REINFORCEMENT

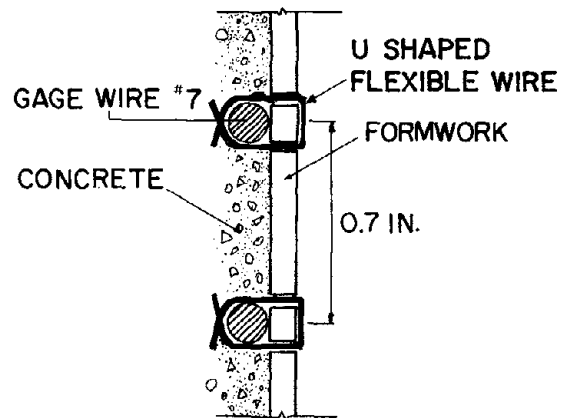


FIG. 2.6 DETAIL SHOWING HOW SPECIFIED SPACING OF THE LATERAL REINFORCEMENT WAS MAINTAINED IN CIRCULAR SPECIMENS WITHOUT COVER

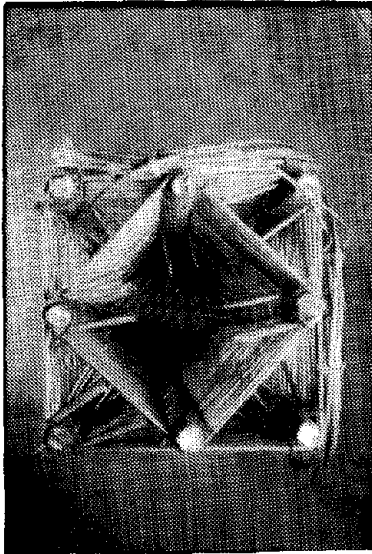


FIG. 2.7 CROSS SECTION VIEW OF
STEEL CAGE (SQUARE SPIRALS)

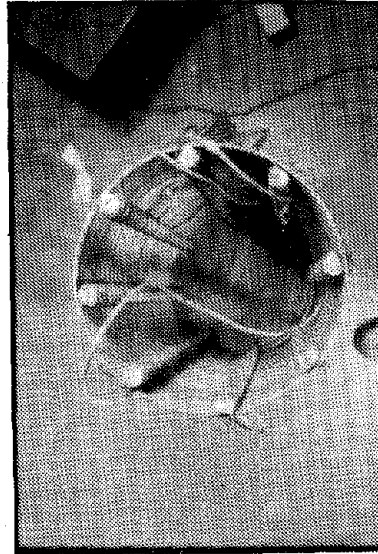


FIG. 2.8 CROSS SECTION VIEW OF
STEEL CAGE (CIRCULAR SPIRALS)

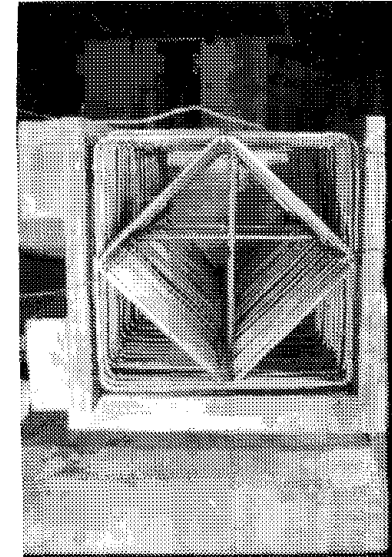


FIG. 2.9 CROSS SECTION VIEW OF
STEEL CAGE (SQUARE HOOPS)

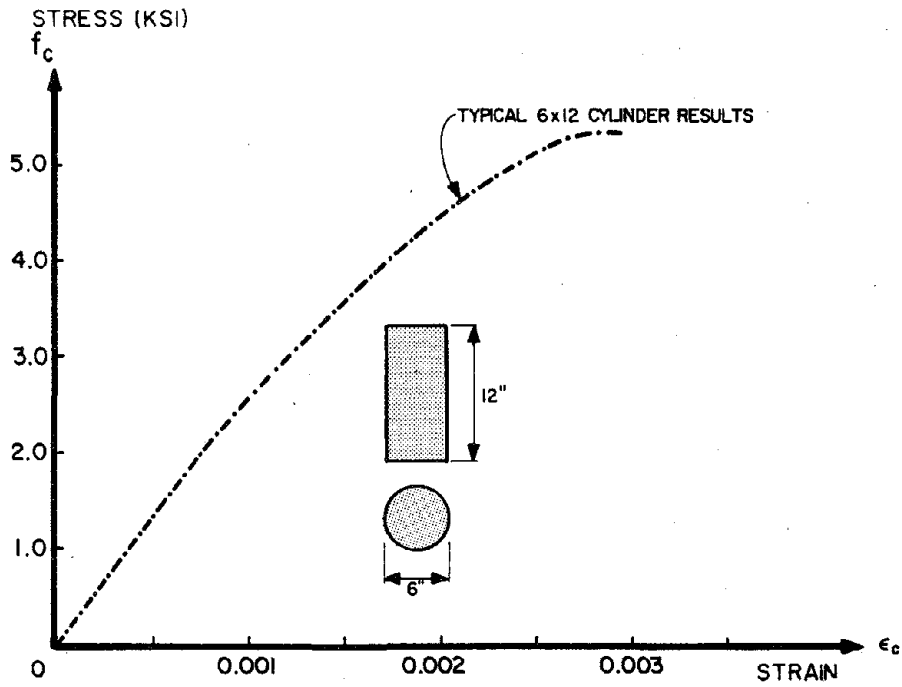


FIG. 2.10 STRESS-STRAIN RELATIONSHIP OF STANDARD 6 IN. X 12 IN. CYLINDER

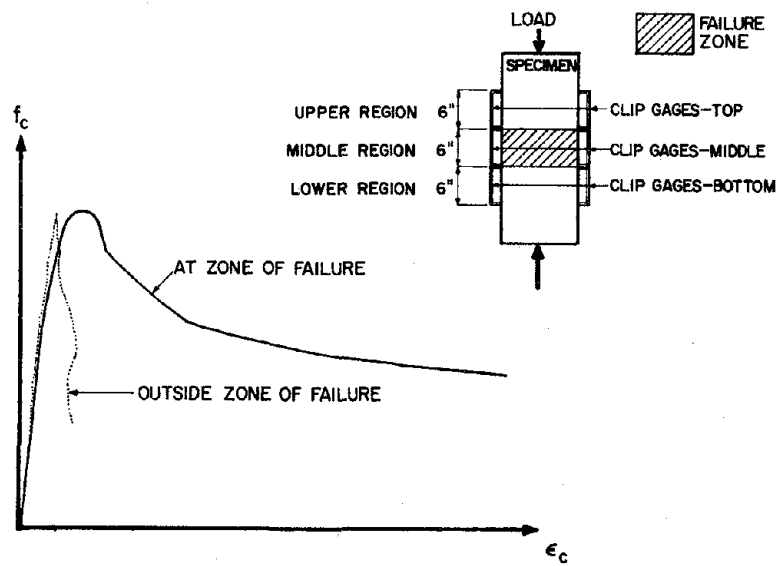


FIG. 3.1 QUALITATIVE STRESS-STRAIN RELATIONSHIPS AT AND OUTSIDE ZONE OF FAILURE

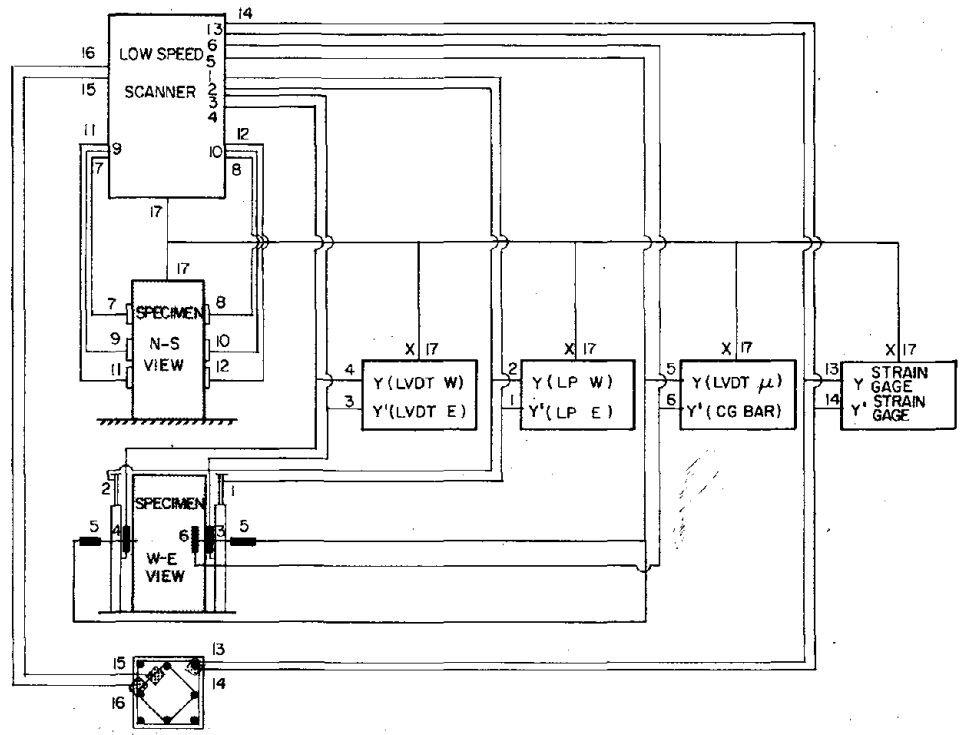


FIG. 3.2 INSTRUMENTATION AND DATA ACQUISITION SYSTEM

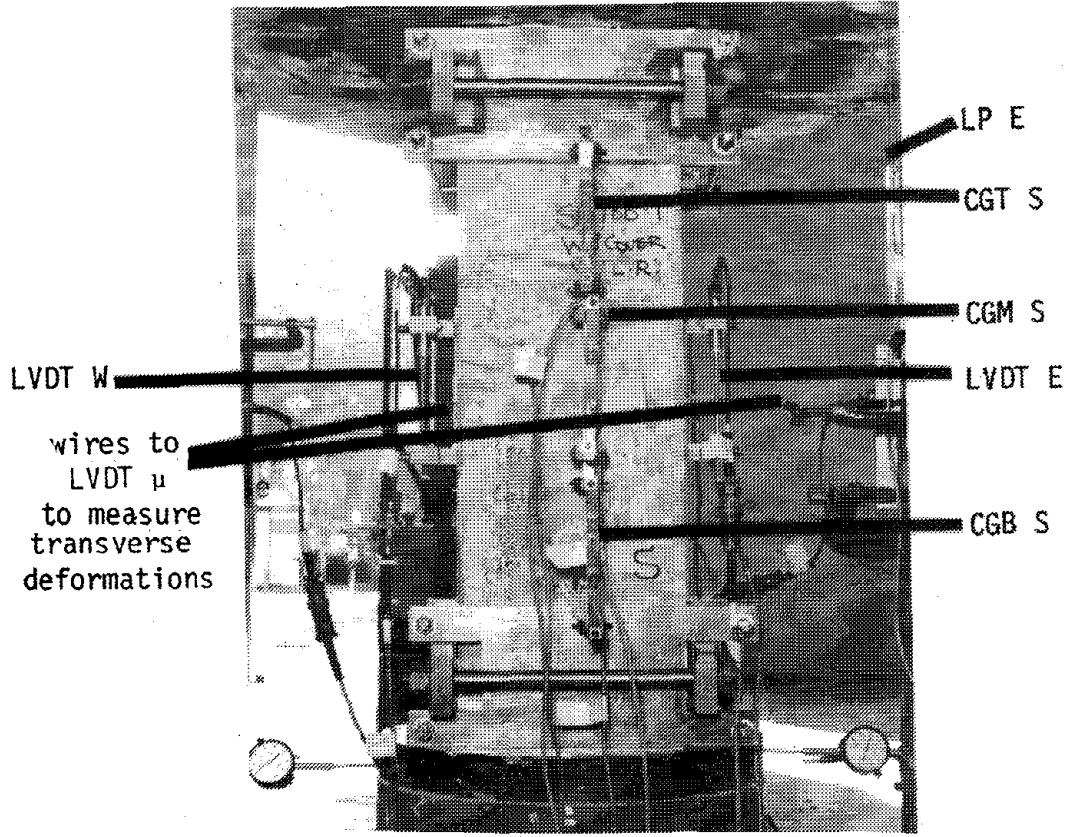


FIG. 3.3 EXTERNAL INSTRUMENTATION

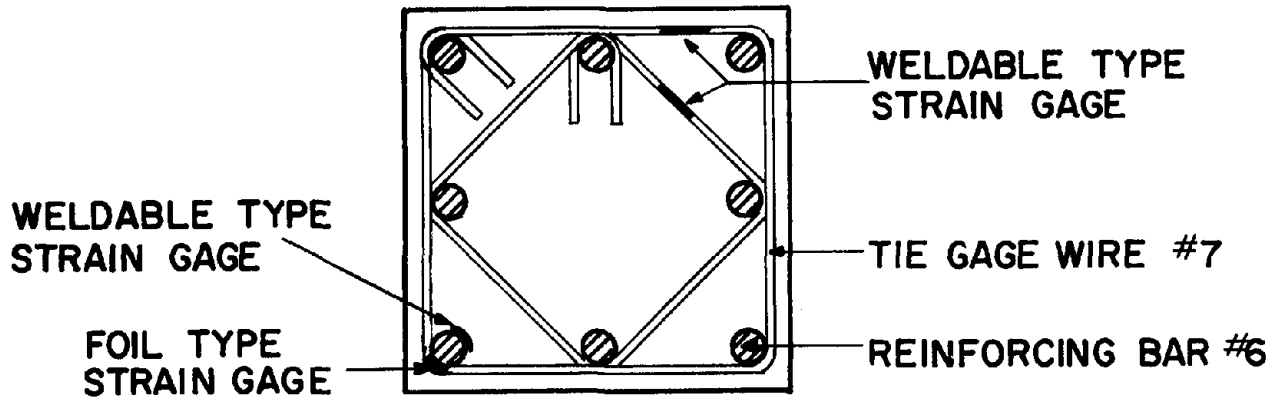


FIG. 3.4 INTERNAL INSTRUMENTATION (SQUARE CROSS SECTION)

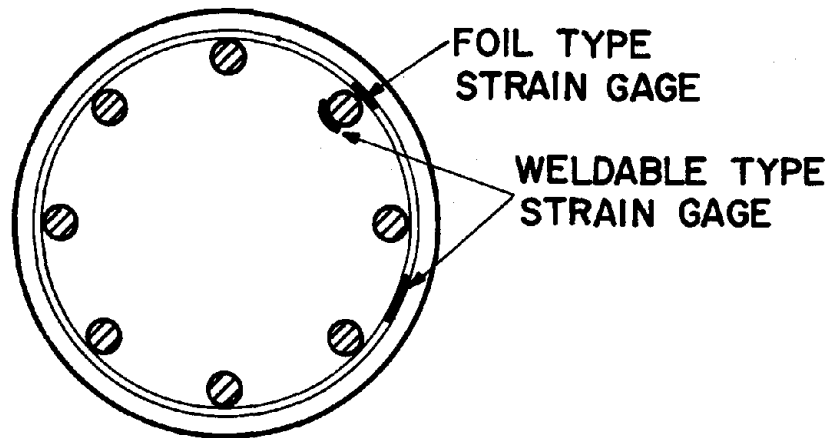


FIG. 3.5 INTERNAL INSTRUMENTATION (CIRCULAR CROSS SECTION)

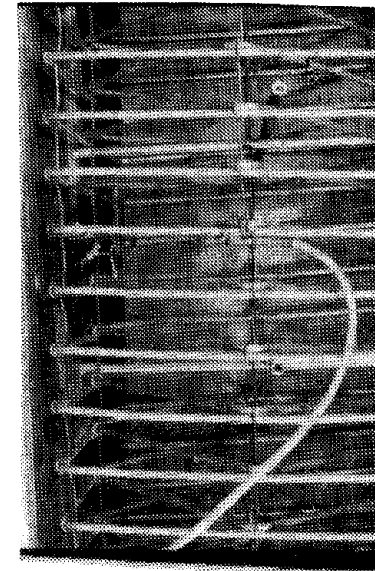


FIG. 3.6A CLOSE-UP OF SPECIMEN (SQUARE CROSS SECTION)

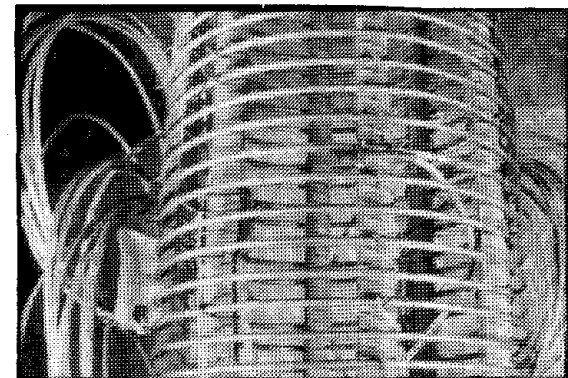


FIG. 3.6B CLOSE-UP OF SPECIMEN (CIRCULAR CROSS-SECTION)

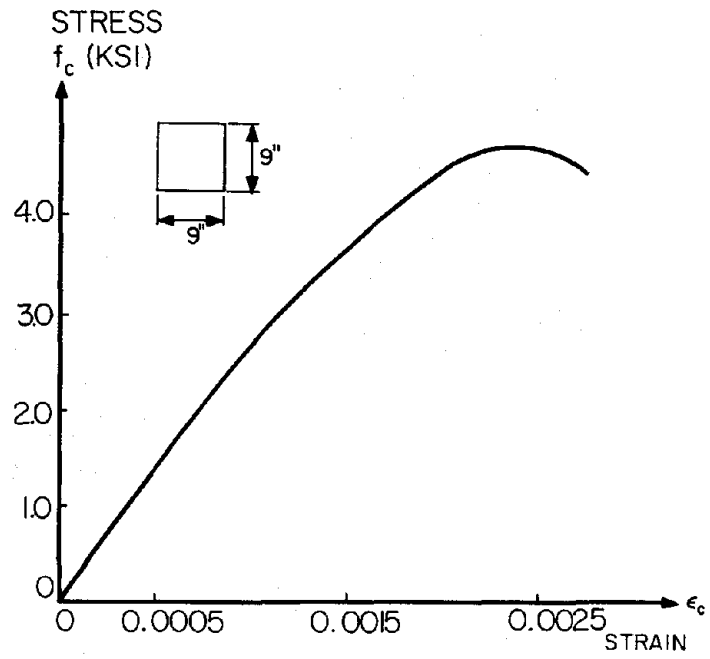


FIG. 4.1 STRESS-STRAIN RELATIONSHIP OF PLAIN CONCRETE CONTROL SPECIMEN

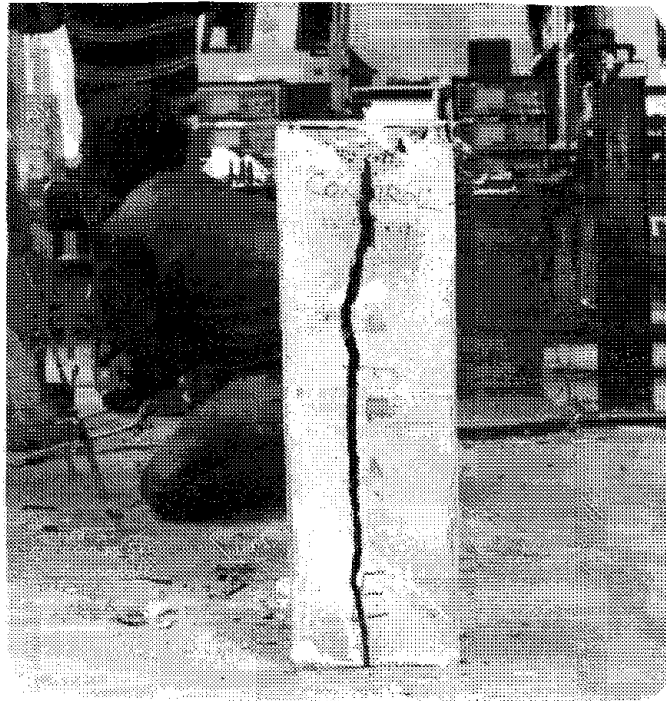


FIG. 4.2 UNCONFINED SPECIMEN AFTER TESTING



FIG. 4.3 TYPICAL FAILURE OF UNCONFINED SPECIMEN

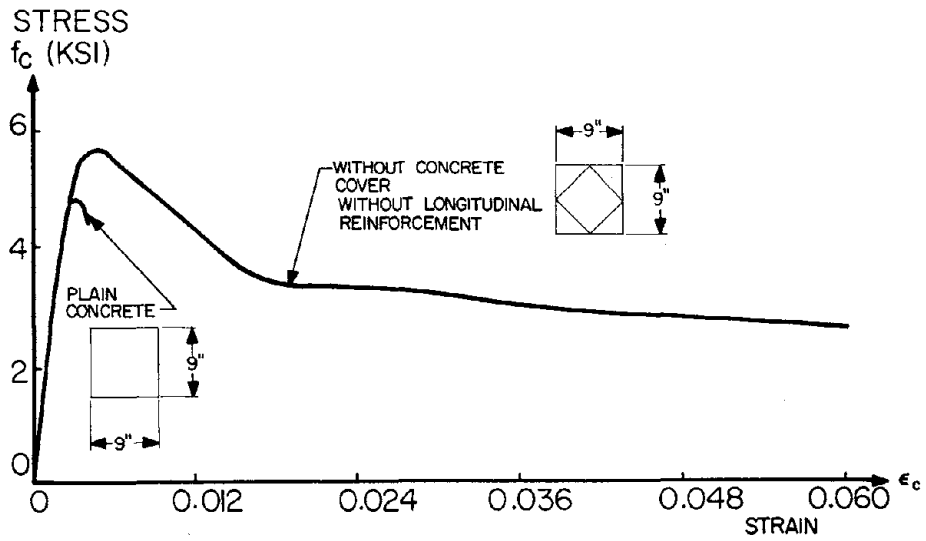


FIG. 4.4 STRESS-STRAIN RELATIONSHIP OF SPECIMEN WITHOUT COVER AND WITHOUT LONGITUDINAL REINFORCEMENT, SQUARE SPIRALS; (1AA-1)

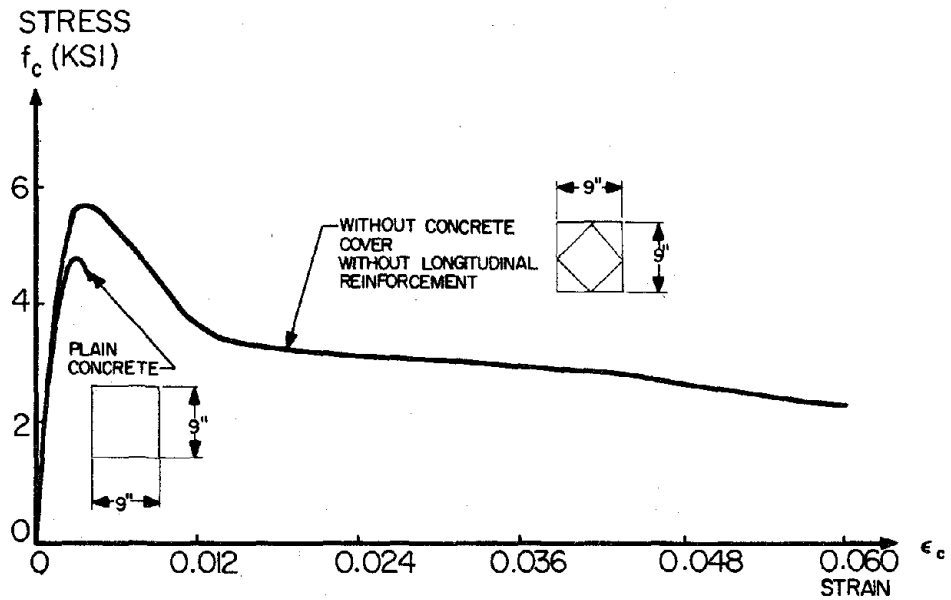


FIG. 4.5 STRESS-STRAIN RELATIONSHIP OF SPECIMEN WITHOUT COVER AND WITHOUT LONGITUDINAL REINFORCEMENT, SQUARE SPIRALS; (1AA-2)

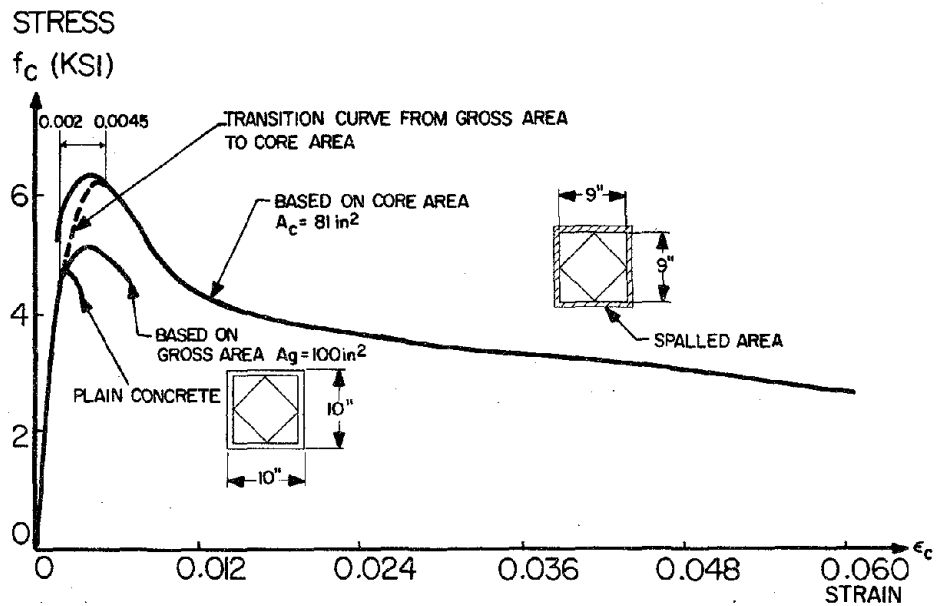


FIG. 4.6 STRESS-STRAIN RELATIONSHIP OF SPECIMEN WITH COVER AND WITHOUT LONGITUDINAL REINFORCEMENT, SQUARE SPIRALS; (1BA-1)

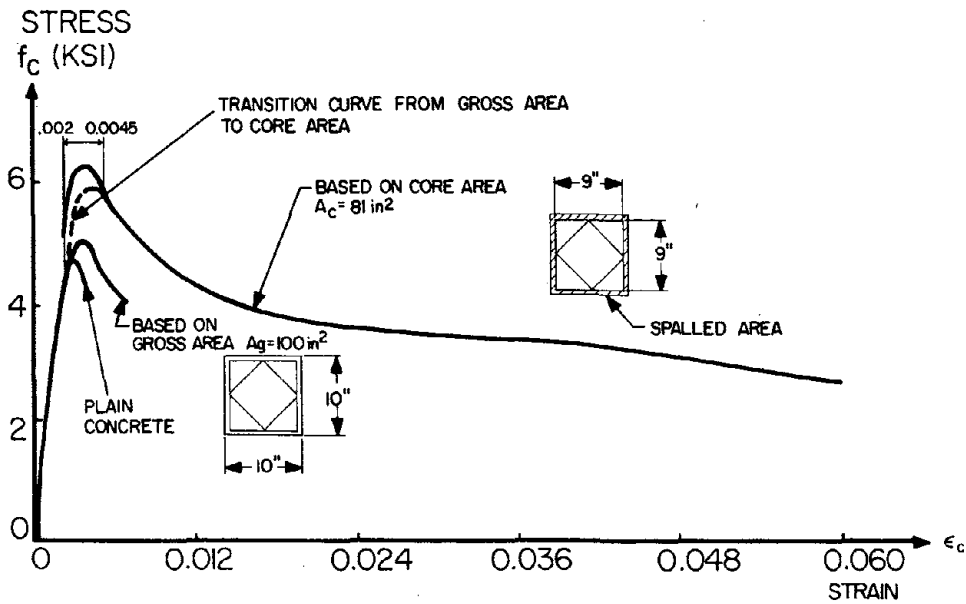


FIG. 4.7 STRESS-STRAIN RELATIONSHIP OF SPECIMEN WITH COVER AND WITHOUT LONGITUDINAL REINFORCEMENT, SQUARE SPIRALS; (1BA-2)

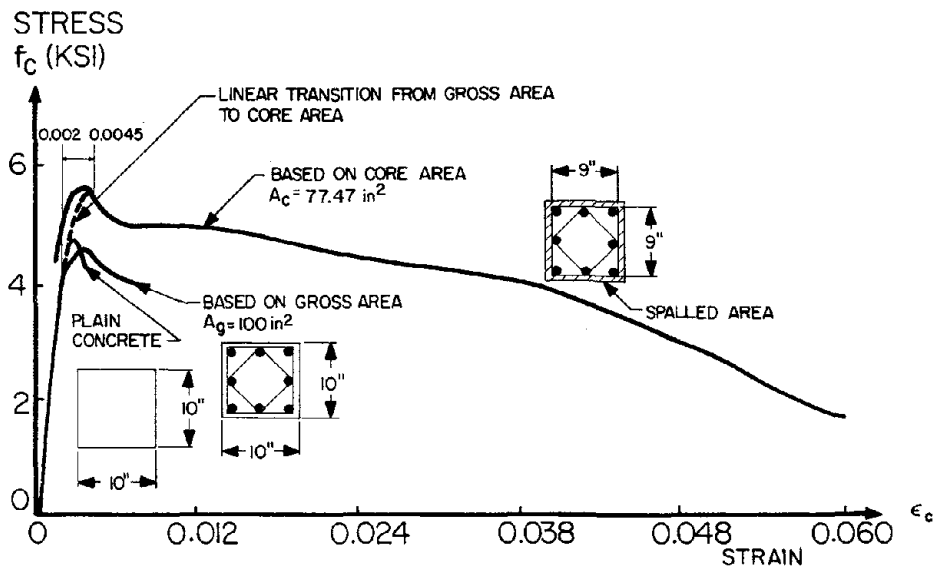


FIG. 4.8 STRESS-STRAIN RELATIONSHIP OF SPECIMEN WITH COVER AND WITH LONGITUDINAL REINFORCEMENT, SQUARE SPIRALS; (1BB-1)

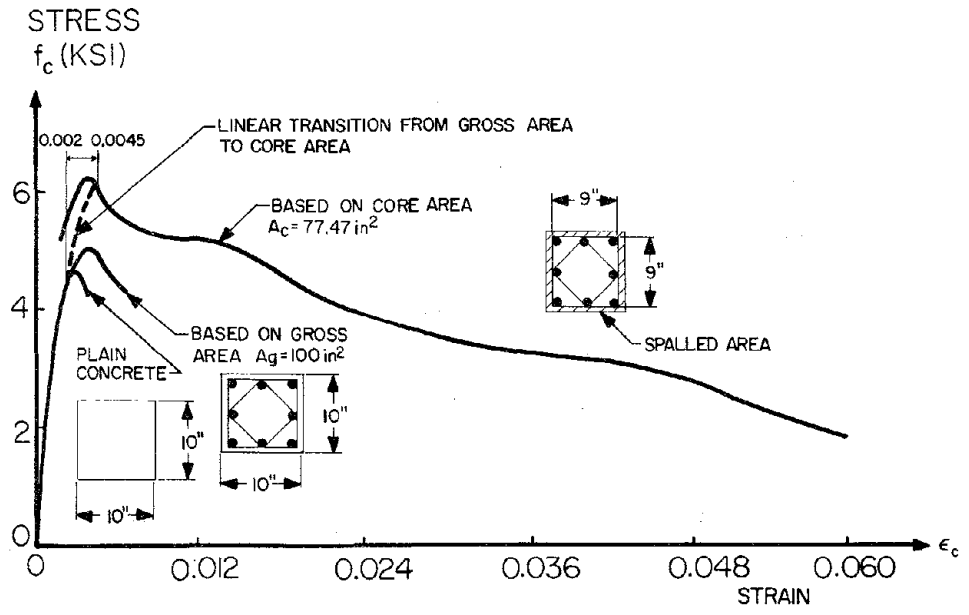


FIG. 4.9 STRESS-STRAIN RELATIONSHIP OF SPECIMEN WITH COVER AND WITH LONGITUDINAL REINFORCEMENT, SQUARE SPIRALS; (1BB-2)

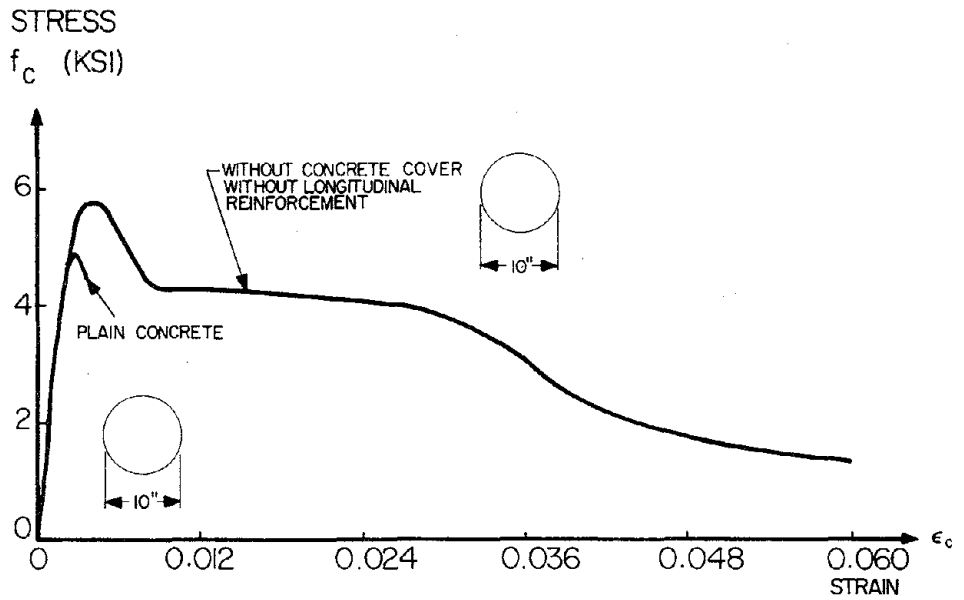


FIG. 4.10 STRESS-STRAIN RELATIONSHIP OF SPECIMEN WITHOUT COVER AND WITHOUT LONGITUDINAL REINFORCEMENT, CIRCULAR SPIRALS; (2AA-1)

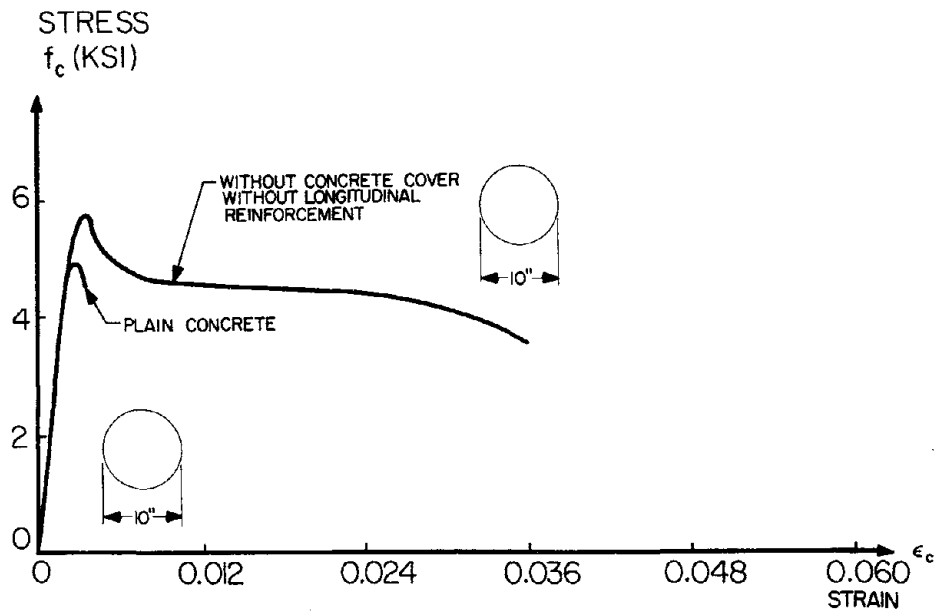


FIG. 4.11 STRESS-STRAIN RELATIONSHIP OF SPECIMEN WITHOUT COVER AND WITHOUT LONGITUDINAL REINFORCEMENT, CIRCULAR SPIRALS; (2AA-2)

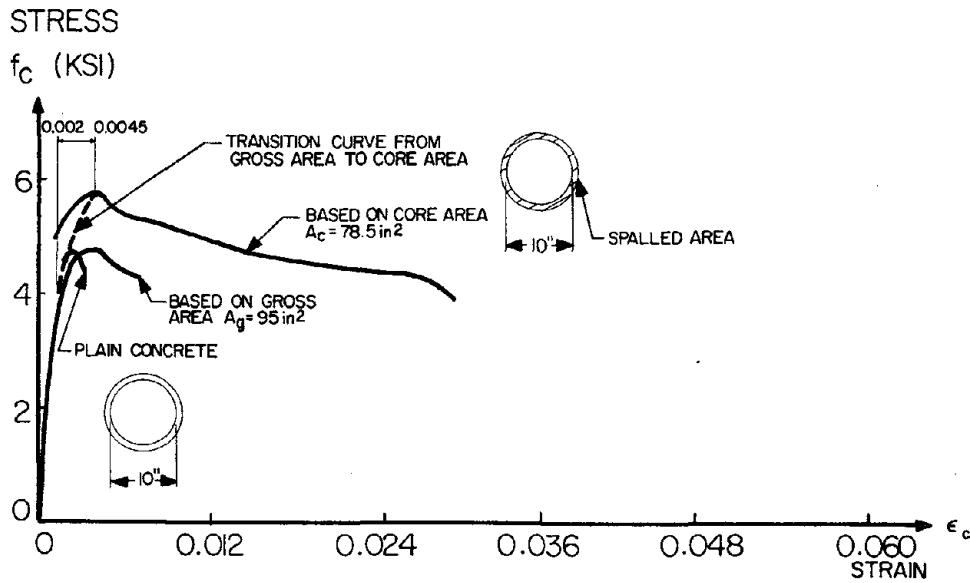


FIG. 4.12 STRESS-STRAIN RELATIONSHIP OF SPECIMEN WITH COVER AND WITHOUT LONGITUDINAL REINFORCEMENT, CIRCULAR SPIRALS; (2BA-1)

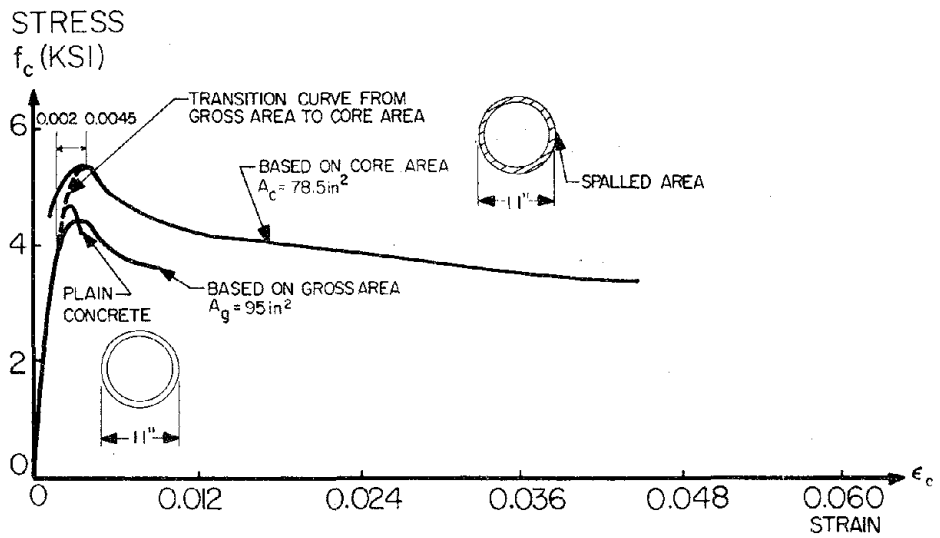


FIG. 4.13 STRESS-STRAIN RELATIONSHIP OF SPECIMEN WITH COVER AND WITHOUT LONGITUDINAL REINFORCEMENT, CIRCULAR SPIRALS; (2BA-2)

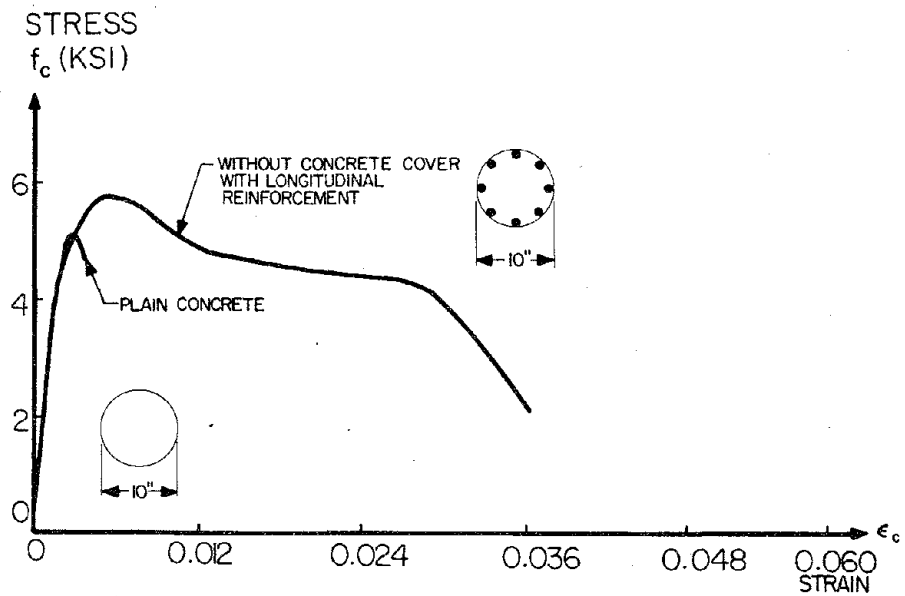


FIG. 4.14 STRESS-STRAIN RELATIONSHIP OF SPECIMEN WITHOUT COVER AND WITH LONGITUDINAL REINFORCEMENT, CIRCULAR SPIRALS; (2AB-1)

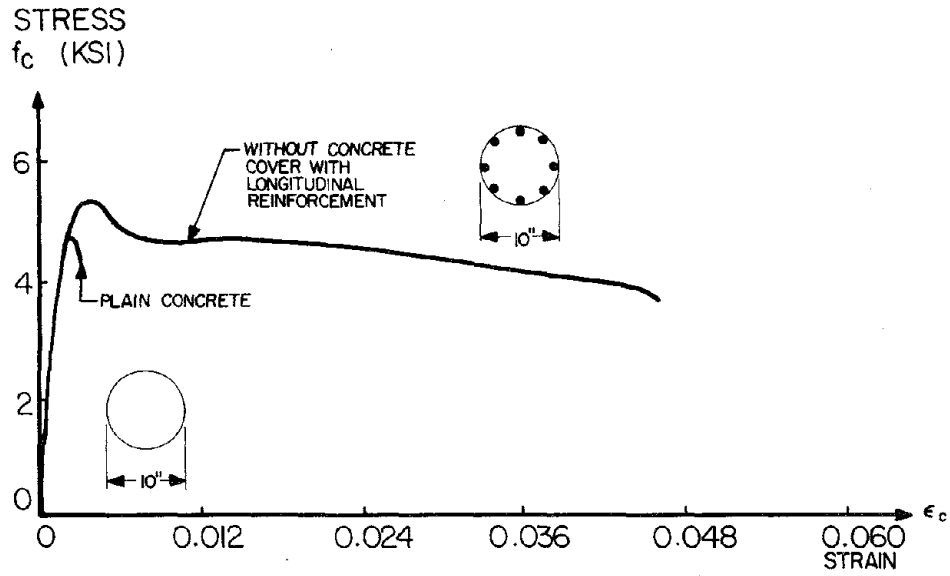


FIG. 4.15 STRESS-STRAIN RELATIONSHIP OF SPECIMEN WITHOUT COVER AND WITH LONGITUDINAL REINFORCEMENT, CIRCULAR SPIRALS; (2AB-2)

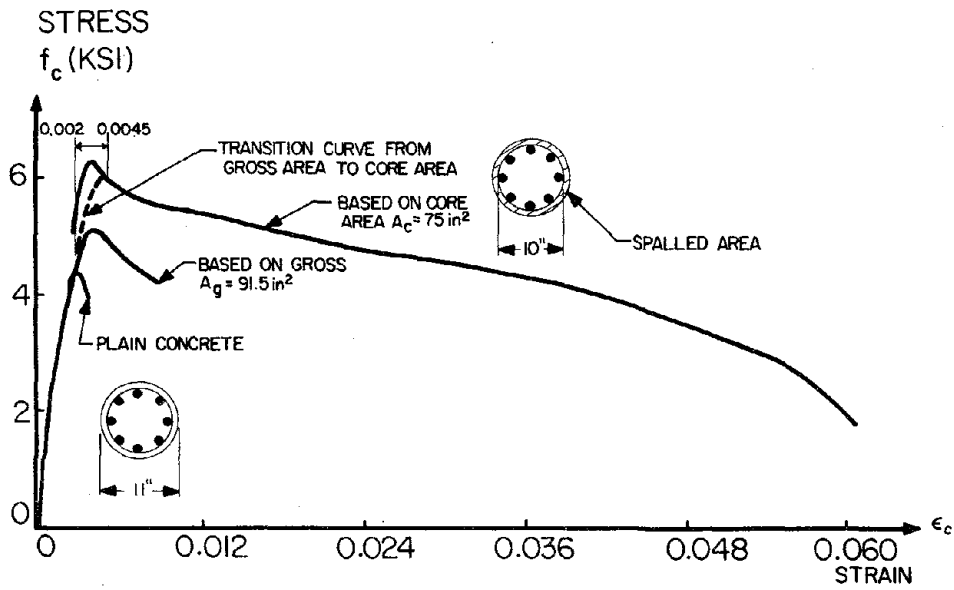


FIG. 4.16 STRESS-STRAIN RELATIONSHIP OF SPECIMEN WITH COVER AND WITH LONGITUDINAL REINFORCEMENT, CIRCULAR SPIRALS; (2BB-1)

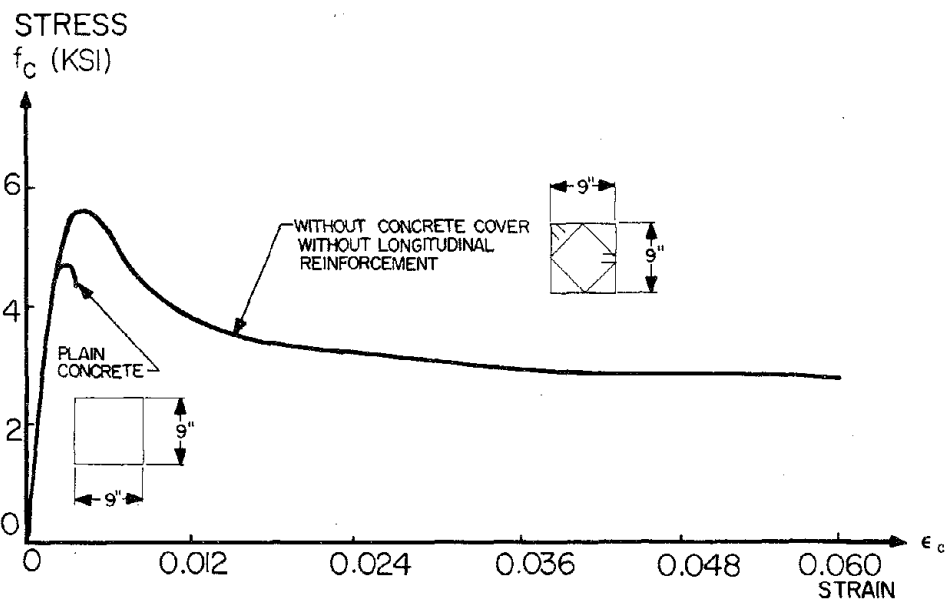


FIG. 4.17 STRESS-STRAIN RELATIONSHIP OF SPECIMEN WITHOUT COVER AND WITHOUT LONGITUDINAL REINFORCEMENT, SQUARE HOOPS; (3AA-1)

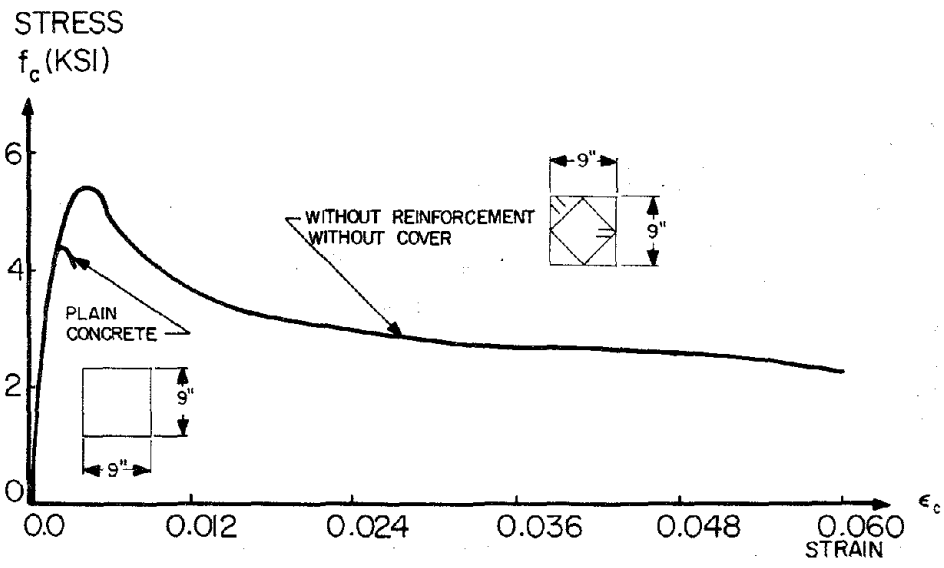


FIG. 4.18 STRESS-STRAIN RELATIONSHIP OF SPECIMEN WITHOUT COVER AND WITHOUT LONGITUDINAL REINFORCEMENT, SQUARE HOOPS; (3AA-2)

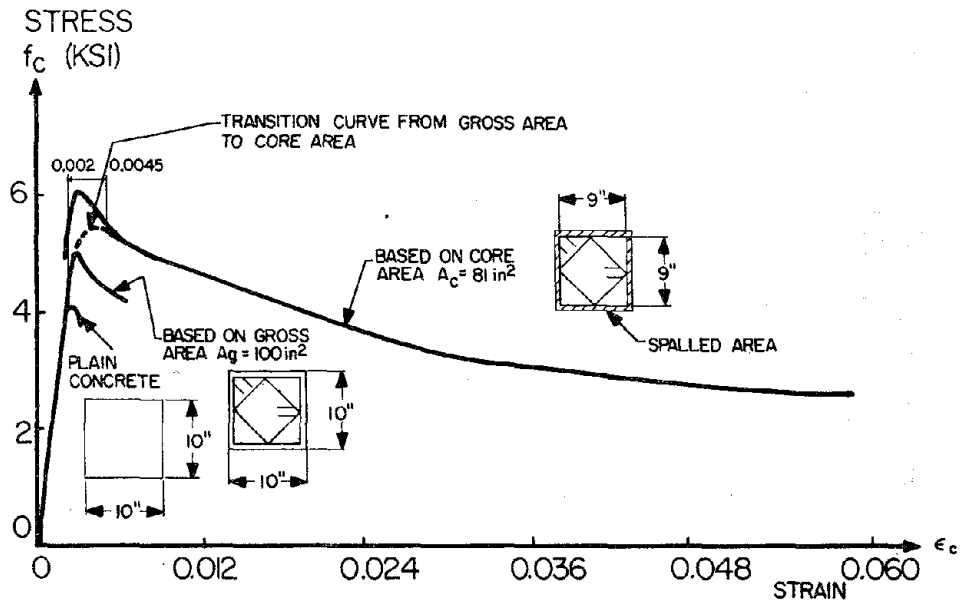


FIG. 4.19 STRESS-STRAIN RELATIONSHIP OF SPECIMEN WITH COVER AND WITHOUT LONGITUDINAL REINFORCEMENT, SQUARE HOOPS; (3BA-1)

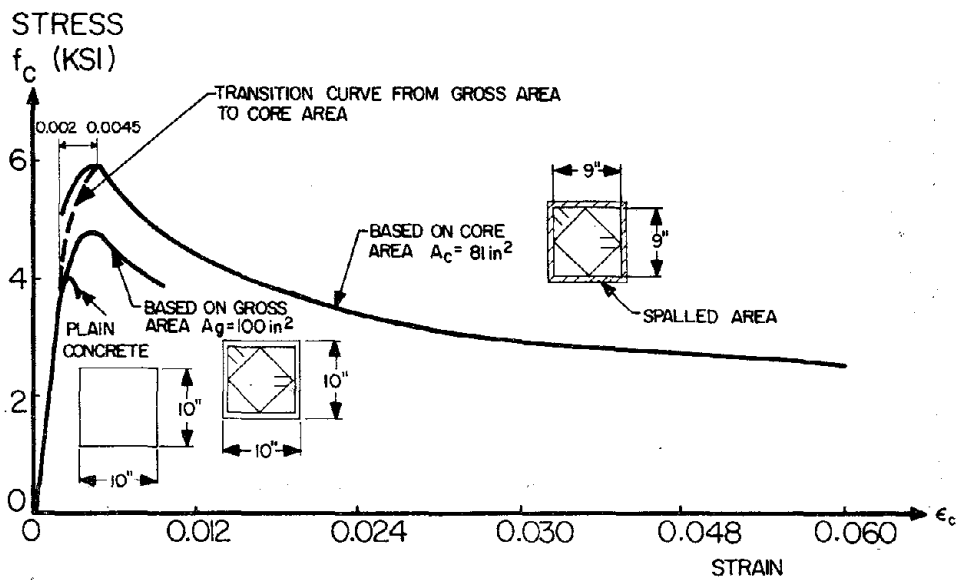


FIG. 4.20 STRESS-STRAIN RELATIONSHIP OF SPECIMEN WITH COVER AND WITHOUT LONGITUDINAL REINFORCEMENT, SQUARE HOOPS (3BA-2)

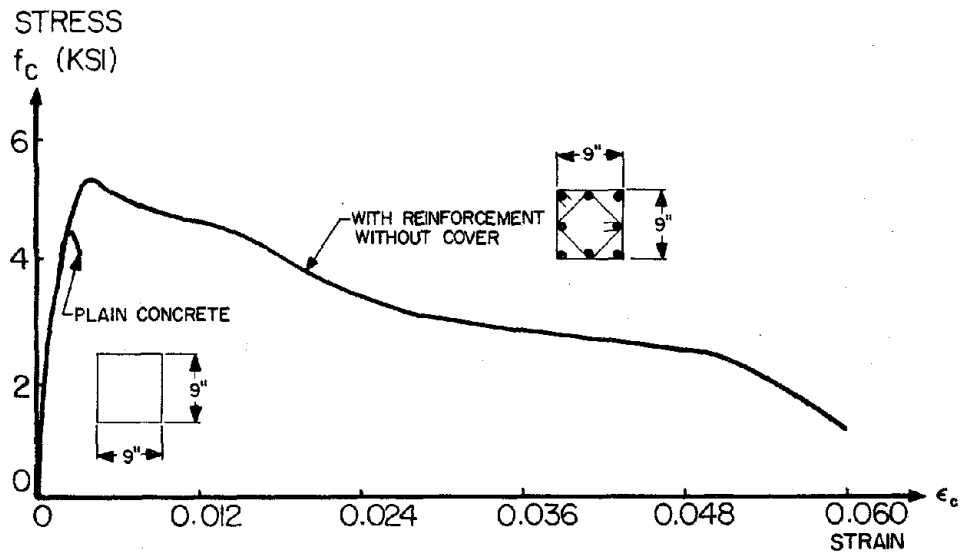


FIG. 4.21 STRESS-STRAIN RELATIONSHIP OF SPECIMEN WITHOUT COVER AND WITH LONGITUDINAL REINFORCEMENT, SQUARE HOOPS; (3AB-1)

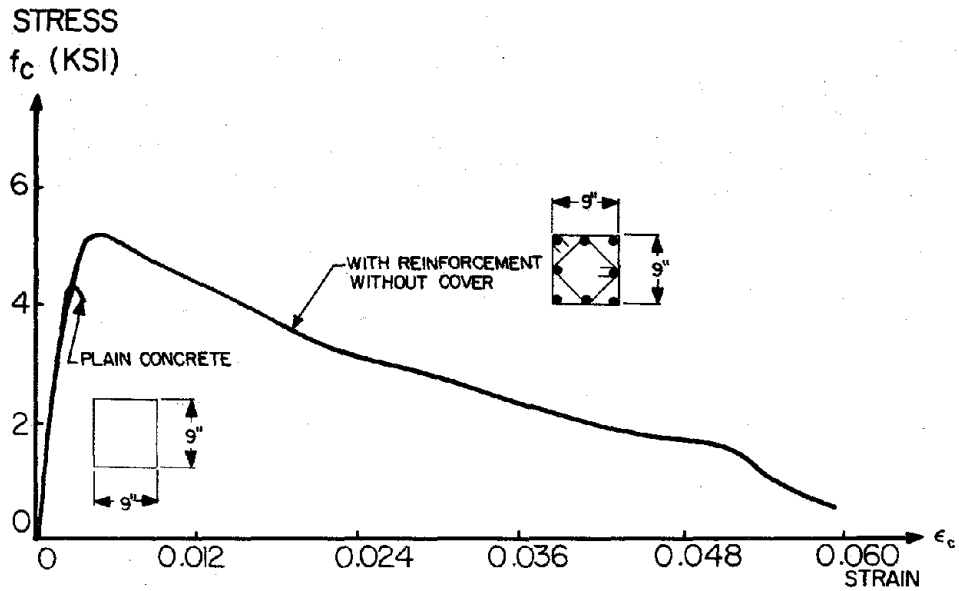


FIG. 4.22 STRESS-STRAIN RELATIONSHIP OF SPECIMEN WITHOUT COVER AND WITH LONGITUDINAL REINFORCEMENT, SQUARE HOOPS; (3AB-2)

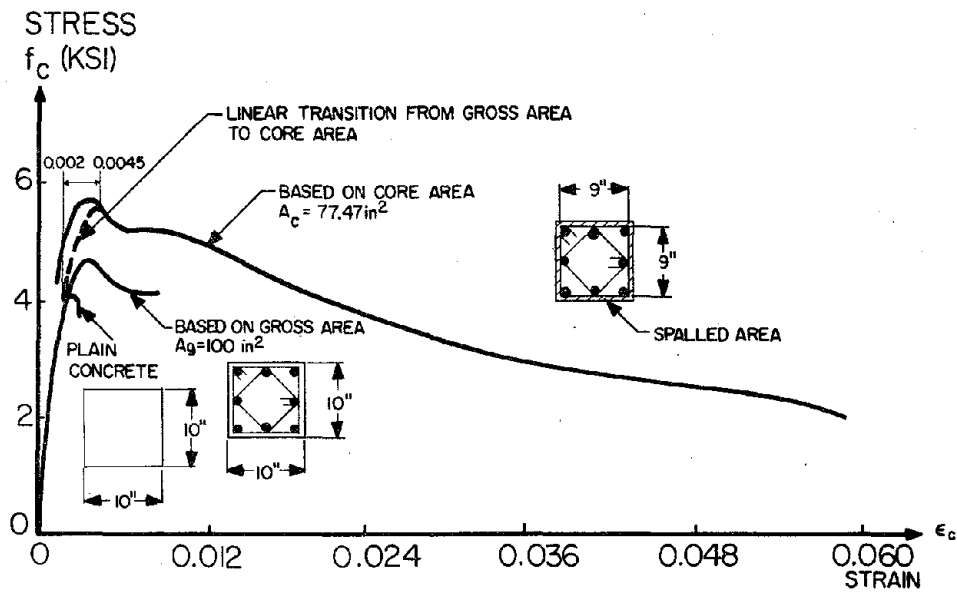


FIG. 4.23 STRESS-STRAIN RELATIONSHIP OF SPECIMEN WITH COVER AND WITH LONGITUDINAL REINFORCEMENT, SQUARE HOOPS; (3BB-1)

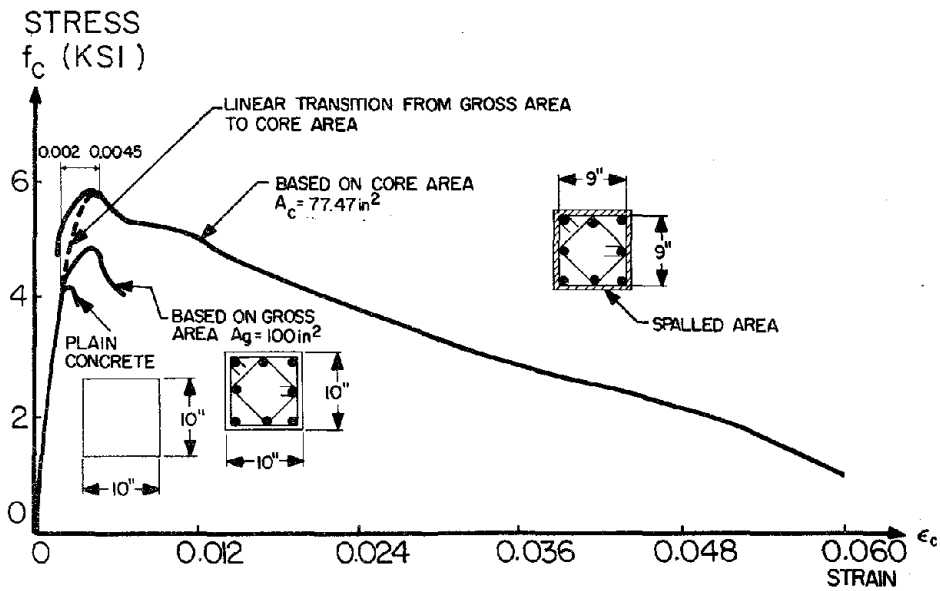


FIG. 4.24 STRESS-STRAIN RELATIONSHIP OF SPECIMEN WITH COVER AND WITH LONGITUDINAL REINFORCEMENT, SQUARE HOOPS; (3BB-2)

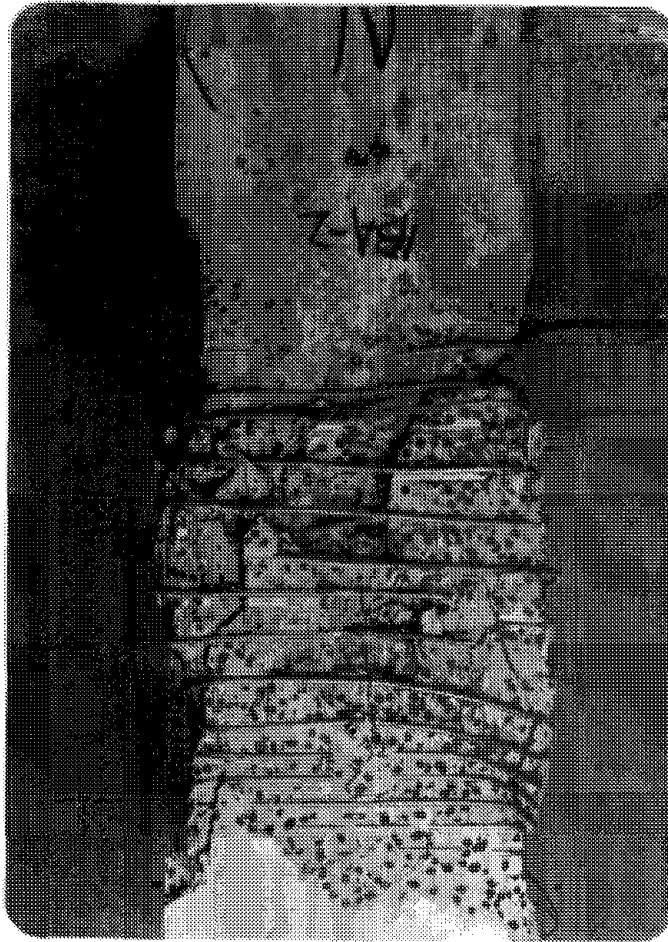


FIG. 4.25 SPECIMEN WITH SQUARE SPIRALS AFTER TESTING
(WITH COVER AND WITHOUT LONGITUDINAL REINFORCEMENT)

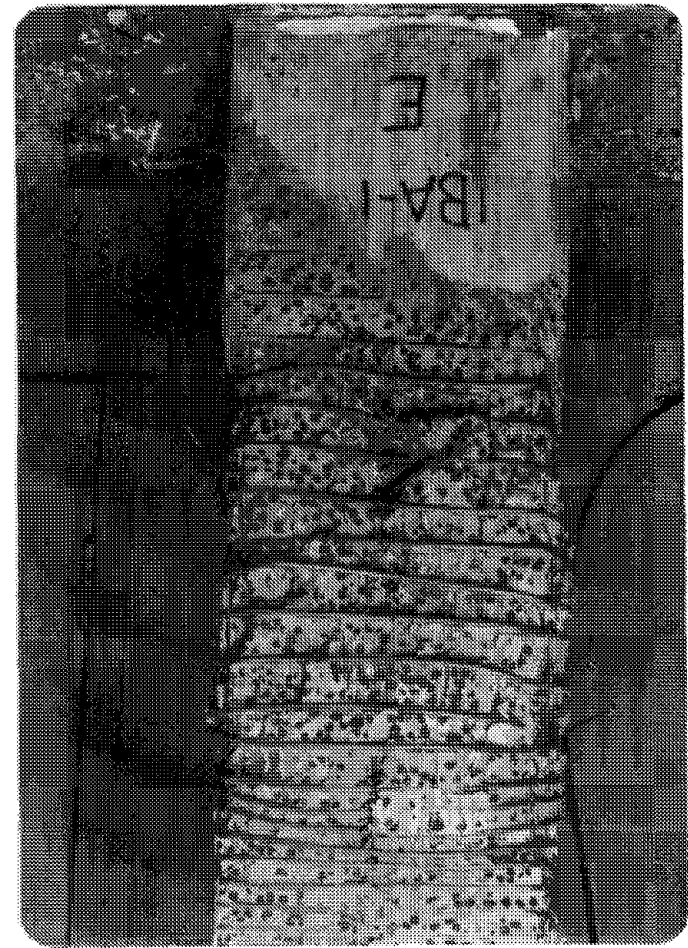


FIG. 4.26 SPECIMEN WITH SQUARE SPIRALS AFTER TESTING
(WITH COVER AND WITHOUT LONGITUDINAL REINFORCEMENT)

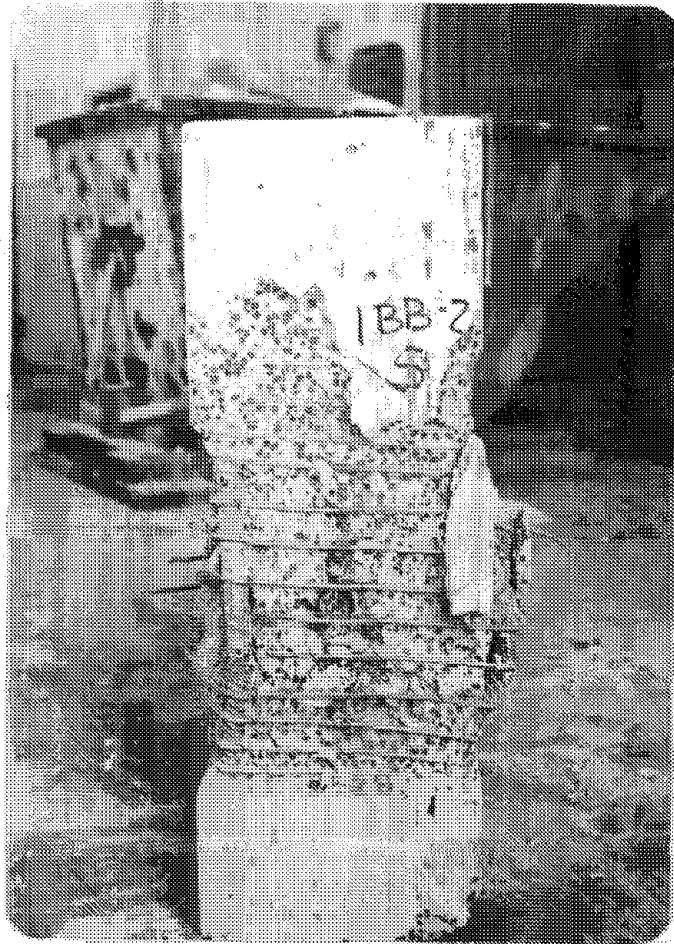


FIG. 4.27 SPECIMEN WITH SQUARE SPIRALS AFTER TESTING
(WITH COVER AND WITH LONGITUDINAL REINFORCEMENT)

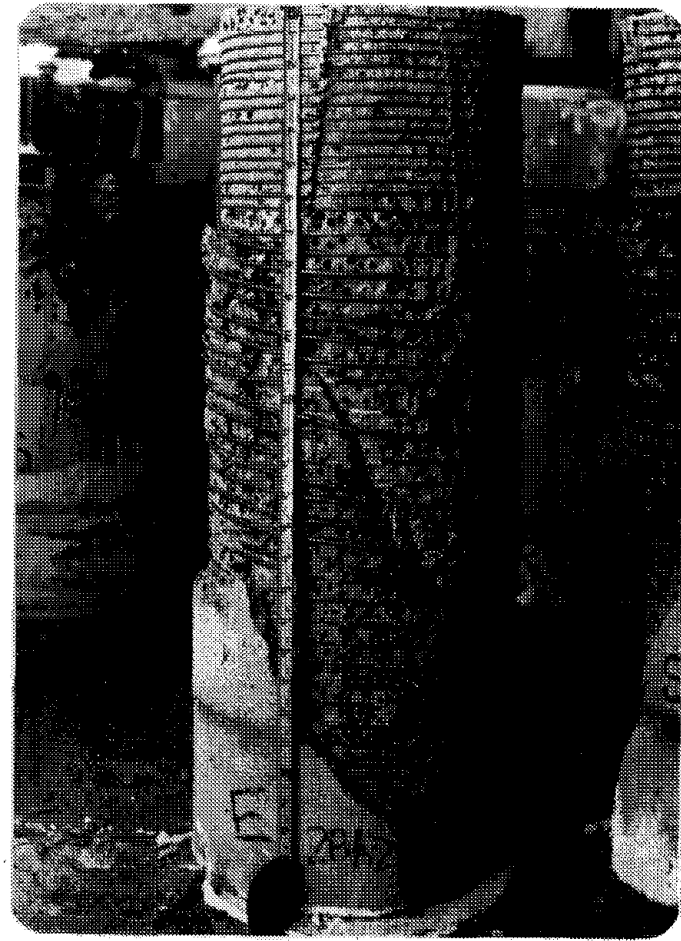


FIG. 4.28 SPECIMEN WITH CIRCULAR SPIRALS AFTER TESTING
(WITH COVER AND WITHOUT LONGITUDINAL REINFORCEMENT)

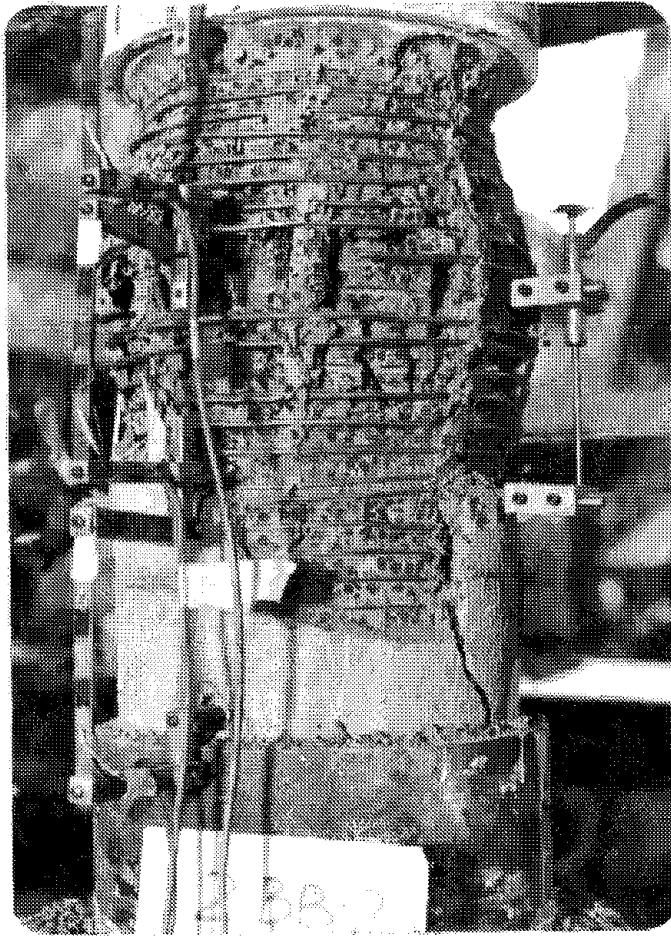


FIG. 4.29 SPECIMEN CONFINED WITH CIRCULAR SPIRALS AFTER TESTING (WITH COVER AND WITH LONGITUDINAL REINFORCEMENT)

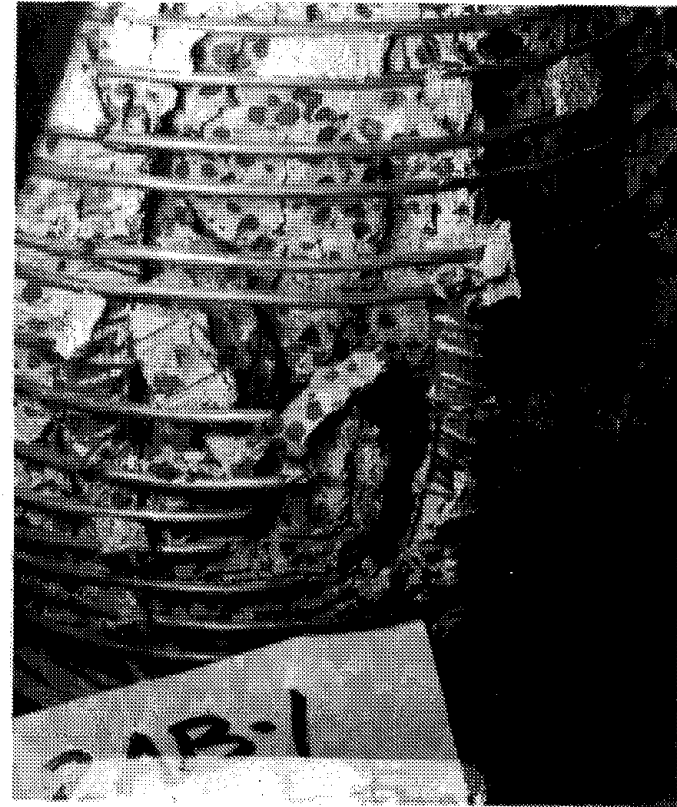


FIG. 4.30 SPECIMEN CONFINED WITH CIRCULAR SPIRALS AFTER TESTING (CLOSE-UP OF REGION OF FAILURE)

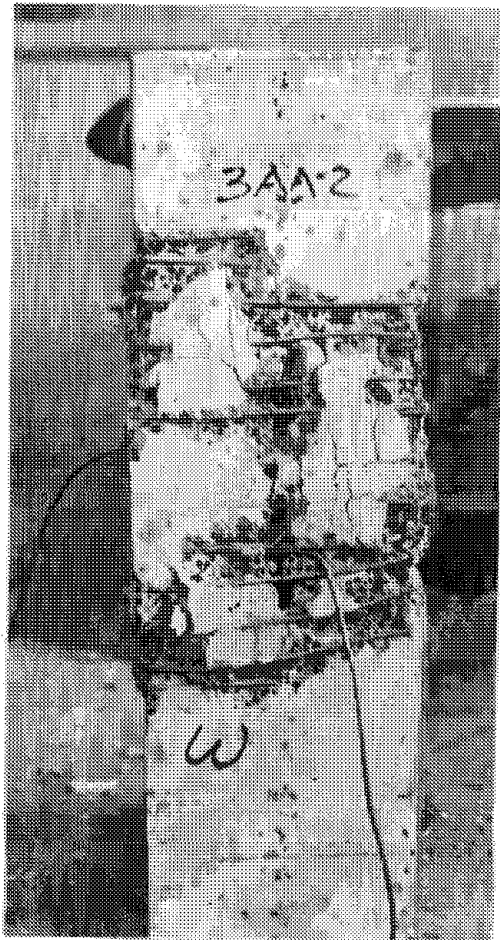


FIG. 4.31 SPECIMEN CONFINED WITH SQUARE HOOPS, AFTER TESTING (WITH COVER AND WITHOUT LONGITUDINAL REINFORCEMENT)



FIG. 4.32 SPECIMEN CONFINED WITH SQUARE HOOPS, AFTER TESTING (WITH COVER AND WITHOUT LONGITUDINAL REINFORCEMENT)

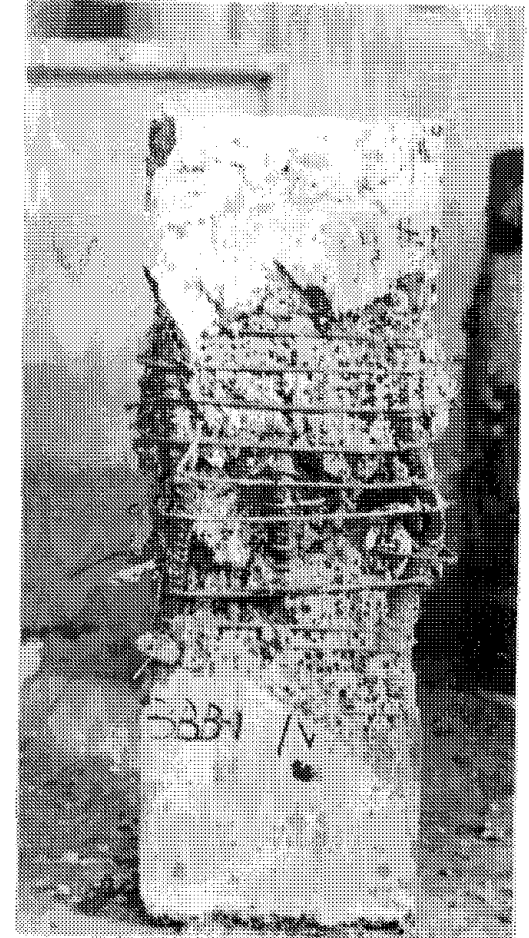


FIG. 4.33 SPECIMEN CONFINED WITH SQUARE HOOPS, AFTER TESTING (WITH COVER AND WITH LONGITUDINAL REINFORCEMENT)

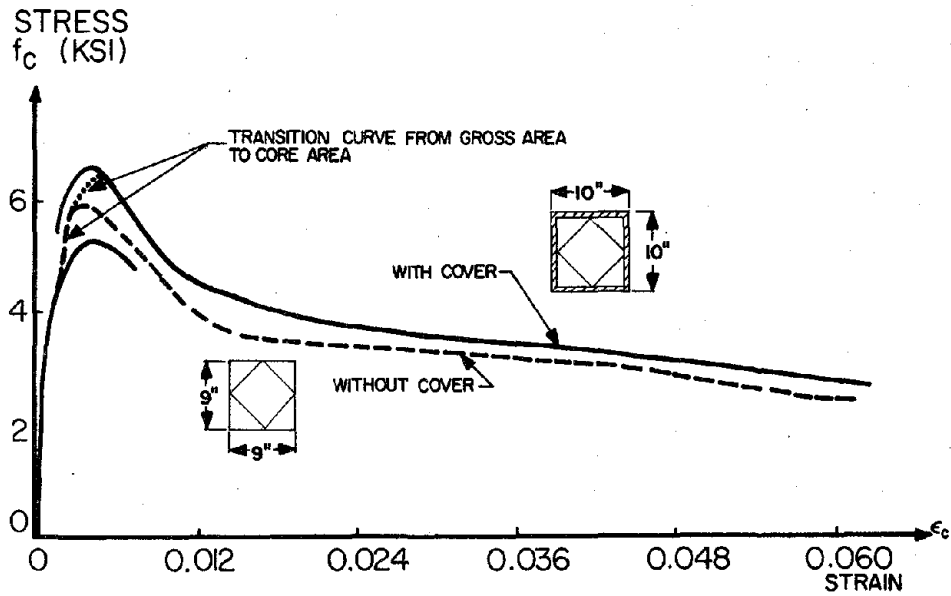


FIG. 4.34 EFFECT OF CONCRETE COVER ON THE STRESS-STRAIN RELATIONSHIP OF CONFINED CONCRETE (SPECIMENS WITHOUT LONGITUDINAL REINFORCEMENT)

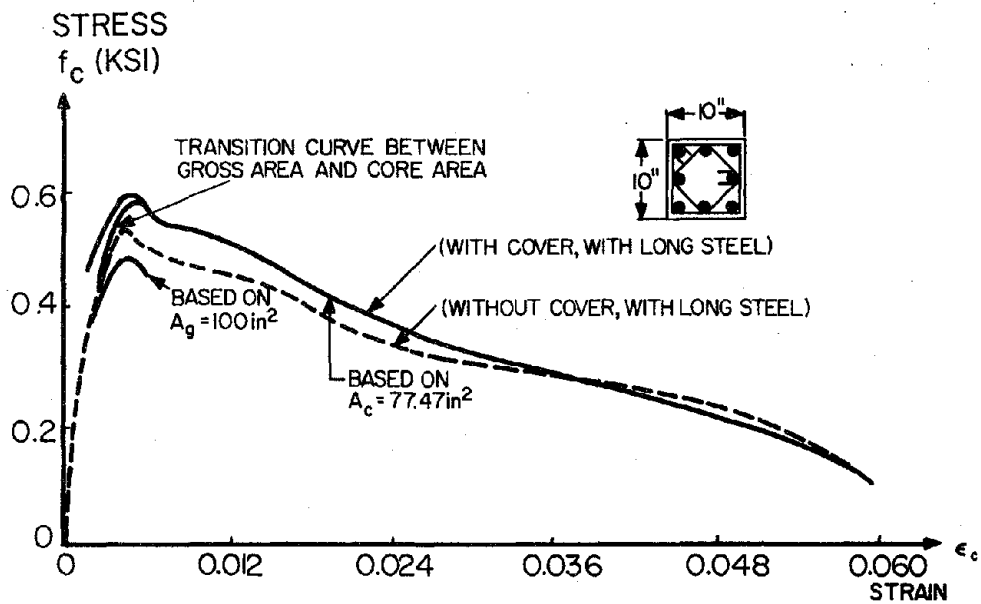


FIG. 4.35 EFFECT OF CONCRETE COVER ON THE STRESS-STRAIN RELATIONSHIP OF CONFINED CONCRETE (SPECIMENS WITH LONGITUDINAL REINFORCEMENT)

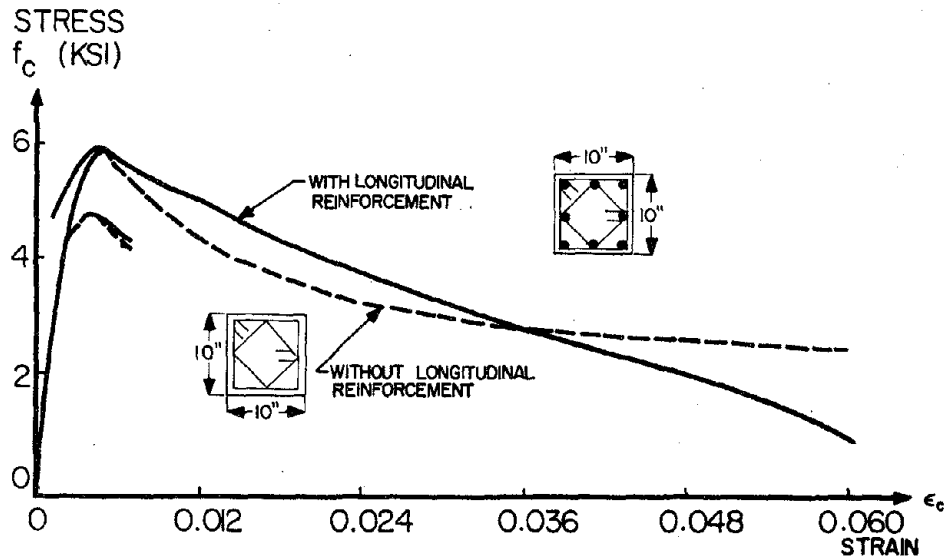


FIG. 4.36 EFFECT OF THE LONGITUDINAL REINFORCEMENT ON THE STRESS-STRAIN RELATIONSHIP OF CONFINED CONCRETE (SPECIMENS WITH COVER)

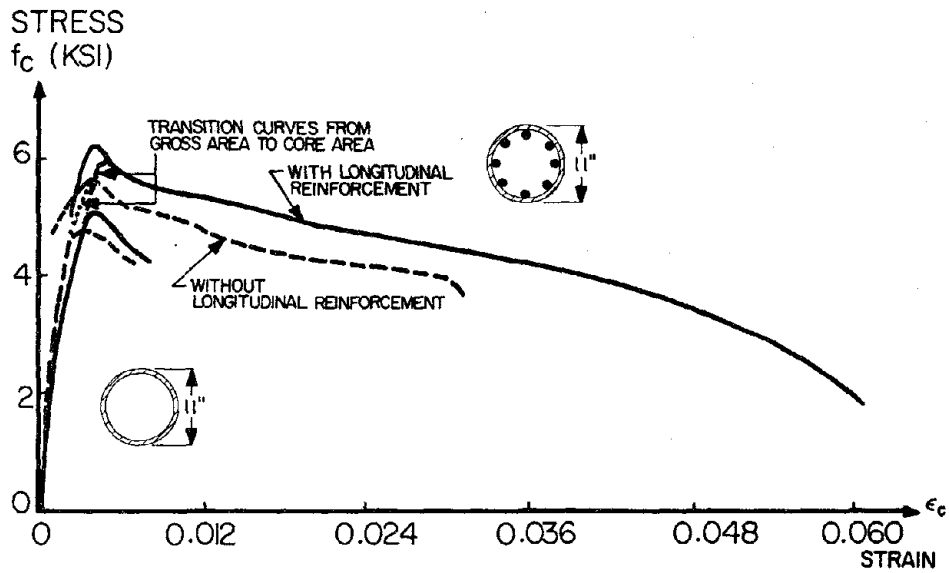


FIG. 4.37 EFFECT OF THE LONGITUDINAL REINFORCEMENT ON THE STRESS-STRAIN RELATIONSHIP OF CONFINED CONCRETE (SPECIMENS WITH COVER)

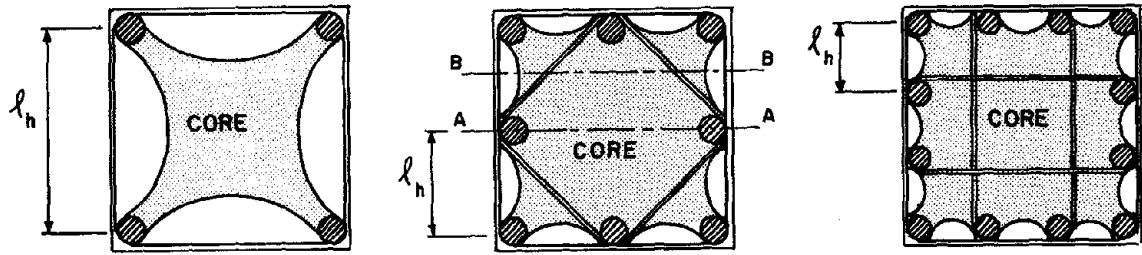


FIG. 4.38a EFFECT OF CONFIGURATION OF THE LONGITUDINAL REINFORCEMENT ON THE BASKETING OF THE CONCRETE CORE

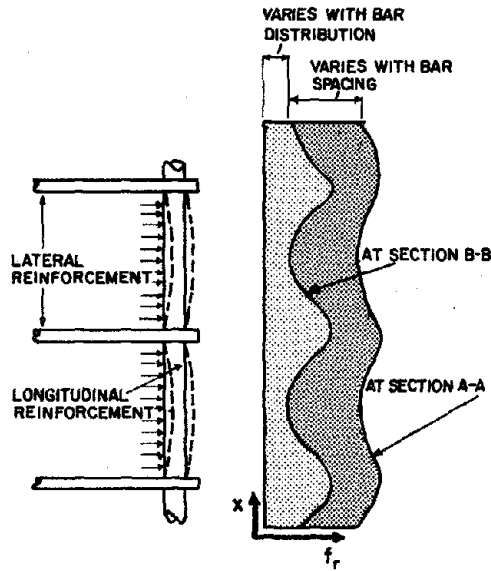


FIG. 4.38b LONGITUDINAL VARIATION OF f_r ON A SPECIMEN

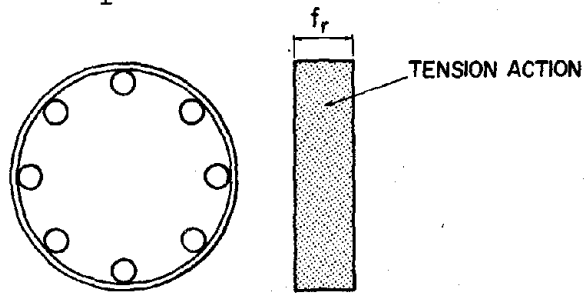


FIG. 4.39a TRANSVERSAL VARIATION OF f_r IN CIRCULAR CROSS SECTION

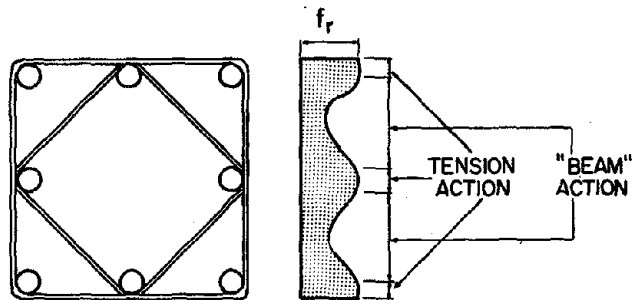


FIG. 4.39b TRANSVERSAL VARIATION OF f_r IN SQUARE CROSS SECTION

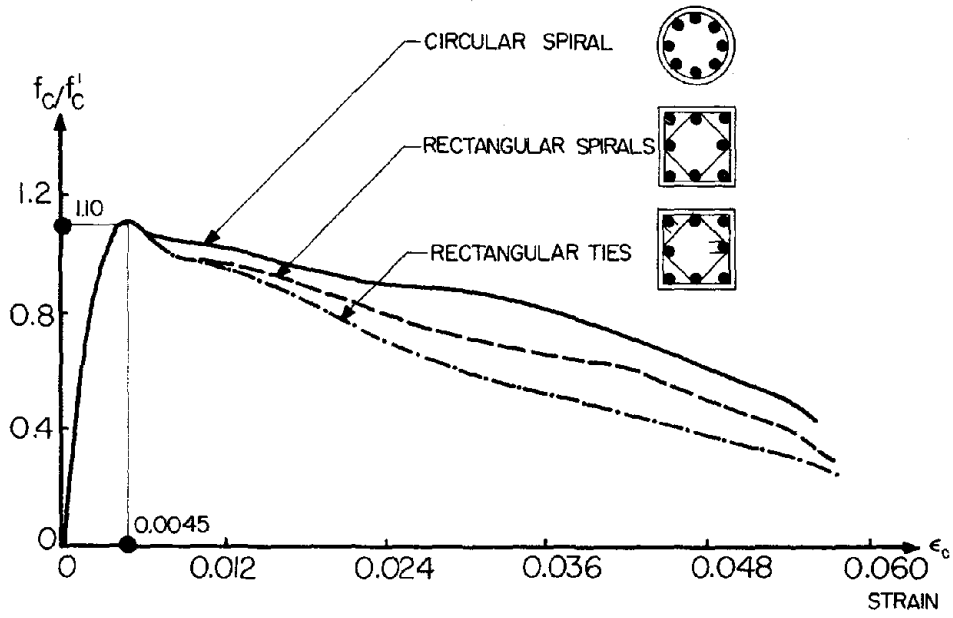


FIG. 4.40 EFFECT OF TYPE OF LATERAL REINFORCEMENT ON THE STRESS-STRAIN RELATIONSHIP OF CONFINED LIGHTWEIGHT CONCRETE

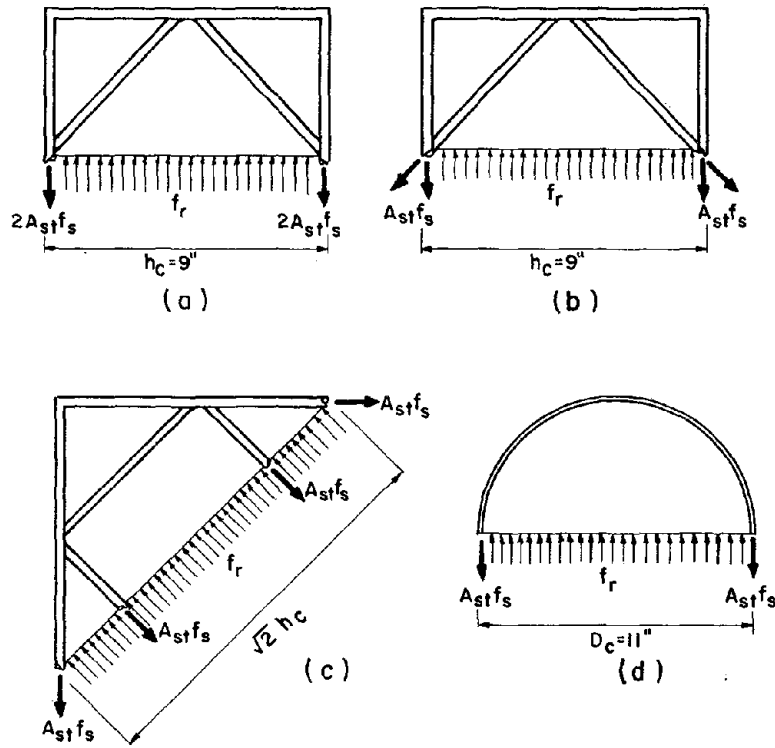


FIG. 4.41 FREE BODY DIAGRAMS USED IN DETERMINING f_r

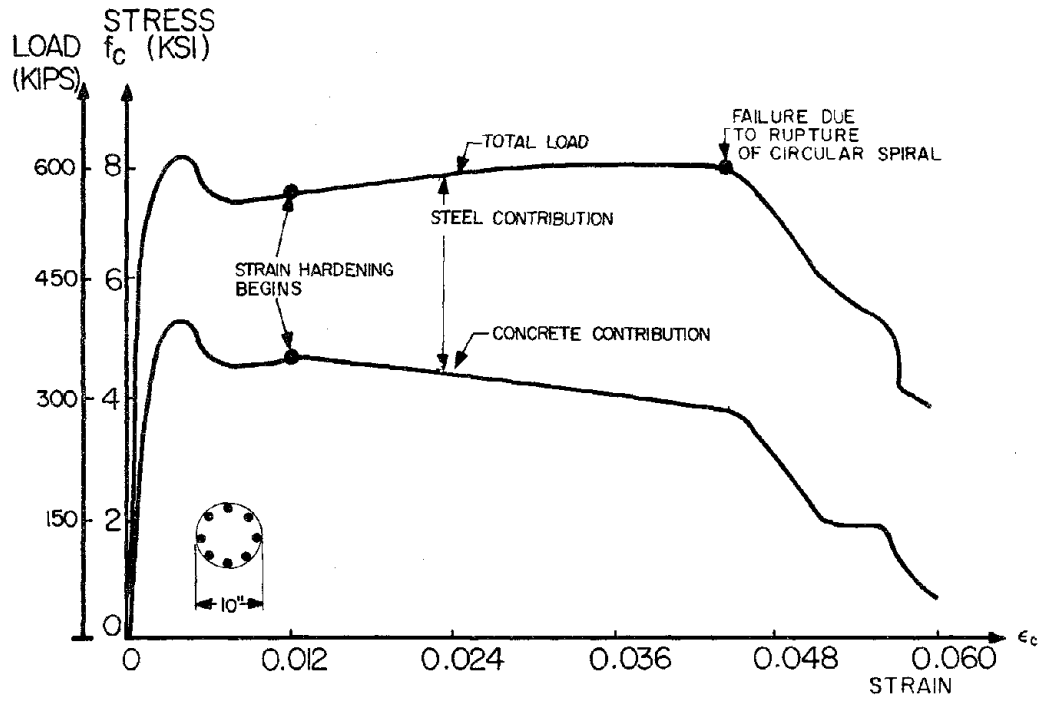


FIG. 4.42 EFFECT OF STRAIN HARDENING OF THE LONGITUDINAL REINFORCEMENT ON CONFINED CONCRETE

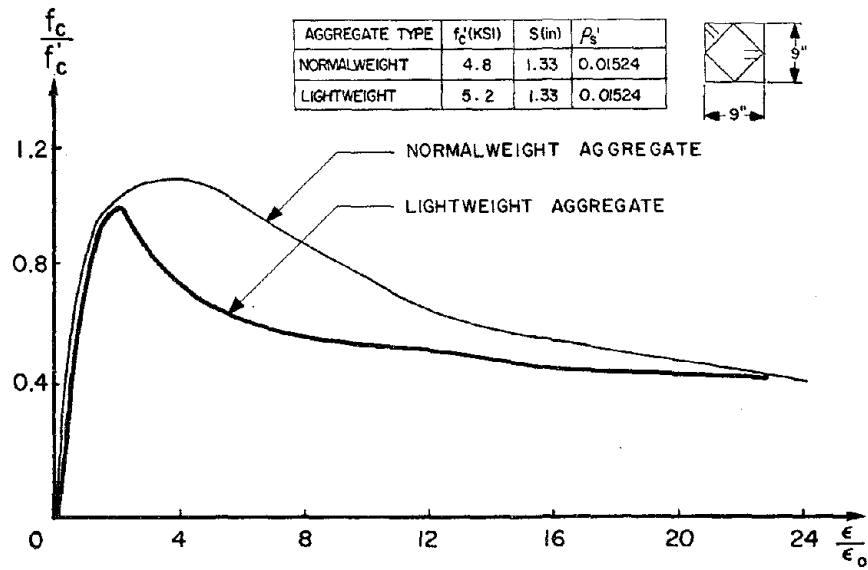


FIG. 5.1 COMPARISON OF NORMAL AND LIGHTWEIGHT CONFINED CONCRETE (SPECIMENS WITHOUT COVER AND WITHOUT LONGITUDINAL REINFORCEMENT)

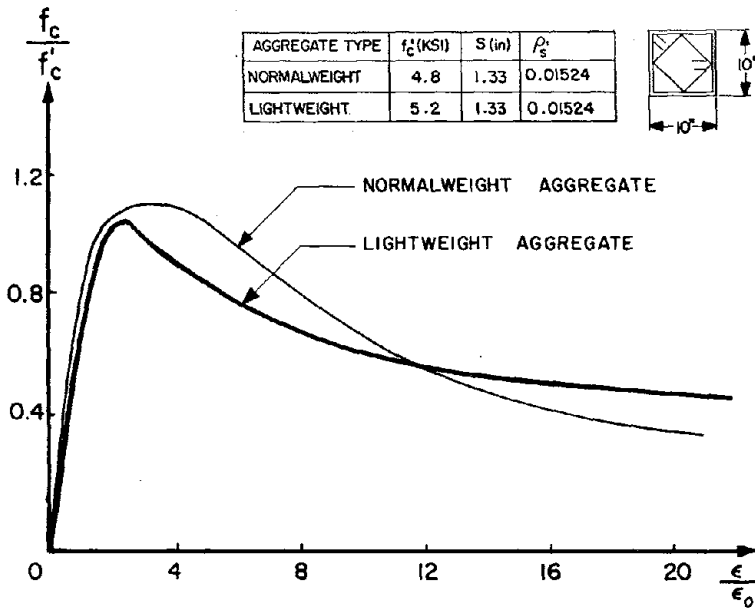


FIG. 5.2 COMPARISON OF NORMAL AND LIGHTWEIGHT CONFINED CONCRETE (SPECIMENS WITH COVER AND WITHOUT LONGITUDINAL REINFORCEMENT)

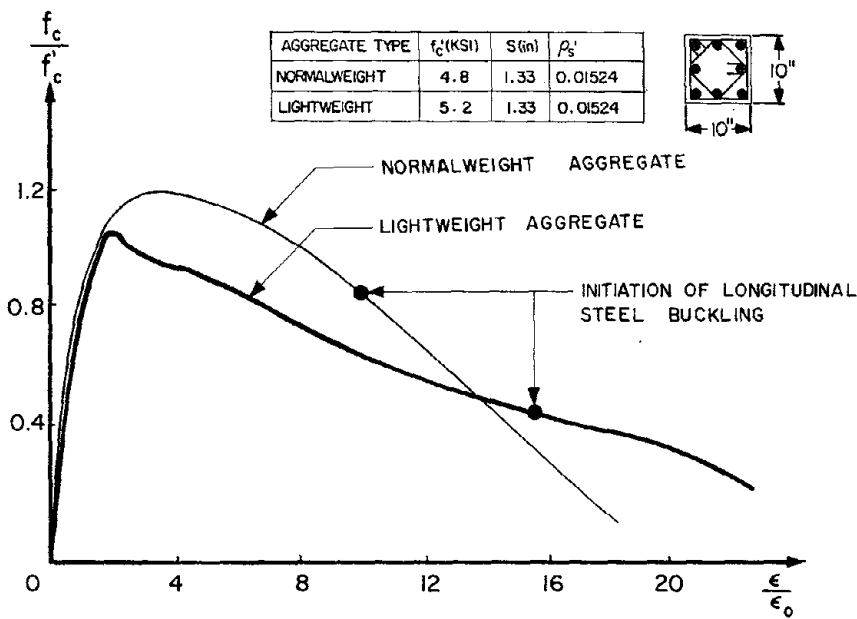


FIG. 5.3 COMPARISON OF NORMAL AND LIGHTWEIGHT CONFINED CONCRETE (SPECIMENS WITH COVER AND WITH LONGITUDINAL REINFORCEMENT)

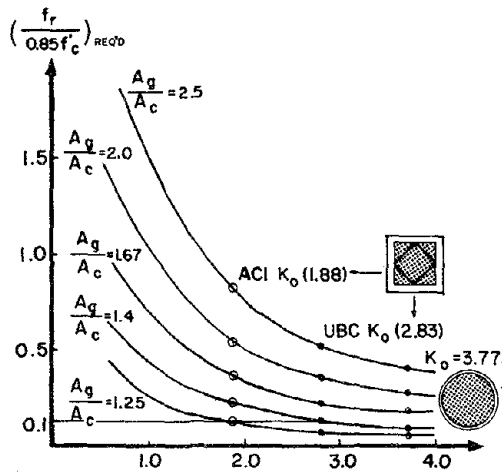


FIG. 6.1 VARIATION OF f_r (required) VS. K_0 FOR DIFFERENT VALUES OF $\frac{A_g}{A_c}$

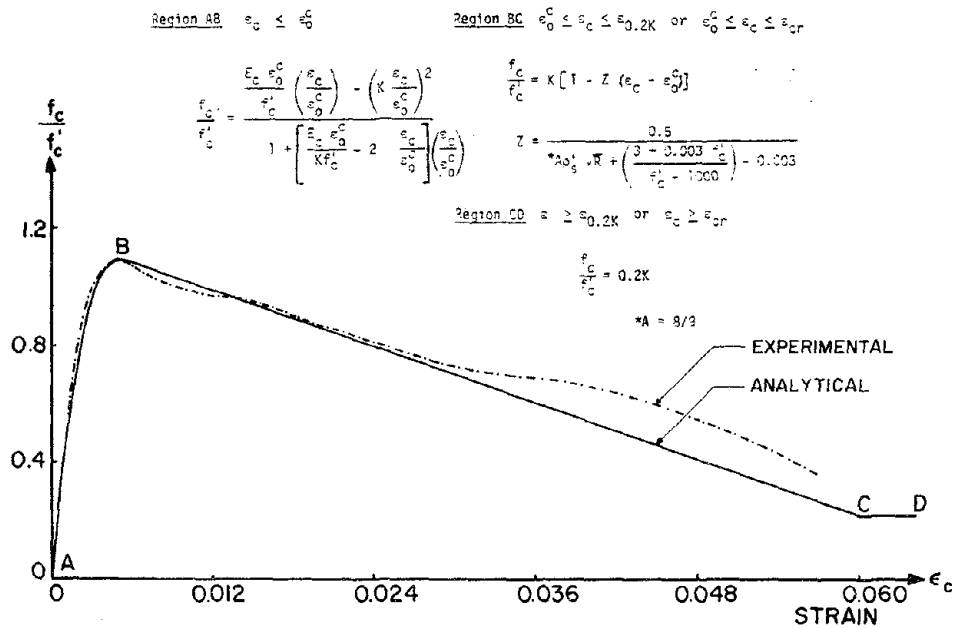


FIG. 7.1 EXPERIMENTAL AND ANALYTICAL STRESS-STRAIN RELATIONSHIP OF CONFINED LIGHTWEIGHT CONCRETE (SQUARE SPIRALS)

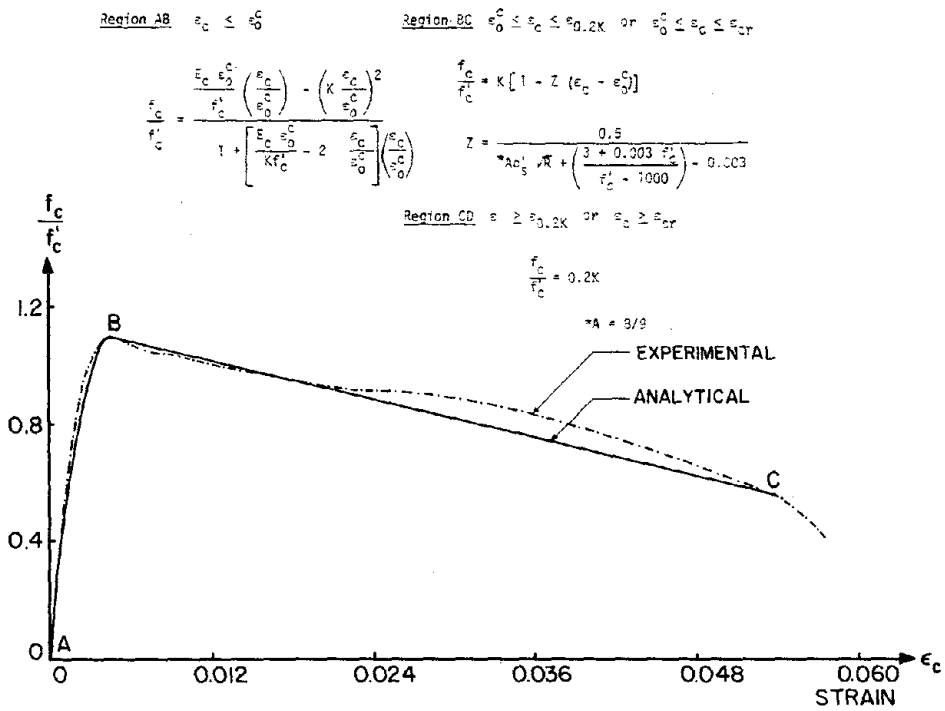


FIG. 7.2 EXPERIMENTAL AND ANALYTICAL STRESS-STRAIN RELATIONSHIP OF CONFINED LIGHTWEIGHT CONCRETE (CIRCULAR SPIRALS)

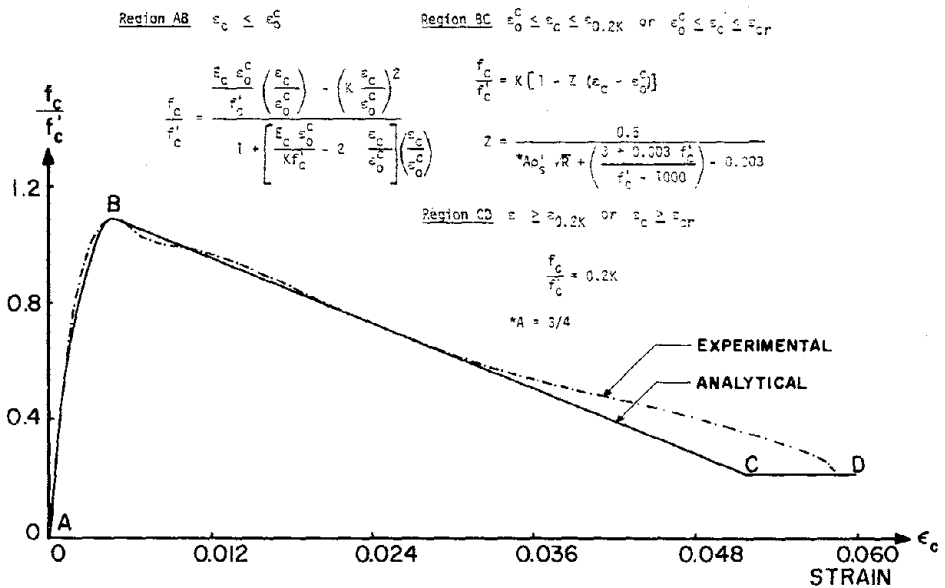


FIG. 7.3 EXPERIMENTAL AND ANALYTICAL STRESS-STRAIN RELATIONSHIP OF CONFINED LIGHTWEIGHT CONCRETE (SQUARE HOOPS)

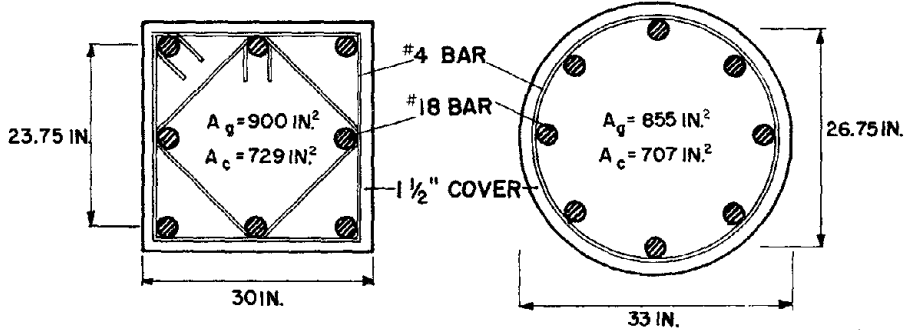


FIG. 9.1a DIMENSIONS OF SQUARE CROSS SECTION USED IN COMPUTING P-M INTERACTION DIAGRAM

FIG. 9.1b DIMENSIONS OF CIRCULAR SECTION USED IN COMPUTING P-M INTERACTION DIAGRAM

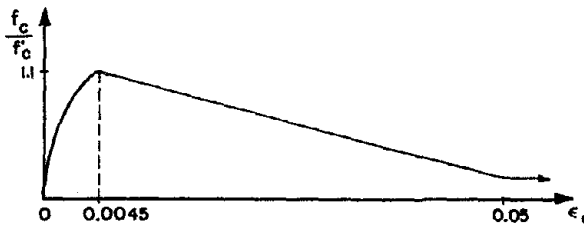


FIG. 9.2a STRESS-STRAIN RELATIONSHIP OF CONFINED CONCRETE USED IN THE ANALYSIS OF SQUARE CROSS SECTION

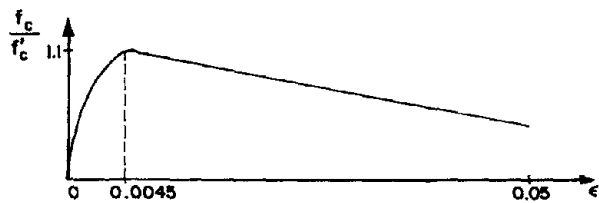


FIG. 9.2b STRESS-STRAIN RELATIONSHIP OF CONFINED CONCRETE USED IN THE ANALYSIS OF SQUARE CROSS SECTION

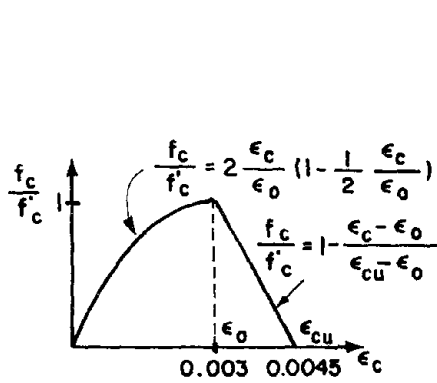


FIG. 9.3a STRESS-STRAIN RELATIONSHIP FOR CONCRETE COVER

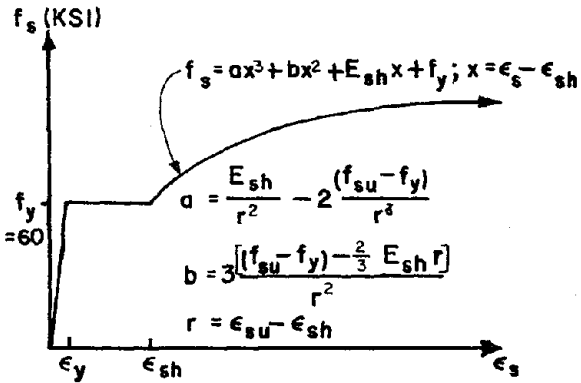


FIG. 9.3b STRESS-STRAIN RELATIONSHIP FOR LONGITUDINAL REINFORCEMENT

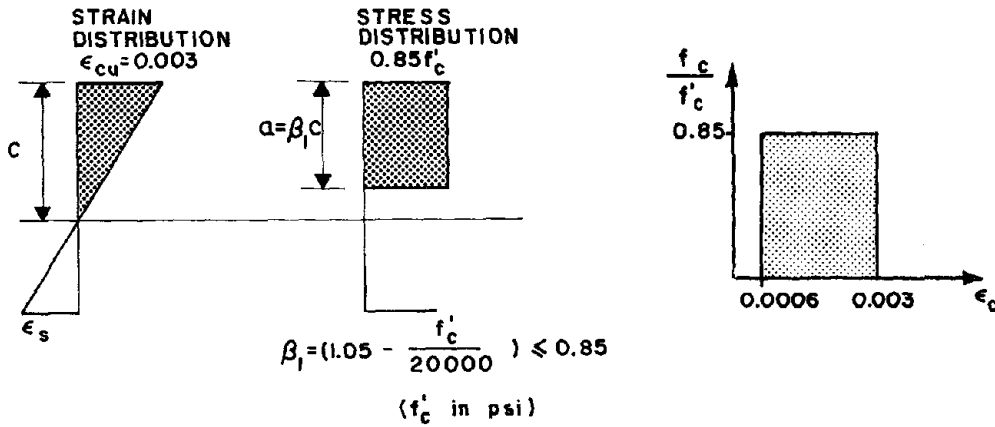


FIG. 9.4a EQUIVALENT STRESS BLOCK ASSUMPTIONS AND IMPLIED STRESS-STRAIN RELATIONSHIP FOR CONCRETE

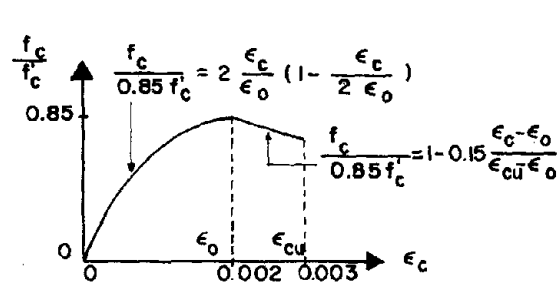


FIG. 9.4b HOGNESTAD STRESS-STRAIN RELATIONSHIP FOR CONCRETE

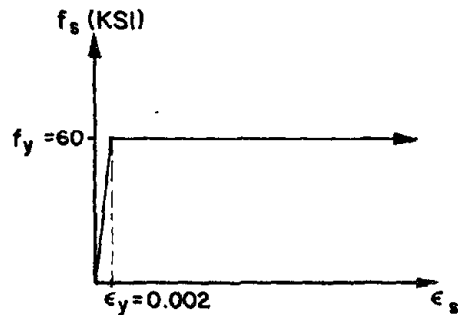


FIG. 9.4c ELASTIC-PERFECTLY PLASTIC RELATIONSHIP FOR STEEL

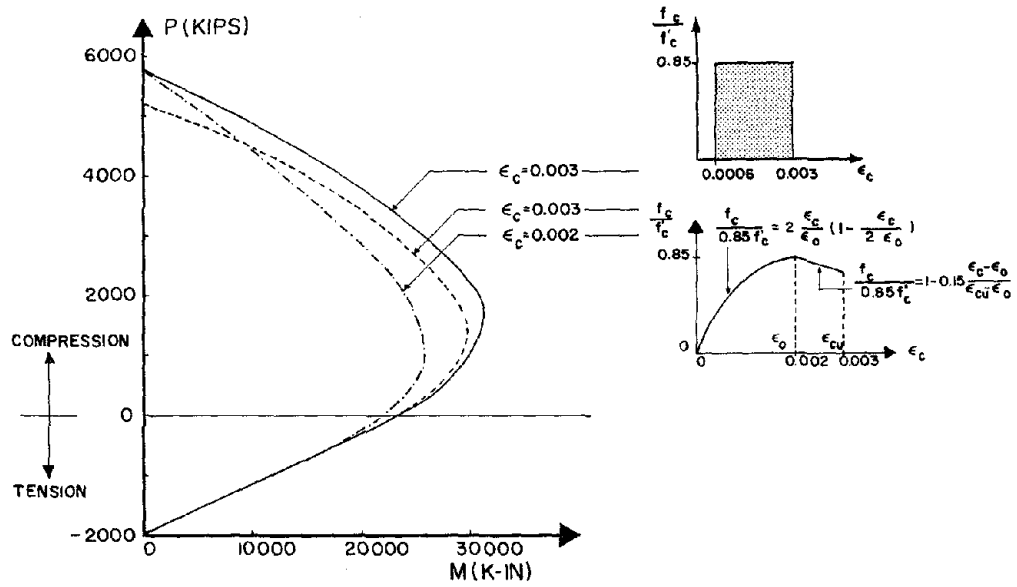


FIG. 9.5 COMPARISON OF AXIAL LOAD-MOMENT (P-M) INTERACTION DIAGRAMS FOR SQUARE CROSS SECTION COMPUTED USING HOGNESTAD'S AND THE EQUIVALENT STRESS BLOCK RELATIONSHIP

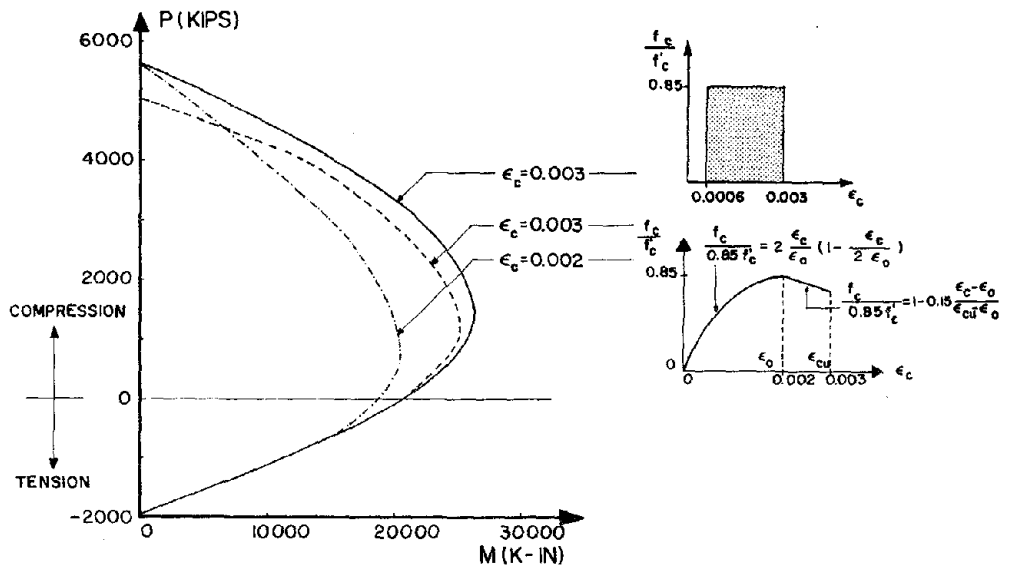


FIG. 9.6 COMPARISON OF AXIAL LOAD-MOMENT (P-M) INTERACTION DIAGRAMS FOR CIRCULAR CROSS SECTION COMPUTED USING HOGNESTAD'S AND THE EQUIVALENT STRESS BLOCK RELATIONSHIP

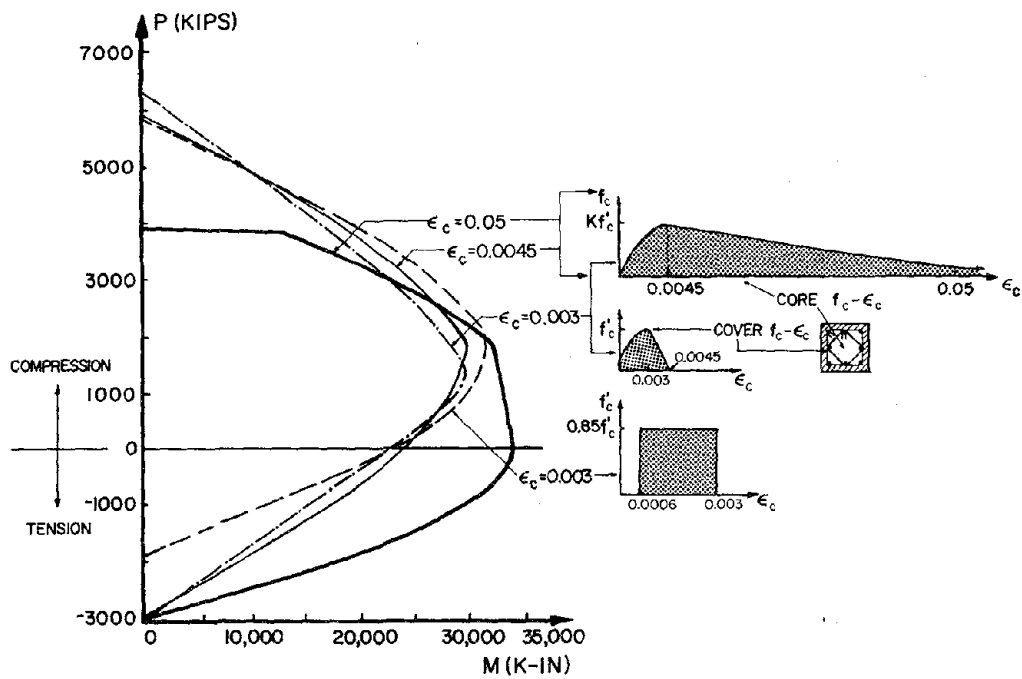


FIG. 9.7 COMPARISON OF AXIAL LOAD-MOMENT (P-M) INTERACTION DIAGRAMS FOR SQUARE CROSS SECTION

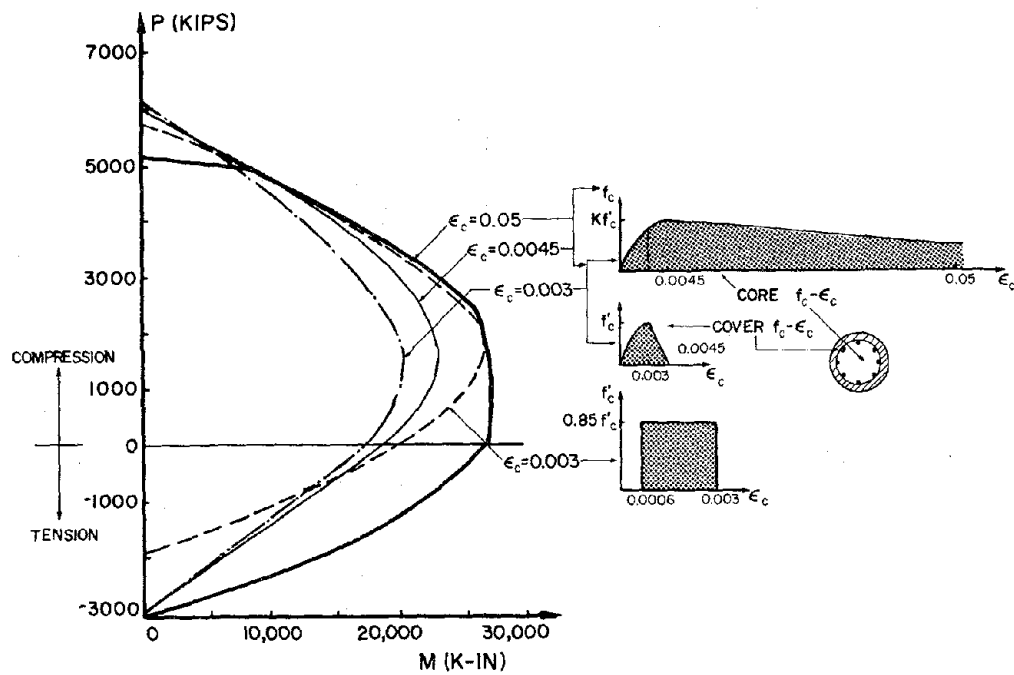


FIG. 9.8 COMPARISON OF AXIAL LOAD-MOMENT (P-M) INTERACTION DIAGRAMS FOR CIRCULAR CROSS SECTION

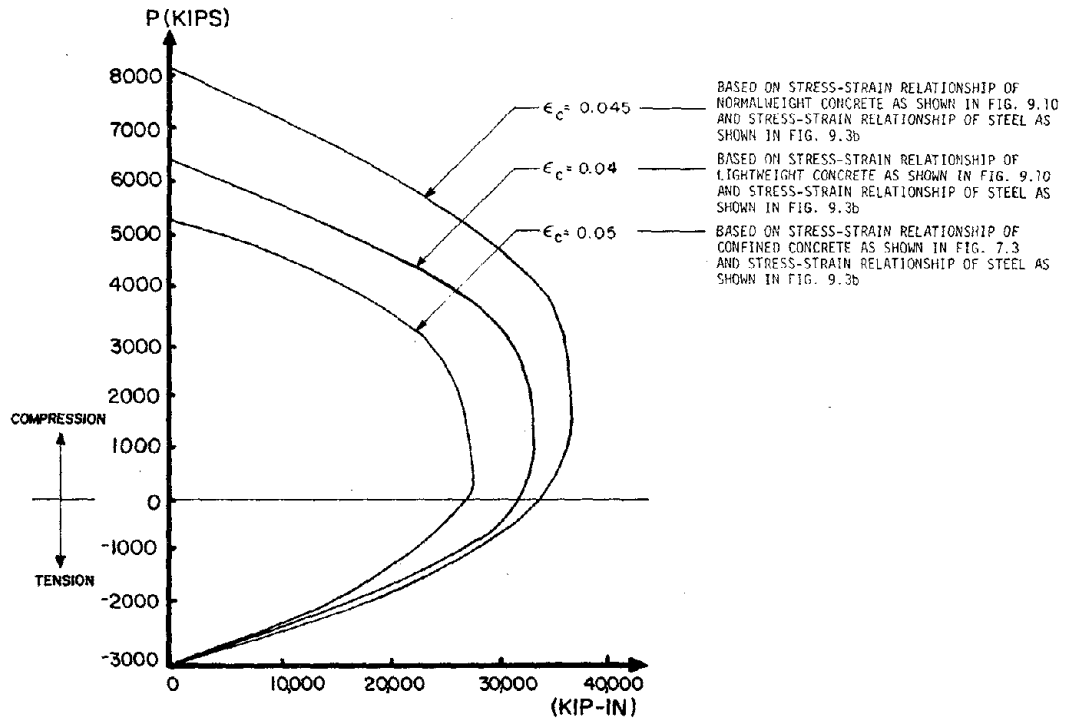


FIG. 9.9 EFFECT OF AMOUNT OF LATERAL CONFINING PRESSURE ON THE AXIAL LOAD-MOMENT (P-M) INTERACTION DIAGRAMS FOR NORMAL AND LIGHTWEIGHT CONCRETE

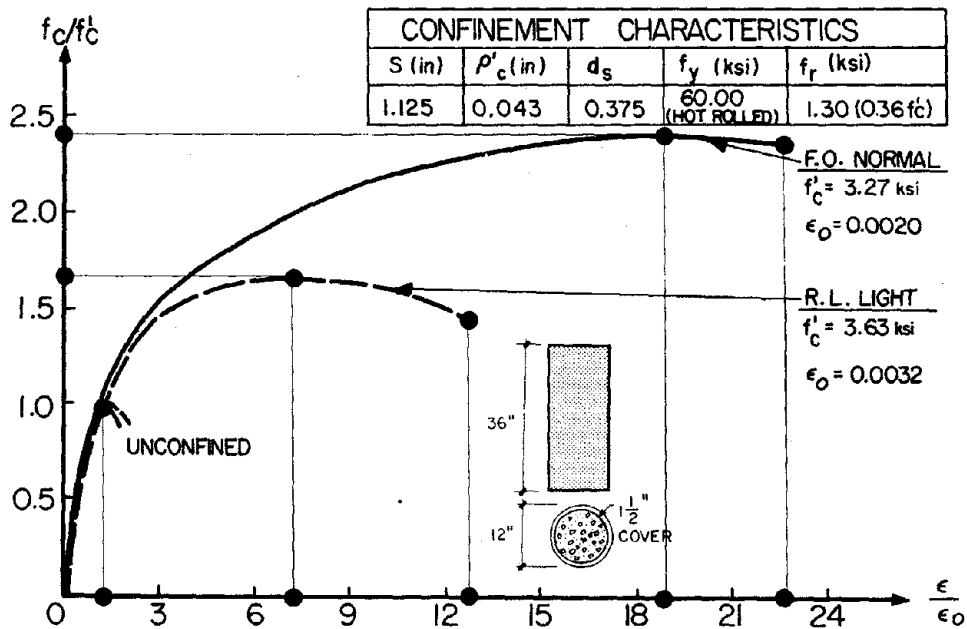


FIG. 9.10 NON-DIMENSIONAL STRESS-STRAIN RELATIONSHIPS FOR CONFINED NORMAL AND LIGHTWEIGHT CONCRETE (REF. 3)

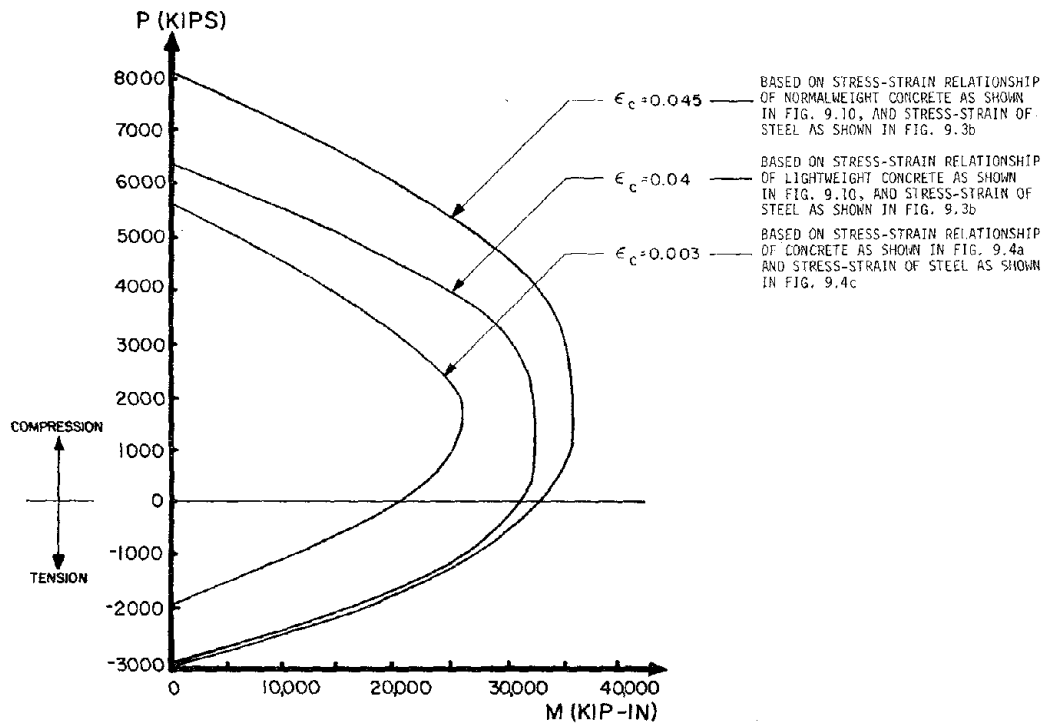


FIG. 9.11 COMPARISON OF AXIAL LOAD-MOMENT (P-M) INTERACTION DIAGRAMS COMPUTED USING THE EQUIVALENT STRESS BLOCK RELATIONSHIP AND THE EXPERIMENTAL CURVES REPORTED IN REFERENCE 3

EARTHQUAKE ENGINEERING RESEARCH CENTER REPORTS

NOTE: Numbers in parentheses are Accession Numbers assigned by the National Technical Information Service; these are followed by a price code. Copies of the reports may be ordered from the National Technical Information Service, 5285 Port Royal Road, Springfield, Virginia, 22161. Accession Numbers should be quoted on orders for reports (PB--- ---) and remittance must accompany each order. Reports without this information were not available at time of printing. Upon request, EERC will mail inquirers this information when it becomes available.

- EERC 67-1 "Feasibility Study of Large-Scale Earthquake Simulator Facility," by J. Penzien, J. G. Bouwkamp, R. W. Clough, and D. Rea - 1967 (PB 187 905)A07
- EERC 68-1 Unassigned
- EERC 68-2 "Inelastic Behavior of Beam-to-Column Subassemblages under Repeated Loading," by V. V. Bertero - 1968 (PB 184 888)A05
- EERC 68-3 "A Graphical Method for Solving the Wave Reflection-Refraction Problem," by H. D. McNiven and Y. Mengi - 1968 (PB 187 943)A03
- EERC 68-4 "Dynamic Properties of McKinley School Buildings," by D. Rea, J. G. Bouwkamp, and R. W. Clough - 1968 (PB 187 902)A07
- EERC 68-5 "Characteristics of Rock Motions during Earthquakes," by H. B. Seed, I. M. Idriss, and F. W. Kiefer - 1968 (PB 188 338)A03
- EERC 69-1 "Earthquake Engineering Research at Berkeley," - 1969 (PB 187 906)A11
- EERC 69-2 "Nonlinear Seismic Response of Earth Structures," by M. Dibaj and J. Penzien - 1969 (PB 187 904)A08
- EERC 69-3 "Probabilistic Study of the Behavior of Structures during Earthquakes," by R. Ruiz and J. Penzien - 1969 (PB 187 886)A06
- EERC 69-4 "Numerical Solution of Boundary Value Problems in Structural Mechanics by Reduction to an Initial Value Formulation," by N. Distefano and J. Schujman - 1969 (PB 187 942)A02
- EERC 69-5 "Dynamic Programming and the Solution of the Biharmonic Equation," by N. Distefano - 1969 (PB 187 941)A03
- EERC 69-6 "Stochastic Analysis of Offshore Tower Structures," by A. K. Malhotra and J. Penzien - 1969 (PB 187 903)A09
- EERC 69-7 "Rock Motion Accelerograms for High Magnitude Earthquakes," by H. B. Seed and I. M. Idriss - 1969 (PB 187 940)A02
- EERC 69-8 "Structural Dynamics Testing Facilities at the University of California, Berkeley," by R. M. Stephen, J. G. Bouwkamp, R. W. Clough and J. Penzien - 1969 (PB 189 111)A04
- EERC 69-9 "Seismic Response of Soil Deposits Underlain by Sloping Rock Boundaries," by H. Dezfulian and H. B. Seed - 1969 (PB 189 114)A03
- EERC 69-10 "Dynamic Stress Analysis of Axisymmetric Structures under Arbitrary Loading," by S. Ghosh and E. L. Wilson - 1969 (PB 189 026)A10
- EERC 69-11 "Seismic Behavior of Multistory Frames Designed by Different Philosophies," by J. C. Anderson and V. V. Bertero - 1969 (PB 190 662)A10
- EERC 69-12 "Stiffness Degradation of Reinforcing Concrete Members Subjected to Cyclic Flexural Moments," by V. V. Bertero, B. Bresler, and H. Ming Liao - 1969 (PB 202 942)A07
- EERC 69-13 "Response of Non-Uniform Soil Deposits to Travelling Seismic Waves," by H. Dezfulian and H. B. Seed - 1969 (PB 191 023)A03
- EERC 69-14 "Damping Capacity of a Model Steel Structure," by D. Rea, R. W. Clough, and J. G. Bouwkamp - 1969 (PB 190 663)A06
- EERC 69-15 "Influence of Local Soil Conditions on Building Damage Potential during Earthquakes," by H. B. Seed and I. M. Idriss - 1969 (PB 191 036)A03

- EERC 69-16 "The Behavior of Sands under Seismic Loading Conditions," by M. L. Silver and H. B. Seed - 1969 (AD 714 982)A07
- EERC 70-1 "Earthquake Response of Gravity Dams," by A. K. Chopra - 1970 (AD 709 640)A03
- EERC 70-2 "Relationships between Soil Conditions and Building Damage in the Caracas Earthquake of July 29, 1967," by H. B. Seed, I. M. Idriss, and H. Dezfulian - 1970 (PB 195 762)A05
- EERC 70-3 "Cyclic Loading of Full Size Steel Connections," by E. P. Popov and R. M. Stephen - 1970 (PB 213 545)A04
- EERC 70-4 "Seismic Analysis of the Charaima Building, Caraballeda, Venezuela," by Subcommittee of the SEAONC Research Committee: V. V. Bertero, P. F. Fratessa, S. A. Mahin, J. H. Sexton, A. C. Scordelis, E. L. Wilson, L. A. Wylie, H. B. Seed, and J. Penzien, Chairman - 1970 (PB 201 455)A06
- EERC 70-5 "A Computer Program for Earthquake Analysis of Dams," by A. K. Chopra and P. Chakrabarti - 1970 (AD 723 994)A05
- EERC 70-6 "The Propagation of Love Waves Across Non-Horizontally Layered Structures," by J. Lysmer and L. A. Drake - 1970 (PB 197 896)A03
- EERC 70-7 "Influence of Base Rock Characteristics on Ground Response," by J. Lysmer, H. B. Seed, and P. B. Schnabel - 1970 (PB 197 897)A03
- EERC 70-8 "Applicability of Laboratory Test Procedures for Measuring Soil Liquefaction Characteristics under Cyclic Loading," by H. B. Seed and W. H. Peacock - 1970 (PB 198 016)A03
- EERC 70-9 "A Simplified Procedure for Evaluating Soil Liquefaction Potential," by H. B. Seed and I. M. Idriss - 1970 (PB 198 009)A03
- EERC 70-10 "Soil Moduli and Damping Factors for Dynamic Response Analysis," by H. B. Seed and I. M. Idriss - 1970 (PB 197 869)A03
- EERC 71-1 "Koyna Earthquake of December 11, 1967 and the Performance of Koyna Dam," by A. K. Chopra and P. Chakrabarti - 1971 (AD 731 496)A06
- EERC 71-2 "Preliminary In-Situ Measurements of Anelastic Absorption in Soils using a Prototype Earthquake Simulator," by R. D. Borcherdt and P. W. Rodgers - 1971 (PB 201 454)A03
- EERC 71-3 "Static and Dynamic Analysis of Inelastic Frame Structures," by F. L. Porter and G. H. Powell - 1971 (PB 210 135)A06
- EERC 71-4 "Research Needs in Limit Design of Reinforced Concrete Structures," by V. V. Bertero - 1971 (PB 202 943)A04
- EERC 71-5 "Dynamic Behavior of a High-Rise Diagonally Braced Steel Building," by D. Rea, A. A. Shah, and J. G. Bouwkamp - 1971 (PB 203 584)A06
- EERC 71-6 "Dynamic Stress Analysis of Porous Elastic Solids Saturated with Compressible Fluids," by J. Ghaboussi and E. L. Wilson - 1971 (PB 211 396)A06
- EERC 71-7 "Inelastic Behavior of Steel Beam-to-Column Subassemblages," by H. Krawinkler, V. V. Bertero, and E. P. Popov - 1971 (PB 211 355)A14
- EERC 71-8 "Modification of Seismograph Records for Effects of Local Soil Conditions," by P. Schnabel, H. B. Seed, and J. Lysmer - 1971 (PB 214 450)A03
- EERC 72-1 "Static and Earthquake Analysis of Three Dimensional Frame and Shear Wall Buildings," by E. L. Wilson and H. H. Dovey - 1972 (PB 212 904)A05
- EERC 72-2 "Accelerations in Rock for Earthquakes in the Western United States," by P. B. Schnabel and H. B. Seed - 1972 (PB 213 100)A03
- EERC 72-3 "Elastic-Plastic Earthquake Response of Soil-Building Systems," by T. Minami - 1972 (PB 214 868)A08
- EERC 72-4 "Stochastic Inelastic Response of Offshore Towers to Strong Motion Earthquakes," by M. K. Kaul - 1972 (PB 215 713)A05

- EERC 72-5 "Cyclic Behavior of Three Reinforced Concrete Flexural Members with High Shear," by E. P. Popov, V. V. Bertero, and H. Krawinkler - 1972 (PB 214 555)A05
- EERC 72-6 "Earthquake Response of Gravity Dams Including Reservoir Interaction Effects," by P. Chakrabarti and A. K. Chopra - 1972 (AD 762 330)A08
- EERC 72-7 "Dynamic Properties of Pine Flat Dam," by D. Rea, C. Y. Liaw, and A. K. Chopra - 1972 (AD 763 928)A05
- EERC 72-8 "Three Dimensional Analysis of Building Systems," by E. L. Wilson and H. H. Dovey - 1972 (PB 222 438)A06
- EERC 72-9 "Rate of Loading Effects on Uncracked and Repaired Reinforced Concrete Members," by S. Mahin, V. V. Bertero, D. Rea and M. Atalay - 1972 (PB 224 520)A08
- EERC 72-10 "Computer Program for Static and Dynamic Analysis of Linear Structural Systems," by E. L. Wilson, K.-J. Bathe, J. E. Peterson and H. H. Dovey - 1972 (PB 220 437)A04
- EERC 72-11 "Literature Survey - Seismic Effects on Highway Bridges," by T. Iwasaki, J. Penzien, and R. W. Clough - 1972 (PB 215 613)A19
- EERC 72-12 "SHAKE - A Computer Program for Earthquake Response Analysis of Horizontally Layered Sites," by P. B. Schnabel and J. Lysmer - 1972 (PB 220 207)A06
- EERC 73-1 "Optimal Seismic Design of Multistory Frames," by V. V. Bertero and H. Kamil - 1973
- EERC 73-2 "Analysis of the Slides in the San Fernando Dams during the Earthquake of February 9, 1971," by H. B. Seed, K. L. Lee, I. M. Idriss, and F. Makdisi - 1973 (PB 223 402)A14
- EERC 73-3 "Computer Aided Ultimate Load Design of Unbraced Multistory Steel Frames," by M. B. El-Hafez and G. H. Powell - 1973 (PB 248 315)A09
- EERC 73-4 "Experimental Investigation into the Seismic Behavior of Critical Regions of Reinforced Concrete Components as Influenced by Moment and Shear," by M. Celebi and J. Penzien - 1973 (PB 215 884)A09
- EERC 73-5 "Hysteretic Behavior of Epoxy-Repaired Reinforced Concrete Beams," by M. Celebi and J. Penzien - 1973 (PB 239 568)A03
- EERC 73-6 "General Purpose Computer Program for Inelastic Dynamic Response of Plane Structures," by A. Kanaan and G. H. Powell - 1973 (PB 221 260)A08
- EERC 73-7 "A Computer Program for Earthquake Analysis of Gravity Dams Including Reservoir Interaction," by P. Chakrabarti and A. K. Chopra - 1973 (AD 766 271)A04
- EERC 73-8 "Behavior of Reinforced Concrete Deep Beam-Column Subassemblages under Cyclic Loads," by D. Küstü and J. G. Bouwkamp - 1973 (PB 246 117)A12
- EERC 73-9 "Earthquake Analysis of Structure-Foundation Systems," by A. K. Vaish and A. K. Chopra - 1973 (AD 766 272)A07
- EERC 73-10 "Deconvolution of Seismic Response for Linear Systems," by R. B. Reimer - 1973 (PB 227 179)A08
- EERC 73-11 "SAP IV: A Structural Analysis Program for Static and Dynamic Response of Linear Systems," by K.-J. Bathe, E. L. Wilson, and F. E. Peterson - 1973 (PB 221 967)A09
- EERC 73-12 "Analytical Investigations of the Seismic Response of Long, Multiple Span Highway Bridges," by W. S. Tseng and J. Penzien - 1973 (PB 227 816)A10
- EERC 73-13 "Earthquake Analysis of Multi-Story Buildings Including Foundation Interaction," by A. K. Chopra and J. A. Gutierrez - 1973 (PB 222 970)A03
- EERC 73-14 "ADAP: A Computer Program for Static and Dynamic Analysis of Arch Dams," by R. W. Clough, J. M. Raphael, and S. Mojtahedi - 1973 (PB 223 763)A09
- EERC 73-15 "Cyclic Plastic Analysis of Structural Steel Joints," by R. B. Pinkney and R. W. Clough - 1973 (PB 226 843)A08
- EERC 73-16 "QUAD-4: A Computer Program for Evaluating the Seismic Response of Soil Structures by Variable Damping Finite Element Procedures," by I. M. Idriss, J. Lysmer, R. Hwang, and H. B. Seed - 1973 (PB 229 424)A05

- EERC 73-17 "Dynamic Behavior of a Multi-Story Pyramid Shaped Building," by R. M. Stephen, J. P. Hollings, and J. G. Bouwkamp - 1973 (PB 240 718)A06
- EERC 73-18 "Effect of Different Types of Reinforcing on Seismic Behavior of Short Concrete Columns," by V. V. Bertero, J. Hollings, O. Küstü, R. M. Stephen, and J. G. Bouwkamp - 1973
- EERC 73-19 "Olive View Medical Center Materials Studies, Phase I," by B. Bresler and V. V. Bertero - 1973 (PB 235 986)A06
- EERC 73-20 "Linear and Nonlinear Sesismic Analysis Computer Programs for Long Multiple-Span Highway Bridges," by W. S. Tseng and J. Penzien - 1973
- EERC 73-21 "Constitutive Models for Cyclic Plastic Deformation of Engineering Materials," by J. M. Kelly and P. P. Gillis - 1973 (PB 226 024)A03
- EERC 73-22 "DRAIN-2D User's Guide," by G. H. Powell - 1973 (PB 227 016)A05
- EERC 73-23 "Earthquake Engineering at Berkeley - 1973 " 1973 (PB 226 033)A11
- EERC 73-24 Unassigned
- EERC 73-25 "Earthquake Response of Axisymmetric Tower Structures Surrounded by Water," by C. Y. Liaw and A. K. Chopra - 1973 (AD 773 052)A09
- EERC 73-26 "Investigation of the Failures of the Olive View Stairtowers during the San Fernando Earthquake and Their Implications on Seismic Design," by V. V. Bertero and R. G. Collins - 1973 (PB 235 106)A13
- EERC 73-27 "Further Studies on Seismic Behavior of Steel Beam-Column Subassemblages," by V. V. Bertero, H. Krawinkler, and E. P. Popov - 1973 (PB 234 172)A06
- EERC 74-1 "Seismic Risk Analysis," by C. S. Oliveira - 1974 (PB 235 920)A06
- EERC 74-2 "Settlement and Liquefaction of Sands under Multi-Directional Shaking," by R. Pyke, C. K. Chan, and H. B. Seed - 1974
- EERC 74-3 "Optimum Design of Earthquake Resistant Shear Buildings," by D. Ray, K. S. Pister, and A. K. Chopra - 1974 (PB 231 172)A06
- EERC 74-4 "LUSH - A Computer Program for Complex Response Analysis of Soil-Structure Systems," by J. Lysmer, T. Udaka, H. B. Seed, and R. Hwang - 1974 (PB 236 796)A05
- EERC 74-5 "Sensitivity Analysis for Hysteretic Dynamic Systems: Applications to Earthquake Engineering," by D. Ray - 1974 (PB 233 213)A06
- EERC 74-6 "Soil Structure Interaction Analyses for Evaluating Seismic Response," by H. B. Seed, J. Lysmer, and R. Hwang - 1974 (PB 236 519)A04
- EERC 74-7 Unassigned
- EERC 74-8 "Shaking Table Tests of a Steel Frame - A Progress Report," by R. W. Clough and D. Tang - 1974 (PB 240 869)A03
- EERC 74-9 "Hysteretic Behavior of Reinforced Concrete Flexural Members with Special Web Reinforcement," by V. V. Bertero, E. P. Popov, and T. Y. Wang - 1974 (PB 236 797)A07
- EERC 74-10 "Applications of Reliability-Based, Global Cost Optimization to Design of Earthquake Resistant Structures," by E. Vitiello and K. S. Pister - 1974 (PB 237 231)A06
- EERC 74-11 "Liquefaction of Gravelly Soils under Cyclic Loading Conditions," by R. T. Wong, H. B. Seed, and C. K. Chan - 1974 (PB 242 042)A03
- EERC 74-12 "Site-Dependent Spectra for Earthquake-Resistant Design," by H. B. Seed, C. Ugas, and J. Lysmer - 1974 (PB 240 953)A03
- EERC 74-13 "Earthquake Simulator Study of a Reinforced Concrete Frame," by P. Hidalgo and R. W. Clough - 1974 (PB 241 944)A13
- EERC 74-14 "Nonlinear Earthquake Response of Concrete Gravity Dams," by N. Pal - 1974 (AD/A 006 583)A06

- EERC 74-15 "Modeling and Identification in Nonlinear Structural Dynamics - I. One Degree of Freedom Models," by N. Distefano and A. Rath - 1974 (PB 241 548)A06
- EERC 75-1 "Determination of Seismic Design Criteria for the Dumbarton Bridge Replacement Structure, Vol. I: Description, Theory and Analytical Modeling of Bridge and Parameters," by F. Baron and S.-H. Pang - 1975 (PB 259 407)A15
- EERC 75-2 "Determination of Seismic Design Criteria for the Dumbarton Bridge Replacement Structure, Vol. II: Numerical Studies and Establishment of Seismic Design Criteria," by F. Baron and S.-H. Pang - 1975 (PB 259 408)A11 [For set of EERC 75-1 and 75-2 (PB 241 454)A09]
- EERC 75-3 "Seismic Risk Analysis for a Site and a Metropolitan Area," by C. S. Oliveira - 1975 (PB 248 134)A09
- EERC 75-4 "Analytical Investigations of Seismic Response of Short, Single or Multiple-Span Highway Bridges," by M.-C. Chen and J. Penzien - 1975 (PB 241 454)A09
- EERC 75-5 "An Evaluation of Some Methods for Predicting Seismic Behavior of Reinforced Concrete Buildings," by S. A. Mahin and V. V. Bertero - 1975 (PB 246 306)A16
- EERC 75-6 "Earthquake Simulator Story of a Steel Frame Structure, Vol. I: Experimental Results," by R. W. Clough and D. T. Tang - 1975 (PB 243 981)A13
- EERC 75-7 "Dynamic Properties of San Bernardino Intake Tower," by D. Rea, C.-Y Liaw and A. K. Chopra - 1975 (AD/A 008 406)A05
- EERC 75-8 "Seismic Studies of the Articulation for the Dumbarton Bridge Replacement Structure, Vol. 1: Description, Theory and Analytical Modeling of Bridge Components," by F. Baron and R. E. Hamati - 1975 (PB 251 539)A07
- EERC 75-9 "Seismic Studies of the Articulation for the Dumbarton Bridge Replacement Structure, Vol. 2: Numerical Studies of Steel and Concrete Girder Alternates," by F. Baron and R. E. Hamati - 1975 (PB 251 540)A10
- EERC 75-10 "Static and Dynamic Analysis of Nonlinear Structures," by D. P. Mondkar and G. H. Powell - 1975 (PB 242 434)A08
- EERC 75-11 "Hysteretic Behavior of Steel Columns," by E. P. Popov, V. V. Bertero, and S. Chandramouli - 1975 (PB 252 365)A11
- EERC 75-12 "Earthquake Engineering Research Center Library Printed Catalog " - 1975 (PB 243 711)A26
- EERC 75-13 "Three Dimensional Analysis of Building Systems (Extended Version)," by E. L. Wilson, J. P. Hollings, and H. H. Dovey - 1975 (PB 243 989)A07
- EERC 75-14 "Determination of Soil Liquefaction Characteristics by Large-Scale Laboratory Tests," by P. De Alba, C. K. Chan, and H. B. Seed - 1975 (NUREG 0027)A08
- EERC 75-15 "A Literature Survey - Compressive, Tensile, Bond and Shear Strength of Masonry," by R. L. Mayes and R. W. Clough - 1975 (PB 246 292)A10
- EERC 75-16 "Hysteretic Behavior of Ductile Moment-Resisting Reinforced Concrete Frame Components," by V. V. Bertero and E. P. Popov - 1975 (PB 246 388)A05
- EERC 75-17 "Relationships Between Maximum Acceleration, Maximum Velocity, Distance from Source, Local Site Conditions for Moderately Strong Earthquakes," by H. B. Seed, R. Murarka, J. Lysmer, and I. M. Idriss - 1975 (PB 248 172)A03
- EERC 75-18 "The Effects of Method of Sample Preparation on the Cyclic Stress-Strain Behavior of Sands," by J. Mulilis, C. K. Chan, and H. B. Seed - 1975 (Summarized in EERC 75-28)
- EERC 75-19 "The Seismic Behavior of Critical Regions of Reinforced Concrete Components as Influenced by Moment, Shear and Axial Force," by M. B. Atalay and J. Penzien - 1975 (PB 258 842)A11
- EERC 75-20 "Dynamic Properties of an Eleven Story Masonry Building," by R. M. Stephen, J. P. Hollings, J. G. Bouwkamp, and D. Jurukovski - 1975 (PB 246 945)A04
- EERC 75-21 "State-of-the-Art in Seismic Strength of Masonry - An Evaluation and Review," by R. L. Mayes and R. W. Clough - 1975 (PB 249 040)A07
- EERC 75-22 "Frequency Dependent Stiffness Matrices for Viscoelastic Half-Plane Foundations," by A. K. Chopra, P. Chakrabarti, and G. Dasgupta - 1975 (PB 248 121)A07

- EERC 75-23 "Hysteretic Behavior of Reinforced Concrete Framed Walls," by T. Y. Wang, V. V. Bertero, and E. P. Popov - 1975
- EERC 75-24 "Testing Facility for Subassemblages of Frame-Wall Structural Systems," by V. V. Bertero, E. P. Popov, and T. Endo - 1975
- EERC 75-25 "Influence of Seismic History on the Liquefaction Characteristics of Sands," by H. B. Seed, K. Mori, and C. K. Chan - 1975 (Summarized in EERC 75-28)
- EERC 75-26 "The Generation and Dissipation of Pore Water Pressures during Soil Liquefaction," by H. B. Seed, P. P. Martin, and J. Lysmer - 1975 (PB 252 648)A03
- EERC 75-27 "Identification of Research Needs for Improving Aseismic Design of Building Structures," by V. V. Bertero - 1975 (PB 248 136)A05
- EERC 75-28 "Evaluation of Soil Liquefaction Potential during Earthquakes," by H. B. Seed, I. Arango, and C. K. Chan - 1975 (NUREG 0026)A13
- EERC 75-29 "Representation of Irregular Stress Time Histories by Equivalent Uniform Stress Series in Liquefaction Analyses," by H. B. Seed, I. M. Idriss, F. Makdisi, and N. Banerjee - 1975 (PB 252 635)A03
- EERC 75-30 "FLUSH - A Computer Program for Approximate 3-D Analysis of Soil-Structure Interaction Problems," by J. Lysmer, T. Udaka, C.-F. Tsai, and H. B. Seed - 1975 (PB 259 332)A07
- EERC 75-31 "ALUSH - A Computer Program for Seismic Response Analysis of Axisymmetric Soil-Structure Systems," by E. Berger, J. Lysmer, and H. B. Seed - 1975
- EERC 75-32 "TRIP and TRAVEL - Computer Programs for Soil-Structure Interaction Analysis with Horizontally Travelling Waves," by T. Udaka, J. Lysmer, and H. B. Seed - 1975
- EERC 75-33 "Predicting the Performance of Structures in Regions of High Seismicity," by J. Penzien - 1975 (PB 248 130)A03
- EERC 75-34 "Efficient Finite Element Analysis of Seismic Structure-Soil-Direction," by J. Lysmer, H. B. Seed, T. Udaka, R. N. Hwang, and C.-F. Tsai - 1975 (PB 253 570)A03
- EERC 75-35 "The Dynamic Behavior of a First Story Girder of a Three-Story Steel Frame Subjected to Earthquake Loading," by R. W. Clough and L.-Y. Li - 1975 (PB 248 841)A05
- EERC 75-36 "Earthquake Simulator Story of a Steel Frame Structure, Volume II - Analytical Results," by D. T. Tang - 1975 (PB 252 926)A10
- EERC 75-37 "ANSR-I General Purpose Computer Program for Analysis of Non-Linear Structural Response," by D. P. Mondkar and G. H. Powell - 1975 (PB 252 386)A08
- EERC 75-38 "Nonlinear Response Spectra for Probabilistic Seismic Design and Damage Assessment of Reinforced Concrete Structures," by M. Murakami and J. Penzien - 1975 (PB 259 530)A05
- EERC 75-39 "Study of a Method of Feasible Directions for Optimal Elastic Design of Frame Structures Subjected to Earthquake Loading," by N. D. Walker and K. S. Pister - 1975 (PB 247 781)A06
- EERC 75-40 "An Alternative Representation of the Elastic-Viscoelastic Analogy," by G. Dasgupta and J. L. Sackman - 1975 (PB 252 173)A03
- EERC 75-41 "Effect of Multi-Directional Shaking on Liquefaction of Sands," by H. B. Seed, R. Pyke, and G. R. Martin - 1975 (PB 258 781)A03
- EERC 76-1 "Strength and Ductility Evaluation of Existing Low-Rise Reinforced Concrete Buildings - Screening Method," by T. Okada and B. Bresler - 1976 (PB 257 906)A11
- EERC 76-2 "Experimental and Analytical Studies on the Hysteretic Behavior of Reinforced Concrete Rectangular and T-Beams," by S.-Y. M. Ma, E. P. Popov, and V. V. Bertero - 1976 (PB 260 843)A12
- EERC 76-3 "Dynamic Behavior of a Multistory Triangular-Shaped Building," by J. Petrovski, R. M. Stephen, E. Gartenbaum, and J. G. Bouwkamp - 1976
- EERC 76-4 "Earthquake Induced Deformations of Earth Dams," by N. Serff and H. B. Seed - 1976
- EERC 76-5 "Analysis and Design of Tube-Type Tall Building Structures," by H. de Clercq and G. H. Powell - 1976 (PB 252 220)A10

- EERC 76-6 "Time and Frequency Domain Analysis of Three-Dimensional Ground Motions, San Fernando Earthquake," by T. Kubo and J. Penzien - 1976 (PB 260 556)A11
- EERC 76-7 "Expected Performance of Uniform Building Code Design Masonry Structures," by R. L. Mayes, Y. Omote, S. W. Chen, and R. W. Clough - 1976
- EERC 76-8 "Cyclic Shear Tests on Concrete Masonry Piers, Part I - Test Results," by R. L. Mayes, Y. Omote, and R. W. Clough - 1976 (PB 264 424)A06
- EERC 76-9 "A Substructure Method for Earthquake Analysis of Structure-Soil Interaction," by J. A. Gutierrez and A. K. Chopra - 1976 (PB 247 783)A08
- EERC 76-10 "Stabilization of Potentially Liquefiable San Deposits using Gravel Drain Systems," by H. B. Seed and J. R. Booker - 1976 (PB 248 820)A04
- EERC 76-11 "Influence of Design and Analysis Assumptions on Computed Inelastic Response of Moderately Tall Frames," by G. H. Powell and D. G. Row - 1976
- EERC 76-12 "Sensitivity Analysis for Hysteretic Dynamic Systems: Theory and Applications," by D. Ray, K. S. Pister, and E. Polak - 1976 (PB 262 859)A04
- EERC 76-13 "Coupled Lateral Torsional Response of Buildings to Ground Shaking," by C. L. Kan and A. K. Chopra - 1976 (PB 257 907)A09
- EERC 76-14 "Seismic Analyses of the Banco de America," by V. V. Bertero, S. A. Mahin, and J. A. Hollings - 1976
- EERC 76-15 "Reinforced Concrete Frame 2: Seismic Testing and Analytical Correlation," by R. W. Clough and J. Gidwani - 1976 (PB 261 323)A08
- EERC 76-16 "Cyclic Shear Tests on Masonry Piers, Part II - Analysis of Test Results," by R. L. Mayes, Y. Omote, and R. W. Clough - 1976
- EERC 76-17 "Structural Steel Bracing Systems: Behavior under Cyclic Loading," by E. P. Popov, K. Takanashi, and C. W. Roeder - 1976 (PB 260 715)A05
- EERC 76-18 "Experimental Model Studies on Seismic Response of High Curved Overcrossings," by D. Williams and W. G. Godden - 1976
- EERC 76-19 "Effects of Non-Uniform Seismic Disturbances on the Dumbarton Bridge Replacement Structure," by F. Baron and R. E. Hamati - 1976
- EERC 76-20 "Investigation of the Inelastic Characteristics of a Single Story Steel Structure using System Identification and Shaking Table Experiments," by V. C. Matzen and H. D. McNiven - 1976 (PB 258 453)A07
- EERC 76-21 "Capacity of Columns with Splice Imperfections," by E. P. Popov, R. M. Stephen and R. Philbrick - 1976 (PB 260 378)A04
- EERC 76-22 "Response of the Olive View Hospital Main Building during the San Fernando Earthquake," by S. A. Mahin, V. V. Bertero, A. K. Chopra, and R. Collins," - 1976
- EERC 76-23 "A Study on the Major Factors Influencing the Strength of Masonry Prisms," by N. M. Mostaghel, R. L. Mayes, R. W. Clough, and S. W. Chen - 1976
- EERC 76-24 "GADFLEA - A Computer Program for the Analysis of Pore Pressure Generation and Dissipation during Cyclic or Earthquake Loading," by J. R. Booker, M. S. Rahman, and H. B. Seed - 1976 (PB 263 947)A04
- EERC 76-25 "Rehabilitation of an Existing Building: A Case Study," by B. Bresler and J. Axley - 1976
- EERC 76-26 "Correlative Investigations on Theoretical and Experimental Dynamic Behavior of a Model Bridge Structure," by K. Kawashima and J. Penzien - 1976 (PB 263 388)A11
- EERC 76-27 "Earthquake Response of Coupled Shear Wall Buildings," by T. Srichatrapimuk - 1976 (PB 265 157)A07
- EERC 76-28 "Tensile Capacity of Partial Penetration Welds," by E. P. Popov and R. M. Stephen - 1976 (PB 262 899)A03
- EERC 76-29 "Analysis and Design of Numerical Integration Methods in Structural Dynamics," by H. M. Hilber - 1976 (PB 264 410)A06

- EERC 76-30 "Contribution of a Floor System to the Dynamic Characteristics of Reinforced Concrete Buildings," by L. E. Malik and V. V. Bertero - 1976
- EERC 76-31 "The Effects of Seismic Disturbances on the Golden Gate Bridge," by F. Baron, M. Arikan, R. E. Hamati - 1976
- EERC 76-32 "Infilled Frames in Earthquake-Resistant Construction," by R. E. Klingner and V. V. Bertero - 1976 (PB 265 892)A13
- UCB/EERC-77/01 "PLUSH - A Computer Program for Probabilistic Finite Element Analysis of Seismic Soil-Structure Interaction," by M. P. Romo Organista, J. Lysmer, and H. B. Seed - 1977
- UCB/EERC-77/02 "Soil-Structure Interaction Effects at the Humboldt Bay Power Plant in the Ferndale Earthquake of June 7, 1975," by J. E. Valera, H. B. Seed, C.-F. Tsai, and J. Lysmer - 1977 (B 265 795)A04
- UCB/EERC-77/03 "Influence of Sample Disturbance on Sand Response to Cyclic Loading," by K. Mori, H. B. Seed, and C. K. Chan - 1977 (PB 267 352)A04
- UCB/EERC-77/04 "Seismological Studies of Strong Motion Records," by J. Shoja-Taheri - 1977 (PB 269 655)A10
- UCB/EERC-77/05 "Testing Facility for Coupled Shear Walls," by L.-H. Lee, V. V. Bertero, and E. P. Popov - 1977
- UCB/EERC-77/06 "Developing Methodologies for Evaluating the Earthquake Safety of Existing Buildings," No. 1 - B. Bresler; No. 2 - B. Bresler, T. Okada, and D. Zisling; No. 3 - T. Okada and B. Bresler; No. 4 - V. V. Bertero and B. Bresler - 1977 (PB 267 354)A08
- UCB/EERC-77/07 "A Literature Survey - Transverse Strength of Masonry Walls," by Y. Omote, R. L. Mayes, S. W. Chen, and R. W. Clough - 1977
- UCB/EERC-77/08 "DRAIN-TABS: A Computer Program for Inelastic Earthquake Response of Three Dimensional Buildings," by R. Guendelman-Israel and G. H. Powell - 1977
- UCB/EERC-77/09 "SUBWALL: A Special Purpose Finite Element Computer Program for Practical Elastic Analysis and Design of Structural Walls with Substructure Option," by D. Q. Le, H. Petersson, and E. P. Popov - 1977
- UCB/EERC-77/10 "Experimental Evaluation of Seismic Design Methods for Broad Cylindrical Tanks," by D. P. Clough - 1977
- UCB/EERC-77/11 "Earthquake Engineering Research at Berkeley - 1976," - 1977
- UCB/EERC-77/12 "Automated Design of Earthquake Resistant Multistory Steel Building Frames," by N. D. Walker, Jr. - 1977
- UCB/EERC-77/13 "Concrete Confined by Rectangular Hoops and Subjected to Axial Loads," by J. Vallenias, V. V. Bertero, and E. P. Popov - 1977
- UCB/EERC-77/14 "Seismic Strain Induced in the Ground during Earthquakes," by Y. Sugimura - 1977
- UCB/EERC-77/15 "Bond Deterioration under Generalized Loading," by V. V. Bertero, E. P. Popov, and S. Viathanatepa - 1977
- UCB/EERC-77/16 "Computer-Aided Optimum Design of Ductile Reinforced Concrete Moment-Resisting Frames," by S. W. Zagajeski and V. V. Bertero - 1977
- UCB/EERC-77/17 "Earthquake Simulation Testing of a Stepping Frame with Energy-Absorbing Devices," by J. M. Kelly and D. F. Tsztoo - 1977
- UCB/EERC-77/18 "Inelastic Behavior of Eccentrically Braced Steel Frames under Cyclic Loadings," by C. W. Roeder and E. P. Popov - 1977
- UCB/EERC-77/19 "A Simplified Procedure for Estimating Earthquake-Induced Deformation in Dams and Embankments," by F. I. Makdisi and H. B. Seed - 1977
- UCB/EERC-77/20 "The Performance of Earth Dams during Earthquakes," by H. B. Seed, F. I. Makdisi, and P. de Alba - 1977

- UCB/EERC-77/21 "Dynamic Plastic Analysis Using Stress Resultant Finite Element Formulation," by P. Lukkunaprasit and J. M. Kelly - 1977
- UCB/EERC-77/22 "Preliminary Experimental Study of Seismic Uplift of a Steel Frame," by R. W. Clough and A. A. Huckelbridge - 1977
- UCB/EERC-77/23 "Earthquake Simulator Tests of a Nine-Story Steel Frame with Columns Allowed to Uplift," by A. A. Huckelbridge - 1977
- UCB/EERC-77/24 "Nonlinear Soil-Structure Interaction of Skew Highway Bridges," by M.-C. Chen and J. Penzien - 1977
- UCB/EERC-77/25 "Seismic Analysis of an Offshore Structure Supported on Pile Foundations," by D.D.-N. Liou - 1977
- UCB/EERC-77/26 "Dynamic Stiffness Matrices for Homogeneous Viscoelastic Half-Planes," by G. Dasgupta and A. K. Chopra - 1977
- UCB/EERC-77/27 "A Practical Soft Story Earthquake Isolation System," by J. M. Kelly and J. M. Eidinger - 1977
- UCB/EERC-77/28 "Seismic Safety of Existing Buildings and Incentives for Hazard Mitigation in San Francisco: An Exploratory Study," by A. J. Meltsner - 1977
- UCB/EERC-77/29 "Dynamic Analysis of Electrohydraulic Shaking Tables," by D. Rea, S. Abedi-Hayati, and Y. Takahashi - 1977
- UCB/EERC-77/30 "An Approach for Improving Seismic-Resistant Behavior of Reinforced Concrete Interior Joints," by B. Galunic, V. V. Bertero, and E. P. Popov - 1977
- UCB/EERC-78/01 "The Development of Energy-Absorbing Devices for Aseismic Base Isolation Systems," by J. M. Kelly and D. F. Tsztoo - 1978
- UCB/EERC-78/02 "Effect of Tensile Prestrain on the Cyclic Response of Structural Steel Connections," by J. G. Bouwkamp and A. Mukhopadhyay - 1978
- UCB/EERC-78/03 "Experimental Results of an Earthquake Isolation System using Natural Rubber Bearings," by J. M. Eidinger and J. M. Kelly - 1978
- UCB/EERC-78/04 "Seismic Behavior of Tall Liquid Storage Tanks," by A. Niwa - 1978
- UCB/EERC-78/05 "Hysteretic Behavior of Reinforced Concrete Columns Subjected to High Axial and Cyclic Shear Forces," by S. W. Zagajeski, V. V. Bertero, and J. G. Bouwkamp - 1978
- UCB/EERC-78/06 "Inelastic Beam-Column Elements for the ANSR-I Program," by A. Riahi, D. G. Row, and G. H. Powell - 1978

- UCB/EERC-78/07 "Studies of Structural Response to Earthquake Ground Motion," by O.A. Lopez and A.K. Chopra - 1978
- UCB/EERC-78/08 "A Laboratory Study of the Fluid-Structure Interaction of Submerged Tanks and Caissons in Earthquakes," by R.C. Byrd - 1978 (PB 284 957)A08
- UCB/EERC-78/09 "Models for Evaluating Damageability of Structures," by I. Sakamoto and B. Bresler - 1978
- UCB/EERC-78/10 "Seismic Performance of Secondary Structural Elements," by I. Sakamoto - 1978
- UCB/EERC-78/11 Case Study--Seismic Safety Evaluation of a Reinforced Concrete School Building," by J. Axley and B. Bresler 1978
- UCB/EERC-78/12 "Potential Damageability in Existing Buildings," by T. Blejwas and B. Bresler - 1978
- UCB/EERC-78/13 "Dynamic Behavior of a Pedestal Base Multistory Building," by R. M. Stephen, E. L. Wilson, J. G. Bouwkamp and M. Button - 1978
- UCB/EERC-78/14 "Seismic Response of Bridges - Case Studies," by R.A. Imbsen, V. Nutt and J. Penzien - 1978
- UCB/EERC-78/15 "A Substructure Technique for Nonlinear Static and Dynamic Analysis," by D.G. Row and G.H. Powell - 1978
- UCB/EERC-78/16 "Seismic Performance of Nonstructural and Secondary Structural Elements," by Isao Sakamoto - 1978
- UCB/EERC-78/17 "Model for Evaluating Damageability of Structures," by Isao Sakamoto and B. Bresler - 1978
- UCB/EERC-78/18 "Response of K-Braced Steel Frame Models to Lateral Loads," by J.G. Bouwkamp, R.M. Stephen and E.P. Popov - 1978
- UCB/EERC-78/19 "Rational Design Methods for Light Equipment in Structures Subjected to Ground Motion," by Jerome L. Sackman and James M. Kelly - 1978
- UCB/EERC-78/20 "Testing of a Wind Restraint for Aseismic Base Isolation," by James M. Kelly and Daniel E. Chitty - 1978
- UCB/EERC-78/21 "APOLLO A Computer Program for the Analysis of Pore Pressure Generation and Dissipation in Horizontal Sand Layers During Cyclic or Earthquake Loading," by Philippe P. Martin and H. Bolton Seed - 1978
- UCB/EERC-78/22 "Optimal Design of an Earthquake Isolation System," by M.A. Bhatti, K.S. Pister and E. Polak - 1978

EERC-11

- UCB/EERC-78/23 "MASH A Computer Program for the Non-Linear Analysis of Vertically Propagating Shear Waves in Horizontally Layered Deposits," by Phillippe P. Martin and H. Bolton Seed - 1978
- UCB/EERC-78/24 "Investigation of the Elastic Characteristics of a Three-Story Steel Frame Using System Identification," by Izak Kaya and Hugh D. McNiven - 1978
- UCB/EERC-78/25 "Investigation of the Nonlinear Characteristics of a Three-Story Steel Frame Using Systems Identification," by Izak Kaya and Hugh D. McNiven
- UCB/EERC-78/26 "Studies of Strong Ground Motion in Taiwan," by Y.M. Hsiung, B.A. Bolt, and J. Penzien - 1978
- UCB/EERC-78/27 "Cyclic Loading Tests of Masonry Single Piers Volume 1 - Height to Width Ratio of 2," by P.A. Hidalgo, R.L. Mayes, H.D. McNiven, and R.W. Clough - 1978
- UCB/EERC-78/28 "Cyclic Loading Tests of Masonry Single Piers Volume 2 - Height to Width Ratio of 1," by S.W.J. Chen, P.A. Hidalgo, R.L. Mayes, R.W. Clough, and H.D. McNiven - 1978
- UCB/EERC-78/29 "Analytical Procedures in Soil Dynamics," by J. Lysmer - 1978
- UCB/EERC-79/01 "Hysteretic Behavior of Lightweight Reinforced Concrete Beam-Column Subassemblages," by B. Forzani, E.P. Popov, and V.V. Bertero - 1979
- UCB/EERC-79/02 "The Development of a Mathematical Model to Predict the Flexural Response of Reinforced Concrete Beams to Cyclic Loads, Using System Identification," by J.F. Stanton and H.D. McNiven - 1979
- UCB/EERC-79/03 "Linear and Nonlinear Earthquake Response of Simple Torsionally Coupled Systems," by C.L. Kan and A.K. Chopra - 1979
- UCB/EERC-79/04 "A Mathematical Model of Masonry for Predicting Its Linear Seismic Response Characteristics," by Y. Mengi and H.D. McNiven - 1979
- UCB/EERC-79/05 "Mechanical Behavior of Lightweight Concrete Confined with Different Types of Lateral Reinforcement," by M.A. Manrique, V.V. Bertero, and E.P. Popov - 1979

